The role of 12/15-lipoxygenases in ROS-mediated neuronal cell death

Dissertation

zur

Erlangung des Doktorgrades

der Naturwissenschaften

(Dr. rer. nat.)

dem

Fachbereich

der Philipps-Universität Marburg

vorgelegt von

Svenja Tobaben

aus Mölln

Marburg/Lahn 2010

Vom Fachbereich Pharmazie (16)

der Philipps-Universität Marburg als Dissertation

am_____

_____angenommen.

Erstgutachter: Prof. Dr. Carsten Culmsee

Zweitgutachter: Prof Dr. Jens Kockskämper

Tag der mündlichen Prüfung am 19.01.2011

Meinen Eltern

Table of contents

1. Introduction

1.1. Apoptosis and necrosis in the brain

Apoptosis and necrosis are two major paradigms of neuronal cell death and therefore leading causes for the devastating effects of progressive neuronal loss after acute brain damage and in neurodegenerative diseases [1-4].

Necrosis is characterized by mitochondrial swelling, loss of ATP, massive calcium influx and dysregulation of the intracellular ion homeostasis. Later stages of necrosis are characterized by cell swelling, membrane lysis and induction of inflammatory processes by released intracellular components such as histamine or prostaglandins [5]. In neurodegenerative diseases neuronal cell death also features hallmarks of necrosis [6] for which reason a better understanding of necrosis pathways and their regulation is important to define new therapeutic targets.

In contrast, apoptosis is characterized by nuclear condensation and DNA fragmentation, membrane blebbing and the subsequent formation of apoptotic bodies [7]. These apoptotic bodies have an intact plasma membrane and are phagocytosed for which reason they do not release intracellular components. Consequently, in contrast to necrosis, apoptosis does not induce inflammatory processes that could further increase the damage to the surrounding tissue [8]. For example, apoptosis is very important in proliferating tissue, for the replacement of senescent or excessive cells without causing necrosis, inflammation and scar formation [9].

It is widely accepted that apoptosis is an active form of cell death requiring an energy dependent processing of apoptosis inducing factors, while necrosis traditionally has been regarded as a passive and uncontrolled form of cell death. However, recent findings suggest that this paradigm needs refinement, since a form of cell death has been reported showing features of both necrosis and apoptosis at the same time. The newly discovered form of cell death, named necroptosis shows signs of necrotic cell death, like plasma-membrane disintegration and mitochondrial swelling, even though it is based on tightly controlled signaling pathways [10].

Having been discovered only recently, the role of necroptosis in neurodegeneration is not yet established and is subjected to ongoing research.

Apoptosis, however has been studied in great detail, revealing its physiological role in non-proliferating tissue like the brain, where apoptosis has been suggested to control the development of synapses by removing excessive and unneeded cells especially during brain development [11].

In contrast to the physiological role of apoptosis, e.g. during brain development, pathological pathways of apoptosis have been associated with the progressive neuronal loss occurring in Alzheimer's Disease and Parkinson's Disease. Further, delayed neuronal death after acute brain damage caused by cerebral ischemia or traumatic brain injury also involved apoptotic-signaling pathways [4].

Overall, it is well established that apoptosis is of great importance in all organisms as it assures removal of damaged, senescent or mutagenic cells thereby preserving the maintenance and function of various tissues and organs. In contrast, dysregulation of apoptosis is known to cause diseases, including neurodegenerative disorders.

Two different apoptosis-inducing pathways can be distinguished, the intrinsic and the extrinsic pathway (Figure 1). The extrinsic pathway is triggered by stimulation of death receptors, as for example, the Fas receptor that is activated by Fas-ligand (FasL). Such activation results in the sequential binding of Fas associated death domain (FADD) and procaspase-8, which thereafter becomes activated.

Caspases are proteolytic enzymes that mediate apoptosis by cleaving important cellular proteins, e.g. actin or laminin, and by activating nucleases like CAD (caspase-activated deoxyribunuclease) that cleave the DNA in the nucleus and thereby induce cell death.

Caspase-8 can directly activate the effector caspase-3, which has many substrates and is regarded as one of the key proteases in the execution of apoptosis. Caspase-3 causes release of CAD (caspase-activated deoxyribunuclease) from the inhibitory ligand ICAD and thereby CAD becomes activated. Together, caspase-3 and CAD effect programmed DNA cleavage.

Furthermore, the upstream caspase-8 can activate pro-apoptotic Bcl-2-proteins like Bid, which sets off the cascade of intrinsic apoptosis.

In contrast to the extrinsic pathway, the intrinsic pathway of apoptosis is characterized by the involvement of mitochondria. High levels of ROS and calcium

as well as activation of the pro-apoptotic protein Bid activate the intrinsic pathway and lead to mitochondrial permeabilization and the subsequent release of pro-apoptotic proteins like apoptosis-inducing factor (AIF), cytochrome c, Omi/HtrA2 or Smac/DIABLO. Upon mitochondrial release, AIF rapidly translocates to the nucleus and induces DNA-damage and cell death in a caspase-independent manner [12]. In contrast, cytosolic cytochrome c forms a complex with Apaf-1 (apoptosis protease-activating factor-1) and pro-caspase-9, the so-called apoptosome, which then catalyzes the activation of execution caspases like caspase-3 but also caspase-6 and caspase-7 [13]. These caspases induce the breakdown of the cellular framework through the activation of CAD or degradation of substrates like actin.

Further, alternative mechanisms of caspase activation during intrinsic pathways of apoptosis may be triggered by release of Smac/DIABLO or Omi/HtrA2 from mitochondria. In the cytosol Smac/DIABLO and Omi/HtrA2 block the anti-apoptotic protein XIAP (x-chromosomal linked inhibitor of apoptosis) and other inhibitors of apoptosis (IAPs) that usually inhibit caspase-activation. Consequently, upon mitochondrial release of Smac/DIABLO or Omi/HtrA2, caspases are released from their physiological inhibitors and are thus activated in an indirect manner [13].

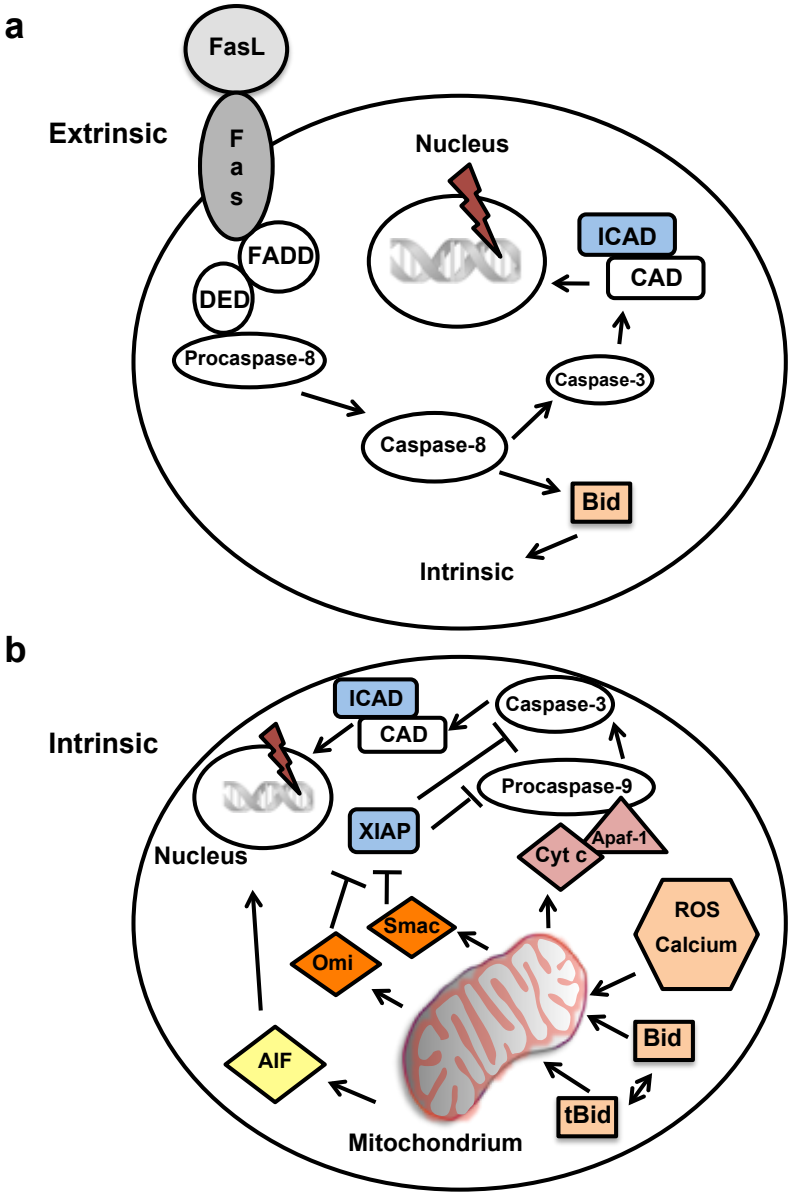

Figure 1: The intrinsic and the extrinsic pathways of apoptosis. (**a**) Extrinsic pathway: The death receptor Fas is activated by its ligand (FasL), inducing the binding of a Fas associated death domain (FADD). The death effector domain (DED) is bound to Pro-caspase-8 and these proteins can bind to the Fas-associated complex and thereby causing the activation of capase-8. Caspase-8 can directly activate caspase-3 thereby inducing the release of CAD (caspase-activated desoxyribonuclease) from its inhibitory ligand ICAD inducing CAD-mediated DNA cleavage. Alternatively, caspase-8 can cleave the pro-apoptotic protein Bid, which activates the intrinsic pathway of apoptosis that involves damage to mitochondria. (**b**) The cleaved Bid protein (tBid), increased calcium-levels or ROS induce mitochondrial membrane permeabilization causing the release of the mitochondrial proteins cytochrome c, Omi/HtrA2, Smac/DIABLO (Smac) or AIF. Cytochrome c forms a complex with Apaf-1 and pro-caspase-9, called the apoptosome. The apoptosome potentiates the activation of caspase-3. The x-chromosomal linked inhibitor of apoptosis (XIAP) is inhibited by the mitochondrial proteins Omi/HtrA2 and Smac, and consequently, caspase-3 and 9 are activated. When released from the mitochondria, AIF translocates to the nucleus where it induces DNA fragmentation.

Many different triggers have been described for induction of neuronal apoptosis, like activation of ionotropic glutamate receptors followed by toxic calcium influx (excitotoxicity), loss of ATP, withdrawal of neurotropic factors and oxidative stress [14-17]. In Parkinson's Disease, for instance, formation of ROS, mitochondrial dysfunction and activation of caspases are well-accepted mechanisms contributing to the degeneration of dopaminergic neurons [1, 18].

Glutamate-induced excitotoxicity is a major trigger of apoptotic pathways that mediate cell death in acute neuronal disorders like trauma or ischemic stroke. Ionotropic glutamate receptors like N-methyl-D-aspartate- (NMDA) receptors, 2-amino-3-(3-hydroxy-5-methylisoxazol-4-yl)proprionate (AMPA) receptors or kainate receptors are activated by high levels of extracellular glutamate leading to increased intracellular calcium levels and the formation of ROS. The forced ROS production is due to mitochondrial membrane leakage and the activation of caspases, nitric oxide synthases or calpains [13].
Excitotoxicity is a well-established cause of neuronal cell death inducing apoptosis or necrosis, depending on the strength of the insult, i.e. the concentration of glutamate over time, and particular conditions such as the availability of energy substrates and oxygen [19].
The comparison of different neurodegenerative diseases reveals, that apoptotic mechanisms are highly conserved, even though the initiating triggers may differ among these diseases [6]. Until today, only a few drugs are available for the treatment of neurodegenerative diseases such as Parkinson's Disease or Alzheimer's Disease. However, the effect of these merely symptomatic therapies is limited, as they do not slow down the progression of neuronal demise. Therefore, it is important to understand the mechanisms of neuronal apoptosis in order to reveal novel targets for causal therapies.

1.1.2. Oxidative stress as mediator of neuronal apoptosis

In the past reactive oxygen species (ROS) have frequently been linked to different neurodegenerative diseases like Parkinson's Disease and Alzheimer's Disease but

also to neuronal death after stroke [20, 21]. ROS include molecules of highly diverse structures like oxygen free radicals (for example superoxide radicals or hydroxyl radicals) and peroxides like hydrogen peroxide or lipid hydroperoxides. Under physiological conditions ROS at low levels are involved in signaling processes and function as mediators in different processes like cellular growth and adaptation responses [22].

In contrast, elevated concentrations of ROS can contribute to membrane damage and can alter DNA and unsaturated lipids as well as membrane proteins. ROS-induced changes in the cellular membranes cause decreased activity of membrane-bound ion channels, receptors and enzymes and thus influence membrane fluidity [23].

As described before ROS are important triggers of the intrinsic apoptotic pathway indicating the importance of ROS formation in neuronal damage. The excessive formation of ROS in neurons can be caused by different activators such as glutamate overload, β-amyloid-plaques [3, 14][24], oxygen-glucose deprivation and massive NO formation, among others [20, 25]. High levels of glutamate have been linked especially to excitotoxicity-induced ROS formation but it has been suggested that glutamate can also mediate oxidative stress independently of ionotropic glutamate receptors [26]. The mechanisms of glutamate-induced oxidative stress are not fully understood and, therefore, it is necessary to delineate neuronal glutamate toxicity in further detail.

In order to investigate the mechanisms of oxidative stress in neurons HT-22 cells were used as a model system. These cells are immortalized mouse hippocampal neurons that are sensitive to glutamate. Since HT-22 cells do not express ionotropic glutamate receptors, glutamate-induced cell death is not mediated by excitotoxicity, but by glutathione depletion. High extracellular glutamate concentrations block the glutamate-cystine-exchanger X_c-, which usually mediates the transport of cystine into the cells. Consequently, glutamate reduces intracellular cystine-levels thereby blocking glutathione (GSH) synthesis [27-29]. Glutathione serves as a radical scavenger that sequesters free radicals and oxidizing species. Thus, with declining levels of glutathione the formation of ROS within the HT-22 cells increases and concomitantly ROS-mediated damage of intracellular structures (i.e. lipid membranes, proteins and DNA) is induced. Furthermore, it has been shown that despite of the absence of NMDA-receptors, cytosolic calcium also contributes to cell

death in HT-22 cells as it increases with some delay in response to the glutamate challenge [30].

The increase in ROS and cytosolic calcium as well as the mitochondrial dysfunction are established key mediators of apoptosis, all of them detectable in cell death of HT-22 cells, rendering the model of glutamate toxicity in this cell line a valuable and applicable model for apoptosis induced by detrimental oxidative stress in neuronal cells. Thus, the underlying mechanisms of cell death in HT-22 cells challenged with millimolar concentrations of glutamate were termed oxytosis. However, the mechanisms of increased ROS formation and downstream oxytosis death pathways induced in the neuronal HT-22 cells required further investigation.

In addition, primary neuronal cultures were used to explore oxidative stress in neurons in further detail. These cells express ionotropic glutamate receptors and therefore glutamate toxicity is mediated by excitotoxic activation of NMDA receptors, characterized by increased intracellular calcium levels in addition to glutamate-induced GSH-depletion and formation of ROS.

1.2. The Bcl-2-proteins and mitochondria in neuronal cell death

The Bcl-2 proteins are a family of pro- and anti-apoptotic B-cell lymphoma-2 (Bcl-2) proteins. These proteins are key mediators of mitochondrial damage and cell death [31]. All members of the Bcl-2 family share a close homology in characteristic regions named the BH (Bcl-2 homology) domains. To date, 4 BH domains have been identified (BH -1-4) [32]. It is important to note that some of the Bcl-2 proteins mediate apoptosis (e.g. Bax, Bak, Bad, Bim, Bid) and others prevent apoptotic mechanisms by interaction with the pro-apoptotic representatives (e.g. Bcl-2, Bcl-xl, Bcl-w). Bcl-2 and Bcl-xl, for instance, can prevent the pro-apoptotic function of Bax by the formation of heterodimer complexes with the pro-apoptotic protein [33].

Bad, Bid, Bik/NBK, Bim/Bod, Bmf, Hrk/DP5, Noxa and Puma/BBC3 share only the BH-3 region with the other members of the protein family and therefore are named BH-3-only proteins. These proteins are exclusively pro-apoptotic and once activated they mediate cell death. Interestingly, the BH-3-only proteins require Bak or Bax to

mediate mitochondrial demise and cell death, proposing signaling network interactions between the pro-apoptotic Bcl-2 proteins.

For example, the pro-apoptotic BH-3-only protein Bid and its truncated form tBid are involved in different pro-apoptotic pathways. The activation of tBid can induce the release of Bax from the Bcl-xl/Bax heterodimers. Furthermore, in the presence of activated Bid, Bax and Bak form a pore in the mitochondrial membrane and thereby allow the release of pro-apoptotic factors like AIF or cytochrome c [31, 34]

As described before cleavage of the Bid protein is necessary for the activation of the intrinsic apoptotic pathway pointing out again the central role of the Bid protein [35, 36]. Pharmacological Bid inhibitors and genetic Bid deletion provided protective effects in different models of neuronal cell death. For example, Bid knockout mice showed less neuronal damage after trauma compared to wild type mice [37] and Bid-deficient neurons were protected against oxygen glucose deprivation (OGD) and cerebral ischemia [38, 39]. Further, Bid activation has been supposed to be involved in glutamate-induced oxidative stress [26] and after cerebral ischemia and death receptor signaling [38, 40].

Several studies have suggested that the inactive full-length Bid is located in the cytosol and that cleavage of Bid is necessary for its activation and its pro-apoptotic function [41]. Caspase-8 is the most prominent activator of Bid mediating Bid cleavage e.g. after stimulation of TNF- or Fas- receptors. Caspase-8 activity was also found enhanced after OGD and also after cerebral ischemia in rodents [42, 43]. In addition, Bid can be cleaved by caspase-1 and also by caspase-2. This has been shown in models of ischemia and hypoxia for caspase-1 [49].

In addition to caspases also calpains and lysosomal hydrolases are able to cleave the Bid protein. Calpains are calcium-activated proteolytic enzymes that metabolize protein kinases and phosphatases as well as cytoskeletal proteins and transport proteins among others [44, 45].

Taken together, high levels of intracellular calcium resulting from glutamate-induced excitotoxicity can activate calpains and thereby mediate apoptosis. Once activated, calpains may cause mitochondrial damage via Bid cleavage and Bid transactivation to mitochondria and the subsequent release of pro-apoptotic proteins like AIF or cytochrome c [31, 46]. In models of acute brain damage like transient forebrain

ischemia or traumatic brain injury calpain inhibitors significantly reduced neuronal cell death indicating that calpain activation mediates acute brain injury [47, 48].
Interestingly, it is known that also full-length Bid can translocate to the mitochondria and induce loss of mitochondrial membrane potential and DNA-damage in glutamate-induced neurotoxicity [50]. In a model of epithelial cells, for example, full-length Bid mediated apoptosis without being cleaved in advance [51]. In the model of HT-22 cells Bid cleavage was hardly detectable after glutamate treatment indicating that full-length Bid translocates to the mitochondria whereas only a small amount of Bid may be cleaved in HT-22 cells [52].
Overall, not only tBid but also full length Bid seem to be key mediators of apoptotic neuronal cell death. Therefore, the investigation of exact mechanisms induced by Bid and tBid is very important for further analysis of neurodegenerative processes.

It became obvious that Bcl-2 proteins are linked to intrinsic pathways of programmed cell death mediating their pro-apoptotic function through mitochondrial damage.
Mitochondria are essential organelles since they produce the main part of energy in the cells through ATP synthesis. On the other hand, mitochondria exhibit a crucial role in apoptotic mechanisms because they generate large amounts of ROS [53] and contain proteins like cytochrome c, AIF or Smac/DIABLO, which induce neuronal cell death once they are released from the mitochondria [53, 54].
Thus, mitochondria are the central cellular organelles mediating the intrinsic apoptosis pathway that can be activated by different stimuli like for example increased calcium levels, pro-apoptotic Bcl-2 family members or reactive oxygen species [55].
Mitochondria produce ATP by electron transfer from one complex of the respiratory enzymes to the next and finally to oxygen. At the same time protons are transported across the mitochondrial inner membrane creating a proton gradient, whose potential is the driving force of ATP synthesis, and an increase of the mitochondrial membrane potential. Since molecular oxygen and electrons are continuously processed in mitochondria, the potential role of mitochondria as a source and a target of reactive oxygen species becomes obvious.

Mitochondrial demise can be caused by several triggers including the disturbance of detoxifying mechanisms like GSH, glutathione peroxidase, superoxide dismutase (SOD) or catalase and also by high intracellular calcium levels (10-100 µM) [56].
Increases in intracellular calcium occur after activation of glutamate receptors and by its release from intracellular stores like the endoplasmatic reticulum (ER).
The pro-apoptotic members of the Bcl-2 protein family represent another potential trigger of mitochondrial membrane permeabilization [57]. As mentioned before the pro-apoptotic Bcl-2 family members Bax and Bak, for instance, may form a pore and thereby induce mitochondrial permeabilization and the release of pro-apoptotic proteins like AIF or cytochrome c [31, 58]. In addition, the pro-apoptotic Bcl-2 family protein Bid induces the intrinsic apoptotic pathway that involves mitochondrial membrane permeabilization thereby releasing pro-apoptotic factors from mitochondria that amplify apoptosis by caspase-dependent and caspase-independent mechanisms.
Mitochondria are dynamic organelles that continuously undergo fission (fragmentation) and fusion processes that are important for mitochondrial biogenesis, repair and for redistribution of mitochondria to parts where high amounts of energy are needed [59-61]. A disturbed balance of fission and fusion has recently been characterized as an important contributor to mitochondrial dysfunction and cellular death [61-63].
Neurons require high levels of energy for which reason they are densely packed with ATP-synthesizing mitochondria. Consequently, disturbed mitochondrial function significantly affects neuronal function and survival. Under physiological conditions several proteins regulate mitochondrial fusion and fission processes, like Drp-1, Fis-1, Opa1 or mitofusins. Opa1 and mitofusin-1 and -2 (Mfn-1/-2) act as fusion proteins whereas Drp1 and Fis1 mediate mitochondrial fission [64]. Dysfunctions in the fission-fusion machinery have been linked to several neurodegenerative diseases, like Alzheimer's Disease or Parkinson's Disease [63, 65, 66]. Consequently, fusion and fission proteins like Drp-1 are interesting targets for the therapy of neurodegenerative diseases and are currently explored in several scientific studies.
Overall, it has been well established that activated Bcl-2 proteins and subsequent mitochondrial damage are important mediators of neuronal cell death but still the detailed mechanisms are not fully understood. Consequently, this thesis

investigated the activation of pro-apoptotic Bcl-2 proteins and focused on upstream mechanisms of mitochondrial demise as well as on mitochondrial death pathways in neuronal cells in order to identify new therapeutic targets to prevent neuronal degeneration and death.

1.3. Lipoxygenases in the brain

Free membrane phospholipids like arachidonic acid (AA) and docosahexaenoic acid (DHA) can be oxidized in an enzymatic or non-enzymatic way to various oxygenated products, which mediate important functions in neuronal cells. The collective name for these metabolites is eicosanoids.

Arachidonic acid is released from phosphatidylcholine by the cytosolic phospholipase A_2 ($cPLA_2$) and DHA is released mainly by the plasmalogen-selective phospholipase A_2 (PlsEtn- PLA_2) [22, 67]. Enzymes like cyclooxygenases (COX), lipoxygenases (LOX) or epoxygenases (EPOX) metabolize AA and induce the formation of prostaglandins, thromboxanes, leukotrienes or epoxyeicosatrienoic acid, respectively. Eicosanoids are important effectors of signal transduction, gene transcription and inflammatory processes [22]. Neurons as well as astrocytes, cerebral vascular endothelial cells, and cerebrospinal fluid contain plenty of eicosanoids [22].

Under physiological conditions leukotrienes and prostaglandins can, for instance, modulate glutamate receptors, thereby mediating the communication between prostaglandin-, leukotriene-, thromboxane- and glutamate receptors. Under pathological situations this crosstalk is disturbed and mediates neuronal damage that depends on the level of COX and LOX [22, 68].

Prostaglandins and related eicosanoids are neuroprotective at nanomolar concentrations, which has been shown for example for PGE_2 in hippocampal neurons in models of excitotoxicity and oxygen glucose deprivation [69]. However, micromolar and millimolar concentrations of PGE_2, as occurring under pathological conditions cause neuronal damage [70].

COX and LOX metabolize DHA to resolvins, docosatrienes and neuroprotectins [22]. Docosanoids is the collective name of these metabolites that antagonize the effect of eicosanoids and can also regulate the expression of cytokines by modulating the function of leukocytes [71, 72]. Different isoforms of COX, LOX and PLA_2 are expressed in neuronal and in non-neuronal tissues [22] where they are involved in inflammatory processes, aging, apoptosis and synaptic activity in the brain [22].

In addition, it is known that disruption of the arachidonic acid (AA) cascade leads to increased production of ROS and hence oxidative damage of membrane proteins, receptors and ion channels. The activation of cyclooxygenases (COX), phospholipase A_2 (PLA_2) and lipoxygenases (LOX) is a potential trigger of enzymatic dysregulation of the AA pathway [73-75]. Further, it has been suggested that activation of COX, PLA_2 and LOX occurs in different neuronal disorders for example after glutamate challenge suggesting a link between glutamate-induced oxidative stress and disruption of the AA cascade [22, 76].

On the other hand, ROS generated by these enzymes leads to further non-enzymatic peroxidation of arachidonic acid and of docosahexaenoic acid (DHA), which is known to cause formation of 4-hydroxynonenal (4-HNE). This and other reactive aldehydes can accelerate neuronal cell death through their ability to modify biomolecules [76, 77][78, 79].

However, the potential role of a disturbed AA cascade in neurodegeneration is still unknown. For this reason this thesis analyzed the role of COX and LOX in neuronal oxytosis in further detail in order to explore the detailed mechanisms of formation and consequences of oxidative stress in glutamate-induced neurotoxicity.

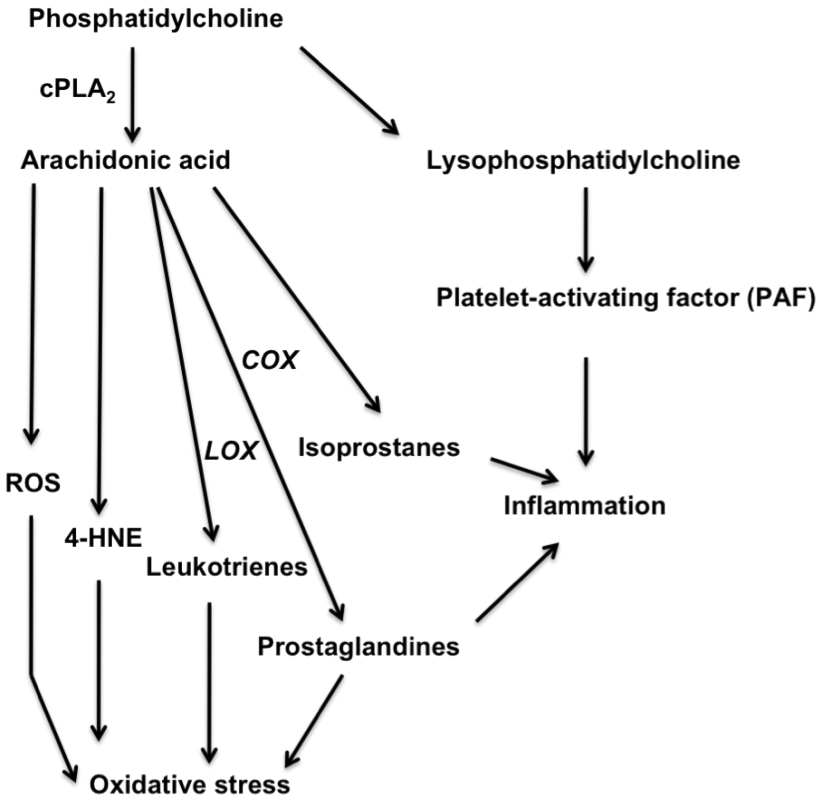

Figure 2: The arachidonic acid metabolism leading to oxidative stress (modified from Phillis et al, 2006). Phosphatidylcholine is metabolized by cytosolic phospholipase A_2 ($cPLA_2$) to arachidonic acid (AA). AA can be metabolized by different enzymes such as cyclooxygenase (COX) or lipoxygenases (LOX). Alternatively, AA is metabolized non-enzymatically and forms toxic aldehydes such as 4-hydroxynonenal (4-HNE). The metabolites can induce inflammation and oxidative stress causing the formation of reactive oxygen species (ROS). In addition, the enzymes have an executionary role in the induction of oxidative stress forming ROS by metabolizing their substrates.

Lipoxygenases are iron-containing dioxygenases, which can insert molecular oxygen into AA. They have a molecular mass of 75 to 78 kDa and consist of one polypeptide chain that is folded into two domains [80, 81]. Lipoxygenases are named by the position at which they oxidize AA and by the stereo-configuration of their resulting products [82]. Three different forms of LOX can be found in the brain: 5-LOX, 12-LOX and 15-LOX and 12-LOX was found to be the most common in neuronal tissues [83].

12-LOX was studied most intensively in rat brain where it generates mainly 12-hydroxyeicosatetraenoic acid (12-HETE) and to some degree 15-HETE [84]. It has been postulated that 12-LOX consists of at least two isoforms, which show different properties regarding substrate specificity, immunological properties and catalytic activity. These two isoforms are often referred to as ‘leukocyte-type’ and ‘platelet-type’ 12-LOX named according to their first time discovery in porcine or bovine

leukocytes and human or bovine platelets, respectively [84, 85]. 'Leukocyte-type 12-LOX' is the isoform expressed and studied in neurons and is often referred to as 12/15-LOX because it generates mainly 12-hydroxyeicosatetraenoic acid (12-HETE) and to some degree 15-HETE [84, 85]. Murine 12/15-LOX has the highest degree of identity with the human 15-LOX showing that the murine 12/15-LOX is a suitable model to study the role of lipoxygenases in neurodegeneration [84].

Previous studies on the role of LOX in the brain suggested that LOX and their products are modulators of synaptic function in the nervous system. These studies focused on the role of neuronal 12-LOX (12/15-LOX) and concluded that 12/15-LOX metabolites might influence long-term-potentiation (LTP) and long-term-depression (LTD) in the hippocampus. For example, 12-HETE and 12-hydroperoxyeicosatetraenoic acid (12-HPETE) both mediated K^+-stimulated glutamate release from synaptosomes in the hippocampus [86]. Furthermore, glutamate induced the formation of 12-HETE in cerebral cortical slices [87]. Others analyzed the role of the 12/15-LOX pathway for the induction of LTD and LTP in the brain in further detail and concluded that 12/15-LOX activation is required for induction of LTD but not for LTP after the activation of metabotropic-glutamate-receptor [88]. These previous results suggested that 12(s)-HPETE is a potential messenger molecule that is involved in the induction of metabotropic glutamate-receptor dependent LTD thereby demonstrating an important role of LOX for physiological neuronal functions in the brain. Taken together, 12/15-LOX have been shown to mediate physiological as well as pathological functions in the brain but there is still not much known about the role of 12/15-LOX in oxidative-stress induced apoptosis.

In addition, some studies analyzed the role of 5-LOX in the brain. For instance, it has been shown that 5-LOX is present in the cytosol of neuronal cells and can translocate to the nuclear envelope. Further studies suggested a link between the expression of glucocorticoids and the stability of 5-LOX in the brain and postulated an interaction of 5-LOX with the growth-factor-receptor-bound-protein 2 (Grb2) [89-91]. The activation of 5-LOX has also been linked to anxiety- and depression-like behaviors [92] indicating a link of 5-LOX and their metabolites to neurotransmitter signaling in the brain. The role of 5-LOX in acute brain damage has also been investigated using 5-LOX knockout mice in a model of focal cerebral ischemia

showing that 5-LOX activation does not mediate neuronal damage after ischemic brain injury [93]. Even though these results suggested different neuronal functions of 5-LOX the role of 5-LOX in neuronal oxytosis has not been investigated.

The induction of excitotoxicity is known to play a key role in neuronal cell death and induces the metabolism of arachidonic acid and thereby the activation of several enzymes such as LOX, COX, EPOX and PLA_2 [94-96]. In accordance with this notion, levels of COX-2 and 5-LOX increase in rat brains after kainate injections [97], which can be significantly reduced by COX- and 5-LOX inhibitors [98, 99]. In addition, COX-1 activation contributes to prostaglandin synthesis and ROS production in models of excitotoxicity [100].
These previous studies suggested that the metabolism of AA and DHA is important in neurodegeneration and that COX and LOX are key mediators of oxidative stress in neurons but the detailed mechanisms are still unknown. Consequently, a more detailed understanding of COX- and LOX-mediated processes in the brain is necessary and therefore part of this thesis.

1.4. NO-toxicity in neurodegeneration

Different isoforms of nitric oxide synthase (NOS) produce nitric oxide (NO) from L-arginine. NO is an important messenger and mediates different physiologic actions. It is a neurotransmitter, neuromodulator and also mediates blood vessel dilation. However, NO can also form highly reactive and toxic molecules that can react with DNA, lipids or proteins and can change their function and thereby cause cellular damage [101]. In fact, several studies have implicated NO as a key molecule in neurodegeneration for example in Alzheimer's Disease, Parkinson's Disease, Huntington's Disease or stroke [102-105].
NOS have been identified in all brain cells, in neurons as well as in glia cells [106, 107]. Three different isoforms have been pointed out: neuronal NOS (nNOS), inducible NOS (iNOS) and endothelial NOS (eNOS). All three NOS isoforms are expressed in different cell types under different conditions [107]. In addition, a mitochondrial NOS (mtNOS) has been suggested [108] but not analyzed in detail.

Neuronal NOS is expressed predominantly in neurons, where NO is a key mediator of cell communication [107]. In the endothelial tissue of blood vessels eNOS is the highest expressed NOS and mediates mainly the relaxation of smooth muscles. Pathogen recognition and cytokine release activate iNOS that is expressed predominantly in immune cells [109] but also in astrocytes and microglia [107], where the produced NO is used to defeat pathogens and to mediate the immune-like activities of glia cells [107].

NO has the ability to modify cysteine residues of proteins what is also referred to as S-nitrosylation. The S-nitrosylated proteins may enhance neuronal survival. S-nitrosylation of NMDA receptors (N-methyl-D-aspartate receptors), for example, “inactivates” the receptors and therefore inhibits excitotoxicity [110-112]. Caspases are also inactivated by S-nitrosylation suggesting that NO-toxicity is not predominantly involved in caspase-dependent apoptosis.

As discussed before, the ability of NO to nitrosylate proteins can mediate cellular survival but on the other hand nitrosylation of special proteins induces cell death.

Additionally, the formation of reactive nitrogen species by reacting with oxygen is an important pathologic function of NO.

A special form of nitrosylation is the 3-nitrotyrosination. When NO reacts with O_2^-, $ONOO^-$ is formed, which can react with proteins, especially with tyrosine residues. The subsequent change in protein function can mediate cellular death.

Moreover, NO interferes with excitotoxicity, as mentioned earlier, and thereby can mediate neuroprotective effects. The protective effect of NO by blocking NMDA receptors depends on the formation of NO^+ (nitrosium ion) [101] that S-nitrosylates the NMDA-receptor and thereby blocks Ca^{2+} influx and promotes cell survival. On the other hand it is important to note that NO may also mediate excitotoxicity under certain conditions [113, 114]. Interestingly, developmental differences seem to control if NO mediates neuronal death or neuronal survival. It has been shown, for example, that NO mediates neuronal survival in immature hippocampal neurons but did not protect mature neurons against NMDA toxicity [115]. How the cells regulate the NOS activity in different developmental periods is not yet defined.

Further, previous studies suggested a link of NO and $ONOO^-$ to the mitochondrial respiratory chain showing that NO and $ONOO^-$ can inhibit complex IV [116-118] and that $ONOO^-$ can inhibit complex I in isolated brain mitochondria [119-121].

An additional mechanism of NO toxicity may be accelerated fission of mitochondria [62]. Several studies have shown that a shift in the fusion/fission balance towards fission can induce neuronal cell death [63, 122] and it has been discussed that NO regulates Drp-1 or mitofusins and therefore mitochondrial dynamics [123, 124].
Moreover, others have postulated a role of Zn^{2+} in NO-induced cell death. Under normal conditions Zn^{2+} is bound to high-affinity ligands, like metallothionein or Zn^{2+} finger-binding proteins but nitrosative stress and even oxidative stress may induce the liberation of high amounts of Zn^{2+} from its stores thereby mediating neuronal cell death [125-127]. In addition, it has been shown that Zn^{2+} increased in the brain after ischemia or trauma showing the role of Zn^{2+} in neurodegeneration.
In summary, these studies showed that misguided NO formation mediate neuronal cell death and postulated several different pathways for NO-mediated toxicity. Therefore, this thesis analyzed the role of NO toxicity in HT-22 cells on order to investigate the role of NO formation in neuronal oxytosis.

1.5. Aims of the thesis

The mechanisms of oxidative stress in neuronal cell death have been matter of intense research in the last couple of years, but still the main trigger of ROS formation and key mediators of downstream cell death signaling remain poorly defined.
In particular, the role of a disturbed arachidonic acid cascade in neurodegeneration has been discussed before [128-130] however, the detailed pathways remain unclear. Furthermore, the Bcl-2 proteins and mitochondria have been investigated precisely in order to explore their functions in neuronal and non-neuronal cells [2, 13, 26, 31-33, 131, 132] but up to now the involved pro-apoptotic pathways are still a matter of debate. The potential link between the disturbed arachidonic acid cascade, the activation of pro-apoptotic Bcl-2 proteins and mitochondrial demise after induction of oxidative stress have not been explored.
Therefore, the investigation of the connection between these important mechanisms of intrinsic pathways of apoptosis was a major aim of this thesis, in order to identify

upstream triggers of oxytosis and downstream regulators of neuronal death that may serve as novel targets for neuroprotective strategies.

Previous studies suggested a major role of 12/15-lipoxygenases in neurons [129, 133, 134] but did not investigate the potential link to other important mediators of programmed cell death.

Moreover, it was the aim of this study to expand the knowledge of LOX in neurodegeneration. This thesis focused especially on the role of 12/15-LOX in oxidative stress-induced neuronal cell death and analyzed the link of 12/15-LOX activation to upstream as well as to downstream mechanisms.

To elucidate the particular role of 12/15-LOX the selective inhibitors PD146176 and AA861 were applied during the experiments. To verify the results gained from experiments relying on the use of inhibitors, 12/15-LOX knockout mice were used and the experiments were also expanded to applications in a model of MCAO in mice to verify the relevance of these findings in vivo.

.

2. Materials and methods

2.1. Chemicals and reagents

All standard chemicals, were obtained from Sigma-Aldrich (Taufkirchen, Germany) and Carl Roth (Karlsruhe, Germany), if not described otherwise.
All buffers and solutions were prepared using demineralized, ultrapure water that was prepared with the SG Ultra Clear UV plus Reinstwassersystem (VWR, Darmstadt, Germany).
For media and solutions that were used in the cell culture the ultrapure, demineralized water was sterilized using a steam autoclave (Systec V-40, Systec GmbH, Wettenberg, Germany).

All media and solutions that were used in the cell culture were sterilized by filtration using 0.22 µM filter sets (Sarstedt, Nürnbrecht, Germany).

2.2. Cell culture materials

Sterile plastic materials for the cell culture were purchased from Greiner (T75 flasks, 6- and 24- well plates, 96- well plates; Frickenhausen, Germany) and Sarstedt (35-mm, 60-mm culture dishes, falcon tubes; Nümbrecht, Germany). The E-plates for the impedance measurements were obtained from Roche, Applied Science (Penzberg, Germany) and the xCELLigence-System was also provided by Roche, Applied Science (Penzberg, Germany).

2.3. Methods

2.3.1. Cell culture and viability assays

2.3.1.1. Cell culture

HT-22 cells were cultured in Dulbecco's modified Eagle medium (DMEM, Invitrogen, Karlsruhe, Germany) supplemented with 10% heat-inactivated fetal calf serum (PAA, Pasching, Austria), 100 U/mL penicillin, 100 µg/mL streptomycin (PAA, Pasching, Austria) and 2 mM stable glutamine (PAA, Pasching, Austria).
The LOX inhibitors PD146176 and AA861 (Sigma-Aldrich, Taufkirchen, Germany) were dissolved in dimethylsulfoxid (DMSO, Sigma-Aldrich, Taufkirchen, Germany). PD146176 was diluted to a concentration of 50 mM and AA861 to a concentration of 10 mM. The stock solutions were stored at -20 °C and diluted with cell culture medium prior to each experiment up to final concentrations of 0.5 µM PD146176 and 0.1 µM AA861.
As the selectivity of AA861 was repeatedly challenged by reports claiming a cross inhibition of 5-LOX, this thesis predominantly focused on PD146176 for most of the experiments.

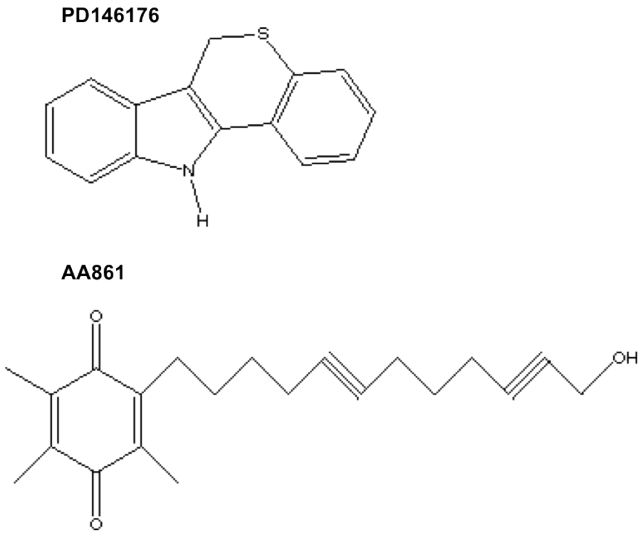

Figure 3: The LOX inhibitors PD146176 and AA861 were used to analyze the role of 12/15-LOX in ROS-induced neuronal cell death. It has been discussed that AA861 also inhibits 5-LOX and is not selective for 12/15-LOX therefore PD146176 was used for most of the experiments in this thesis.

Diphenyleneiodonium chloride (DPI, Enzo Life Science, Lörrach, Germany) was dissolved in DMSO to a concentration of 15.9 mM. This stock solution was stored at -20 °C) diluted with DMEM medium to a concentration of 0.1 μM before each experiment.

The 5-LOX inhibitors YS121 and C06 [135, 136] (kind gift of Prof. Dr. Steinhilber, Frankfurt, Germany) were dissolved in DMSO to prepare stock solutions and diluted with DMEM or EBSS immediately before the experiments. The stock solutions had a concentration of 5 mM and were stored at – 20 °C. YS121 was diluted to final concentrations of 0.41 μM and 4.1 μM with DMEM and C06 was used in final concentrations of 0.065 μM and 0.65 μM.

A glutamate stock solution was prepared at a concentration of 100 mM by solving DL-glutamic acid monohydrate (Sigma-Aldrich, Taufkirchen, Germany) in DMEM. The stock solution was stored at -20 °C and diluted with DMEM to concentrations of 2 - 5 mM immediately before use. These glutamate solutions were used to treat the cells and cell viability was evaluated 12 - 18 h later.

For treatment with hydrogen peroxide (H_2O_2, Sigma-Aldrich, Taufkirchen, Germany) H_2O_2 (stock with a concentration of 30%) was diluted with DMEM to concentrations of 500 – 700 μM. The solutions were always prepared immediately before use.

Sodium nitroprusside (Sigma-Aldrich, Taufkirchen, Germany) was dissolved in DMEM immediately before the treatment of the cells and diluted to concentrations of 20 – 400 μM.

Glucose oxidase (Sigma-Aldrich, Taufkirchen, Germany) has been used to achieve a continuous production of H_2O_2. For treating the cells glucose oxidase was dissolved in sodium acetate solution (50 mM, pH 5.1, Merck, Darmstadt, Germany) and diluted to concentrations of 10 – 20 mU.

DEANONOate (Enzo Life Science, Lörrach, Germany) was dissolved in Ethanol 96% (Sigma-Aldrich, Taufkirchen, Germany) to a concentration of 100 mM and stored at -20 °C for at most 1 week. This stock solution was diluted to concentrations of 500 μM – 2 mM in DMEM immediately before the treatment.

For induction of oxidative stress through Fe^{2+} toxicity iron (II) sulfate heptahydrate (Sigma-Aldrich, Taufkirchen, Germany) was dissolved in DMEM to concentrations of 2 mM, 5 mM and 7.5 mM. The Fe(II) salt solutions were prepared immediately before the treatment.

The eNOS and nNOS inhibitor Nω-Nitro-L-arginine (L-NNA, Sigma-Aldrich, Taufkirchen, Germany) was dissolved in 1M hydrochloric acid (HCl, Sigma-Aldrich, Taufkirchen, Germany) and diluted to concentrations up to 1 mM with DMEM.
The antioxidant N-acetyl-L-cysteine (NAC, Sigma-Aldrich, Taufkirchen, Germany) was dissolved in DMEM to concentrations of 5 – 20 mM. The solutions were prepared freshly before use and the pH was adjusted to 7.2 by addition of sodium hydroxide solution (NaOH, Sigma-Aldrich, Taufkirchen, Germany). It is important to note that NAC reacts with MTT (see below) and has to be washed away before the evaluation of cell viability using the MTT assay.
L-ascorbic acid (Sigma-Aldrich, Taufkirchen, Germany) was dissolved in DMEM to obtain solutions of 0.5 and 1 mM. The solutions were prepared immediately before the experiments
The calcium chelator ethylenediaminetetraacetic acid (EDTA, Sigma-Aldrich, Taufkirchen, Germany) was dissolved in water to obtain a stock solution and used in final concentrations of 200 μM to 1 mM. 1,2-Bis(2-Aminophenoxy)ethane-*N,N,N′,N′*-tetraacetic acid (BAPTA-AM, Sigma-Aldrich, Taufkirchen, Germany) was dissolved in DMSO to obtain a stock solution at a concentration of 10 mM and used at final concentrations of 10 and 20 μM.
The mitochondrial complex I inhibitor rotenone (Sigma-Aldrich, Taufkirchen, Germany) was added in final concentrations of 10 – 100 μM in DMEM. A stock solution of rotenone (100 mM in DMSO) was prepared and stored at -20 °C.
4-Hydroxynonenal-dimethylacetal, (HNE, Sigma-Aldrich, Taufkirchen, Germany) was dissolved in 1 mM cold HCl according to the manufacturer's protocol and diluted to concentrations of 5 – 30 μM with DMEM.
In order to analyze the toxicity of the used solvents of the different inhibitor, the cells were treated with medium containing the highest concentration of the solvent, which may be present during the experiment.

2.3.1.2. Cell viability assays

Quantification of cell viability in HT-22 cells was performed in 96-well plates by 3-(4,5-Dimethylthiazol-2-yl)-2,5-diphenyltetrazolium bromide (MTT) reduction at 0.25

mg/ml for 1.5 h at 37 °C. The reaction was terminated by removing the media and freezing the plate at -80 °C for at least 1 h. Absorbance was then determined after solving MTT dye in DMSO at 570 nm versus 630 nm (FluoStar, BMG Labtech, Offenburg, Germany).

In addition, real time detection of cellular viability was performed by measurements of cellular impedance by using the xCELLigence system (Roche Applied Science, Penzberg, Germany). The HT-22 cells were seeded in 96 well E-plates (Roche, Applied Science, Penzberg, Germany) whose well bottoms are covered with gold electrodes. The presence of the cells on top of the electrodes induces an increase in the impedance. The more cells are attached on the electrodes, the larger the increases in impedance. The system allows to calculate the so-called “cell index” that increases when the cells attach to the electrodes. Thus, the Roche xCELLigence system detects cellular growth, cellular survival and death, and especially the kinetics of these processes during the experiments. The results are presented as a curve showing the cell index as a function of time. It is important to note that the system is very sensitive to changes in temperature and, therefore, the medium was never removed completely for treatments to prevent a persistent breakdown of the impedance [*Real-time detection of neuronal cell death by impedance-based analysis using the xCELLigence System.*; Sebastian Diemert, Julia Grohm, Svenja Tobaben, Amalia Dolga, Carsten Culmsee, Application note for Roche Applied Science, 2010 Aug]

For annexin-V/propidium iodide-staining, HT-22 cells were cultured in 24-well plates and challenged with glutamate (3 and 5mM). The cells were harvested 12-15 hours after the onset of the glutamate treatment by using Trypsin/EDTA, washed once in PBS and resuspended in binding buffer (PromoKine, Heidelberg, Germany). Then 1 µl/100 µl of propidium iodide and annexin-V-FITC solutions (PromoKine Annexin V-FITC Detection Kit) were added respectively, and incubated for 5 minutes at room temperature. Apoptotic and necrotic cells were detected using a FACScan (Becton, Dickinson and Company, Heidelberg, Germany). Annexin-V and propidium iodode fluorescence were exited at a wavelength of 488 nm. Emissions were detected at 530±40 nm for annexin-V and at 680±30 nm for propidium iodide of 10000 cells per sample.

2.3.2. Embryonic cortical cultures

Cortices were removed from embryonic day 16 Sprague-Dawley rats (Janvier, Le Genest St Isle, France), wild type or Alox15-mice (Jackson Laboratory, Bar Harbor, Maine, USA) and dissociated by trypsinization and trituation as followed: Isolated cortices were incubated in Hank's balanced salt solution (HBSS, diluted from 10x HBSS, Invitrogen, Karlsruhe, Germany) containing 1 mg/ml trypsin (Sigma-Aldrich, Taufkirchen, Germany) for 15 minutes at 37°C. The cortices were then washed with HBSS and mixed with HBSS containing 1 mg/ml trypsin inhibitor (Sigma-Aldrich, Taufkirchen, Germany) and the cell suspension was incubated for further 2 minutes at room temperature. Afterwards, the cortices were washed two times with HBSS, and triturated in MEM+ obtained from Eagle's minimum essential medium (Invitrogen, Germany) by addition of 1 mM HEPES (Biomol, Hamburg, Germany), 26 mM $NaHCO_3$, 40 mM glucose, 20 mM KCl, 1.2 mM L-glutamine (each Sigma-Aldrich, Taufkirchen, Germany), 1 mM sodium pyruvate (Biochrom, Berlin, Germany), 10% (v/v) fetal calf serum (FCS) (Invitrogen, Karlsruhe, Germany) and 10 mg/l gentamicin sulfate (Sigma-Aldrich, Taufkirchen, Germany).

Cells were seeded in 35-mm culture dishes coated with polyethylenimine (Sigma-Aldrich, Taufkirchen, Germany). After 4 hours the MEM+ was replaced by Neurobasal medium (Invitrogen, Karlsruhe, Germany).

Cells were treated 6 days after preparation with 20 µM of glutamate in Earl's balance salt solution (EBSS, diluted from 10 x EBSS, add 2.2 g/l Sodium hydrocarbonate, both Sigma-Aldrich, Taufkirchen, Germany). Before adding glutamate the cells were washed once with EBSS in order to completely remove the Neurobasal medium.

After 18 to 24 hours the neurons were fixed with paraformaldehyde (4 % in PBS, Sigma-Aldrich, Taufkirchen, Germany) and stained with the fluorescent DNA-binding dye 4', 6-diamidino-2-phenylindole dihydrochloride (DAPI) (Sigma-Aldrich, Taufkirchen, Germany). The percentage of pyknotic nuclei was quantified from pictures obtained with a fluorescence microscope (DMI 6000 B, Leica, Wetzlar, Germany) connected to a CCD camera (DFC 360 FX, Leica, Wetzlar, Germany) without knowledge of the treatment history. For this quantification, at least 200 cells

were analyzed from 5 areas per cell culture dish, and experiments were performed at least 3 times with n=5 per treatment condition.

2.3.3. Plasmids and gene transfer

Plasmid pCDNA 3.1+ was obtained from Invitrogen (Karlsruhe, Germany). The tBid vector and control vectors were generated as previously described [137]. The mitoGFP vector was a kind gift from Andreas Reichert (Frankfurt, Germany). For plasmid transfections 8 x 10^4 HT-22 cells were seeded in 24-well plates. Antibiotic containing growth medium was removed and replaced with 900 µl antibiotic-free growth medium. Lipofectamine 2000 (Invitrogen, Karlsruhe, Germany) and ptBID plasmid, mitoGFP plasmid or empty vector pCDNA 3.1+ were dissolved separately in Optimem I (Invitrogen, Karlsruhe, Germany). The Lipofectamine 2000 solution was vortexed for 2 min. After 10 min of incubation at room temperature each DNA solution was combined with the respective volume of the Lipofectamine solution, mixed gently, and allowed to form DNA plasmid liposomes for further 20 min at room temperature. The liposome transfection mixture was added to the antibiotic-free cell culture medium to a final concentration of 1µg DNA, and 1.5 µl/ml Lipofectamine 2000 in HT-22 cells. Controls were treated with 100 µl/ml Optimem only, and vehicle controls with 1.5 µl/ml Lipofectamine 2000.

2.3.4. Detection of oxidative stress

Intracellular reactive oxygen species (ROS) were detected by dichlorodihydrofluoresceine-diacetate (DCF, Invitrogen, Karlsruhe, Germany). Within 6 - 17 h after glutamate treatment HT-22 cells were loaded with 1 µM CM-DCF (Invitrogen, Karlsruhe, Germany) for 30 min and DCF fluorescence was monitored using a CyanTM MLE flow cytometer (DakoCytomation, Copenhagen, Denmark) at an excitation wavelength of 488 nm and an emission wavelength of 530 nm.

For detection of cellular lipid peroxidation, cells were loaded with 2 µM BODIPY 581/591 C11 (Invitrogen, Karlsruhe, Germany) for 60 min in standard medium 6 – 17 h after glutamate treatment. The supernatants were collected in order to include also the already detached cells into the measurements. The attached cells were collected after incubating with 1x Trypsin-EDTA (TE) for 3 minutes. After detaching of the HT-22 neurons TE reaction was stopped by adding 1000 µl serum-containing medium to each well, the cells were collected, and transferred to their respective supernatant. Cells were then centrifuged at 1000 rpm, supernatants were removed, the pellets washed once in PBS, centrifuged and resuspended in 500 µl PBS and then kept on ice until the measurement. Flow cytometry was performed using 488 nm UV line argon laser for excitation and BODIPY emission was recorded on channels FL1 at 530 nm (green) and FL2 at 585 nm (red). Data were collected from at least 20000 cells per treatment condition. Lipid peroxides induce a shift from red to green fluorescence that can be detected by flow cytometry (Becton, Dickinson and Company, Heidelberg, Germany).

2.3.5. Detection of the mitochondrial membrane potential

To detect the mitochondrial membrane potential in HT-22 cells the MitoProbe™ JC-1 Assay Kit - for flow cytometry was used (Invitrogen, Karlsruhe, Deutschland). This assay contains 5, 5', 6, 6'- tetrachloro-1, 1', 3, 3'-tetraethyl-benzimidazolyl-carbocyanine iodide (JC-1). HT-22 cells were stained with JC-1 according to the manufacturer's protocol and analyzed by subsequent flow cytometry. After glutamate challenge (12 hours), JC-1 was added at a final concentration of 2 µM. Living-control cells were left untreated and damage-control cells were treated with carbonyl cyanide m-chlorophenylhydrazone (final concentration of 50 µM) (CCCP, included in the MitoProbe™ JC-1 Assay Kit) 5 minutes before staining to induce mitochondrial membrane depolarization. The supernatants were collected in order to include also the already detached cells into the measurements. The attached cells were collected after incubating with 1x Trypsin-EDTA (TE) for 3 minutes. After detaching of the HT-22 neurons TE reaction was stopped by adding 1000 µl serum-containing medium to each well, the cells were collected, and transferred to their

respective supernatants. Cells were then centrifuged at 1000 rpm, supernatants were removed, and the pellets were washed once in PBS, centrifuged and resuspended in 500 µl PBS and then kept on ice until the measurement. Mitochondrial membrane potential was determined using the JC-1 fluorophore (Invitrogen, Karlsruhe, Germany) and FACScan analysis (Becton, Dickinson and Company, Heidelberg, Germany). JC-1 green fluorescence was excited at 488 nm and emission was detected using a 530±40 nm filter. JC-1 red fluorescence was excited at 488 nm and emission was detected using a 613±20 nm filter. Equal loading of the cells with JC-1 dye was detected by the green fluorescence. Living cells with intact mitochondria are able to accumulate and reduce JC-1, which is then detected by the red fluorescence.

2.3.6. Detection of ATP levels

HT-22 cells were seeded in white 96 well plates (Greiner bio one, Frickenhausen, Germany) for luminescence measurements. Twenty-four hours after seeding the cells were damaged with glutamate (3 - 5 mM). DPI and PD146176 were added one hour before glutamate treatment. ATP levels were detected at 3 –18 hours after the onset of glutamate exposure by detection of luminescence using the ViaLight MDA Plus-Kit (Lonza, Verviers, Belgium). The cells were treated first with a " Nucleotide releasing reagent" (100 µl/well) and incubated for 5 min at room temperature. Afterwards the "ATP monitoring reagent" was injected into each well (20 µl/well) and luminescence was detected immediately (FluoStar, BMG Labtech, Offenburg, Germany). The emitted light intensity was measured for quantification of ATP levels.

The method uses an enzyme called luciferase, which catalyzes the following reaction:

$$ATP + Luciferin + O_2 \Rightarrow Oxyluciferin + AMP + PP_i + CO_2 + LIGHT.$$

2.3.7. Immunocytochemistry

For immunocytochemistry HT-22 cells were fixed with 4% PFA. The cells were permeabilized with 0.4% Triton X-100 (Sigma-Aldrich, Taufkirchen, Germany) in PBS for 5 minutes at room temperature. Cells were then incubated in blocking solution (3% horse serum in PBS, PAA, Pasching, Austria) for 30 min and then exposed to a polyclonal anti-AIF antibody (1:100 in blocking solution) overnight at 4°C. This was followed by incubation for 1 h with biotinylated anti-goat IgG antibody and 30 minutes in the presence of streptavidin oregon green 514 conjugate (Invitrogen, Karlsruhe, Germany) according to the manufacturers protocol. The specificity of AIF immunoreactivity was controlled by omission of the primary antibody. Nuclei were counterstained with DAPI. Images were acquired using a fluorescence microscope (DMI 6000 B, Leica, Wetzlar, Germany) connected to a CCD camera (DFC 360 FX, Leica, Wetzlar, Germany).

2.3.8. Immunoblots

HT-22 cells were treated as described above. Nuclear extracts were obtained by using a nuclear extraction kit (Active Motif, Rixensart, Belgium). For the extraction HT-22 cells were seeded in 75 cm^2 cell culture flasks (1 million cells/flask). In order to obtain good amounts of protein in the nuclear fractions 3 flasks were used for each treatment condition. The cells were pretreated with PD146176 (0.5 µM) for 1 h before adding glutamate. Twelve hours after the exposure to glutamate the extraction was started according to the manufacturers protocol. It is important to note that the purity of the extracts improved significantly when the nuclei were washed 1 time with PBS or hypotonic buffer before the addition of the complete lysis buffer.

For total cell protein extracts HT-22 cells were seeded in 24 well culture plates. At least 4 wells per condition were pooled. Cells were washed in PBS and lysed with 100 µl lysis buffer.

Protein lysis buffer:	Mannitol 0.25 M Tris 0.05 M EDTA 1M EGTA 1M, these components were mixed and adjusted to pH 7.8 with HCl 1M, this mixture can be stored at -20 °C DTT 1mM Triton-X 1% 1 tablet Complete Mini protease inhibitor cocktail per 10 ml (Roche Applied Science, Penzberg, Germany), these components were added to the mixture immediately before use

Protein extracts were kept on ice. To remove insoluble membrane fragments, extracts were centrifuged at 15,000 x g for 15 min at 4° C. The supernatants were stored at -80° C until further use.
The protein concentrations of the different extracts were determined by BCA-assay (Perbio Science, Bonn, Germany). 5 µl of each protein extract and of protein standard solutions was mixed with 200 µl of the BCA-solution and heated at 60 °C for 30 minutes. Then 100 µl of each probe was used to measure the absorption at 562 nm in a 96 well-plate with a plate reader (FluoStar, BMG Labtech, Offenburg, Germany). The protein concentration of the probes was calculated in relation to the protein standards by linear regression.

For gel electrophoresis and western blot analysis, the following solutions were used:

For the preparation of Polyacrylamide gels:

0.5 M Tris:	7.88 g Tris-HCl in 100 ml water, adjusted to pH 6.8 by concentrated HCl

1.5 M Tris:	23.6 g Tris-HCl in 100 ml water, adjusted to pH 8.8 by concentrated HCl
10 % APS:	1 g Ammoniumpersulfate (APS) in 10 ml water
10 % SDS:	10 g Sodium dodecyl sulfate (SDS) in 10 ml water

In addition to these solutions, N,N,N′,N′-Tetramethylethylenediamine (TEMED, Promega, Mannheim, Germany) and ultrapure, demineralized water were used to prepare the Polyacrylamide gels. The 0.5 M Tris solution was used for the loading gels whereas the 1.5 M Tris buffer was used for the preparation of the separating gels. It is important to note that the addition of APS and TEMED induces the polymerization of the gels.

For the gel electrophoresis the following buffers were used:

Electrophoresis buffer:	3.0 g Trizma base 14.4 g Glycine 1 g SDS in 1000 ml water
Loading buffer:	7 ml 1M Tris-HCl pH 6,8 3 ml Glycerol 1 g SDS 0.93 g DTT 100 µl β-Mercaptoethanol 1.2 mg Bromophenol blue sodium salt

For Western blot analysis the following buffers were used:

Transfer buffer:	3.0 g Trizma base 14.4 g Glycine 100 ml Methanol p.a. ad 1000 ml water

TBST:	2.42 g Trizma base 29.2 g Sodium chloride 0.5 ml Tween 20 ad 1000 ml water
Blocking buffer:	5 g Non-fatty milk powder In 100 ml TBST
Stripping buffer:	15 g Glycine 1 g SDS 10 ml Tween 20 ad 1 l water, adjusted to pH 2.2 by concentrated HCl

Discontinuous polyacrylamid gels (separating gel 10% or 15% polyacrylamid, loading gel 3.5% polyacrylamid) were cast using the Mini-Protean 3 cell with 1.0 mm spacer and 10-pocket combs (Bio-RAD, Munich, Germany).

The separating gels contained following components:

2.5 ml 1.5 M Tris
0.1 ml SDS 10%
3.34 ml (10%) or 5 ml (15%) 30% Acrylamid/Bis solution 29:1
0.05 ml 10% APS
0.01 ml TEMED and ultrapure, demineralized water ad 10 ml

Stacking gels were prepared with

2.5 ml 0.5 M Tris
0.1 ml SDS 10%
1.2 ml (3.5% gel) 30% Acrylamid/Bis solution 29:1
0.05 ml 10% APS
0.01 ml TEMED and water ad 10 ml

An amount of 25 µg protein of each sample was filled up to 20 µl with water. 4 µl loading buffer were added and heated at 95°C for 5 minutes. Afterwards the samples were loaded onto the gels and 10 µl of PageRuler™ Prestained Protein

Ladder (Fermentas, St. Leon-Rot, Germany) was added in one lane to determine the size of the detected proteins. Electrophoresis was performed in the Mini-Protean® Tetra Cell (Bio-RAD, Munich, Germany) at 60 V for 20 minutes and then at 120 V for circa 2 hours in electrophoresis buffer.

After electrophoresis, proteins were blotted onto a porablot polyvinylidenfluorid membrane (PVDF, Bio-RAD, Munich, Germany) according to the Bio-Rad protocol at 15 V for 35 – 50 minutes (depending on the size of the proteins that should be analyzed). Blotting was performed in a Trans-Blot SD semi-dry transfer cell (Bio-Rad, Munich, Germany) using methanol-containing transfer buffer. The blots were washed with TBST and blocked for 1 hour in blocking buffer (5% non-fat dry milk-powder in TBST).

Briefly, the blot was probed with an anti-AIF goat polyclonal antibody (sc-9416, 1 : 1000, Santa Cruz Biotechnology, Santa Cruz, CA, USA) or anti-nitro-tyrosin antibody at 4°C overnight. Membranes were then exposed to the appropriate HRP-conjugated rabbit anti-goat secondary antibody (1:2500, Vector Laboratories, Burlingame, CA, USA) or anti-rabbit secondary antibody (1:2500, Vector Laboratories, Burlingame, CA, USA) respectively, followed by a chemiluminescence detection of antibody binding using the Molecular Imager ChemiDoc ® XRS System (Bio – Rad, Munich, Germany). Equal protein loading and purity of the extracts was controlled by re-probing the membrane with a monoclonal anti-α-tubulin antibody (T9026, 1 : 20 000, Sigma-Aldrich, Taufkirchen, Germany) and an anti-HDAC1 antibody (dianova, Hamburg, Germany 1 : 1000), respectively. For total cell lysates an anti-actin antibody (MP Biomedicals, Illkirch, France) was used to control for equal loading. ChemiDoc ® software (Bio – Rad, Munich, Germany) was used for quantification of western blot signals.

2.3.9. Calcium measurements

Calcium levels in primary cortical neurons were detected with the fluorescence dyes Fura-2 and Fluo-4-AM.

For single cell measurement primary cortical neurons were plated on cover slips at a density of 3 x 10^4 cells/cm^2. On day 6 after the preparation cells were treated with

PD146176 (0.5 µM, 1 h pretreatment) and stained with fura-2 acetoxymethyl ester (5 µM) (Invitrogen, Karlsruhe, Germany) for 1 hour at 37 °C. The neurons were analyzed using a Polychrome II monochromator and an IMAGO CCD camera (Till Photonics, Martinsried, Germany) coupled to an inverted microscope (IX70; Olympus, Hamburg, Germany) at 340 and 380 nm for measuring $[Ca^{2+}]_i$. The cover slips were fixed on the microscope and then glutamate (20 µM) was added. The measurements were started before adding glutamate in order to detect the fast increases in intracellular calcium immediately after the exposure to glutamate. This method allows the simultaneous detection of increased $[Ca^{2+}]_i$ levels in marked single neurons.

In order to analyze a higher number of cells, primary cortical cultures were seeded in 96 well plates at a density of 16 x 10^4 cells/cm^2. On day 6 after the preparation the cells were pretreated with PD146176 (0.5 µM) and stained with Fluo-4AM (5 µM in DMSO) (Invitrogen, Karlsruhe, Germany) for 1 hour at 37 °C. Pluronic® F-127 (0.02 % in the final solution, Invitrogen, Karlsruhe, Germany) and probenecid (2.5 mM) were added according to the manufacturer's protocol (Invitrogen, Karlsruhe, Germany) in order to allow penetration of the dye into the cell and to prevent leakage of the dye after the staining. After one hour the dye was washed away and glutamate was added to each well and fluorescence was detected using a plate reader at an excitation wavelength of 488 nm and an emission wavelength of 520 nm (FluoStar, BMG Labtech, Offenburg, Germany).

2.3.10. Oxygen glucose deprivation (OGD)

Primary cortical neurons were seeded in 35 mm cell culture dishes at a density of 5 x 10^4 cells/cm^2. The OGD is an in vitro model for ischemia that is based on the application of medium without glucose and the deprivation of oxygen by exposure to a mixture of 5 % carbon dioxide CO_2 and 95 % nitrogen (N_2) in an air-tight chamber. The air-tight chamber is located in an incubator to obtain a temperature of 37 °C and linked to a gas bottle containing the mixture of 5 % carbon dioxide CO_2 and 95 % N_2. The oxygen concentration is controlled with an oxygen sensor (Oxy 3690 MP, Greisinger electronic, Regenstauf, Germany) that also regulates the influx of the

gas mixture. In order to prevent the desiccation of the dishes, a cup filled with ultrapure water was placed in the air-tight chamber (Figure 4). It is important to note that all dishes were opened when they were placed in the chamber to make sure that no oxygen is left in the surrounding of the probes.

Validation of the OGD chamber and the protocol was performed using the NMDA receptor antagonist MK-801 (Sigma-Aldrich, Taufkirchen, Germany) because it has been established that inhibition of the NMDA glutamate receptors significantly reduced OGD-induced neuronal death. MK-801 was dissolved in DMSO and a stock solution was prepared at a concentration of 100 mM and stored at -20 °C. Prior to the experiments the stock solution was diluted to a final concentration of 10 µM in EBSS. MK-801 was added 1 h before the onset of OGD and was present in the medium throughout the experiment.

The PD146176 groups were pretreated with the 12/15-LOX inhibitor at a final concentration of 0.5 µM for one hour and the 12/15-LOX inhibitor was also present in the medium during the experiment. Before the induction of OGD all cells were washed two times with EBSS without glucose (EBSS w/o glucose) in order to completely remove the glucose.

EBSS w/o glucose:	264 mg/l $CaCl_2$ x $2H_2O$
	400 mg/l KCl
	200 mg/l $MgSO_4$ x $7H_2O$
	6.8 g/l NaCl
	2.2 g/l $NaHCO_3$
	158 mg/l NaH_2PO_4 x $2H_2O$
	10mg/l Phenolred
	in 1 liter ultrapure, demineralized water
	pH 7.2, adjusted with 1 M HCl

The medium was sterilized by filtration using a 0.22 µm filter.

For OGD the cells were transferred to the air-tight chamber that was filled with 5 % carbon dioxide CO_2 and 95 % N_2 and they were kept in EBSS w/o glucose. The cells stayed in the OGD chamber for four hours. The controls were kept in the normal incubator with EBSS containing glucose or Neurobasal respectively. After four hours of OGD, EBSS medium containing glucose, was added to all dishes and

cells stayed in the standard cell culture incubator for another 18 - 24 hours. For further analysis of cell death cells were fixed with paraformaldehyde 4 % in PBS (PFA 4%) and stained with the fluorescent DNA-binding dye 4', 6-diamidino-2-phenylindole dihydrochloride (DAPI) (Sigma-Aldrich, Taufkirchen, Germany). The percentage of pyknotic nuclei was quantified using a fluorescence microscope (DMI 6000 B, Leica, Wetzlar, Germany) connected to a CCD camera (DFC 360 FX, Leica, Wetzlar, Germany) without knowledge of the treatment history. At least 200 cells were analyzed from 5 areas per cell culture dish and experiments were performed at least 3 times with n=5 per treatment condition.

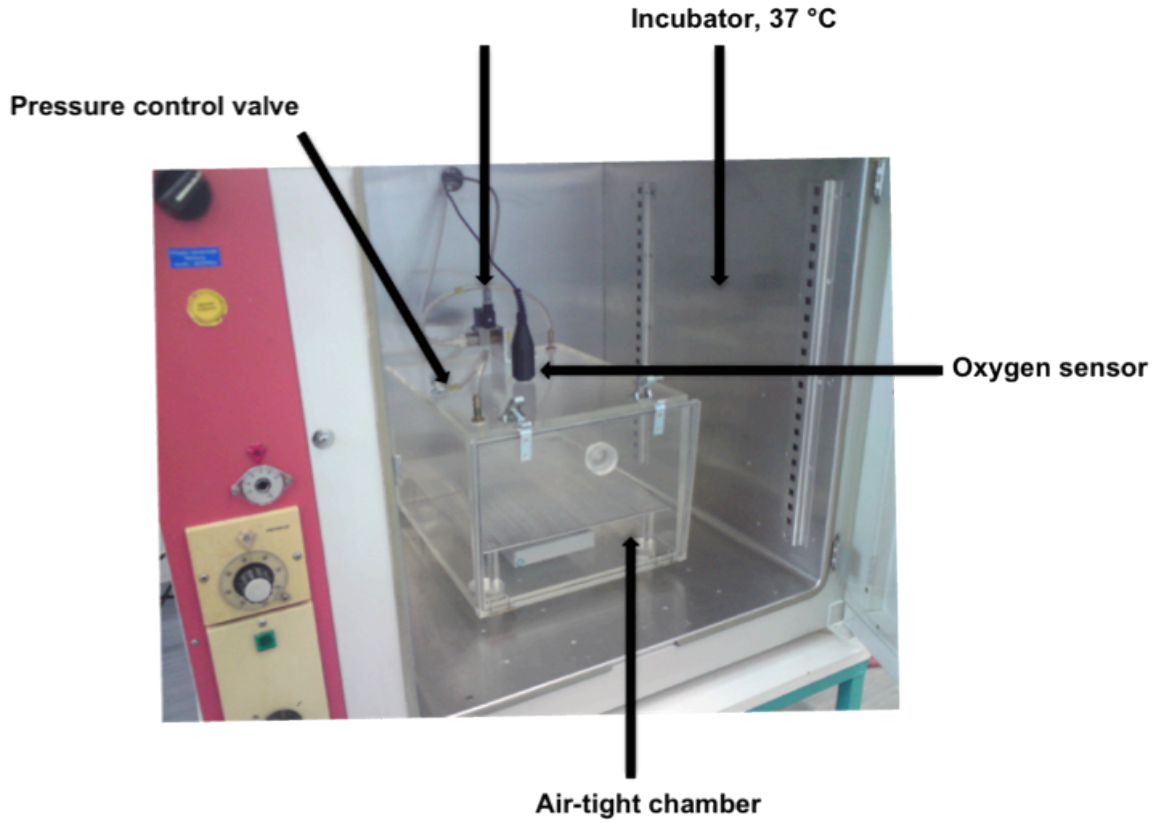

Figure 4: For oxygen glucose deprivation (OGD) an air-tight chamber was heated up to 37°C and filled with 5% CO_2 and 95% N_2. Before the treatment the cells were washed two times with EBSS w/o glucose. After 4 hours of OGD the cells were removed from the chamber and the medium was changed to EBSS containing glucose. After 20 – 24 h of reoxygenation the cells were fixed with PFA 4% and stained with DAPI for the quantification of pyknotic nuclei. The 12/15-LOX inhibitors were present in the medium from 1 h before the induction of OGD and throughout the experiment.

2.3.11. Middle cerebral artery occlusion (MCAO) in mice and determination of the neuroscore

The MCAO experiments were performed by Uta Mamrak and Nicole Terpolilli (Ludwig-Maximilians-Unversität, Munich, Germany). The 12/15-LOX inhibitor was injected to C57BL/6 mice in doses of 0.4 and 4 mg/kg body weight prior to the induction of MCAO. Transient focal ischemia was induced for 45 min by a silicon-coated nylon filament that was introduced into the internal carotid artery to occlude the middle cerebral artery (MCA). Surgery was performed in deep isoflurane/N_2O anesthesia with controlled ventilation, and ischemia and reperfusion were verified by laser Doppler measurements. The infarct volume was calculated on the basis of the histomorphometric data from 11 consecutive sections obtained 24 h after onset of ischemia. Statistical analysis was performed using the Mann-Whitney-U-test.
For determination of the neuroscore the C57BL/6 mice were examined at 1 and 24 h after reperfusion. The neuroscore is used to analyze the motor activity of the mice. The neuroscore was determined by the following criteria: 1) the motor function of each leg was rated independently; 2) sensory deficits of the legs and tail were rated separately; and 3) the ability to walk on a beam was tested on 1.5- and 2.5-cm beams. The total score for healthy animals without cognitive deficits was 0 points.

2.4. Statistical analysis

All data are presented as means ± standard deviation (SD). For statistical comparisons between two groups Mann-Whitney U-test was used. Multiple comparisons were performed by analysis of variance (ANOVA) followed by Scheffé's post hoc test. Calculations were performed with the Winstat standard statistical software package (R. Fitch Software, Bad Krozingen, Germany).

3. Results

3.1. Glutamate induces oxidative stress in HT-22 cells

In HT-22 immortalized mouse hippocampal neurons glutamate induces cell death by inhibition of the xC-transporter and subsequent glutathione (GSH) depletion. Since glutathione functions as one of the major endogenous radical scavengers in the cell, its depletion leads to the accumulation of reactive oxygen species (ROS) up to levels that are critical for cell survival.

It is important to note that sensitivity to glutamate toxicity varies in HT-22 neurons depending on density and passage number of the cells. Consequently, in different experiments HT-22 cells were treated with varying concentrations of glutamate (2 – 5 mM) depending on their sensitivity at the time.

The characterization of glutamate-induced cell death in HT-22 cells showed that the cells die in a time- and concentration dependent manner after the glutamate challenge (Figure 5a, 5b). Cell death was evaluated using the MTT assay and impedance measurements.

Impedance measurements were based on the xCELLigence system (Roche, Applied Science), which allows real time analysis of cell proliferation and cell death kinetics. After exposure to glutamate HT-22 neurons round up and detach from the well bottom, thus the impedance decreases. Impedance measurements permit the detection of kinetic processes while the MTT assay detects one specific endpoint.

A supposed increase of ROS after the glutamate challenge was measured at different time points after onset of glutamate treatment using the fluorescent dyes DCF and BODIPY followed by FACS analysis. DCF (Dichlorodihydrofluoresceine-diacetate) is a cell-permeant indicator for reactive oxygen species that is nonfluorescent until the acetate groups are removed by intracellular esterases and oxidation occurred within the cell.

DCF was used to detect total ROS levels in HT-22 cell while BODIPY (BODIPY® 581⁄591 C11, Invitrogen, Karlsruhe, Germany) detected lipid peroxides formed after glutamate treatment in HT-22 cells.

The results obtained from cells exposed to glutamate for 6 h, 8 h and 18 h show a time-dependent increase in lipid peroxidation after the glutamate challenge (Figure 5c). It is interesting to note that glutamate induced a first increase of the number of cells containing lipid peroxides within 6 – 8 hours after glutamate exposure and a more pronounced accumulation of lipid peroxides at 16 – 18 hours after glutamate treatment (Figure 5c). Similar to the ROS formation detected with BODIPY, the measurements using DCF showed a two-phase increase in oxidative stress, as detected by an initial increase in the fluorescent signal within 6 – 8 hours followed by a more pronounced increase at 16 - 18 hours after the glutamate challenge (Figure 5d).

In correlation with the survival experiments these data indicate a first increase in ROS formation before the onset of detectable cell death and a second strong increase in ROS when cellular damage becomes evident.

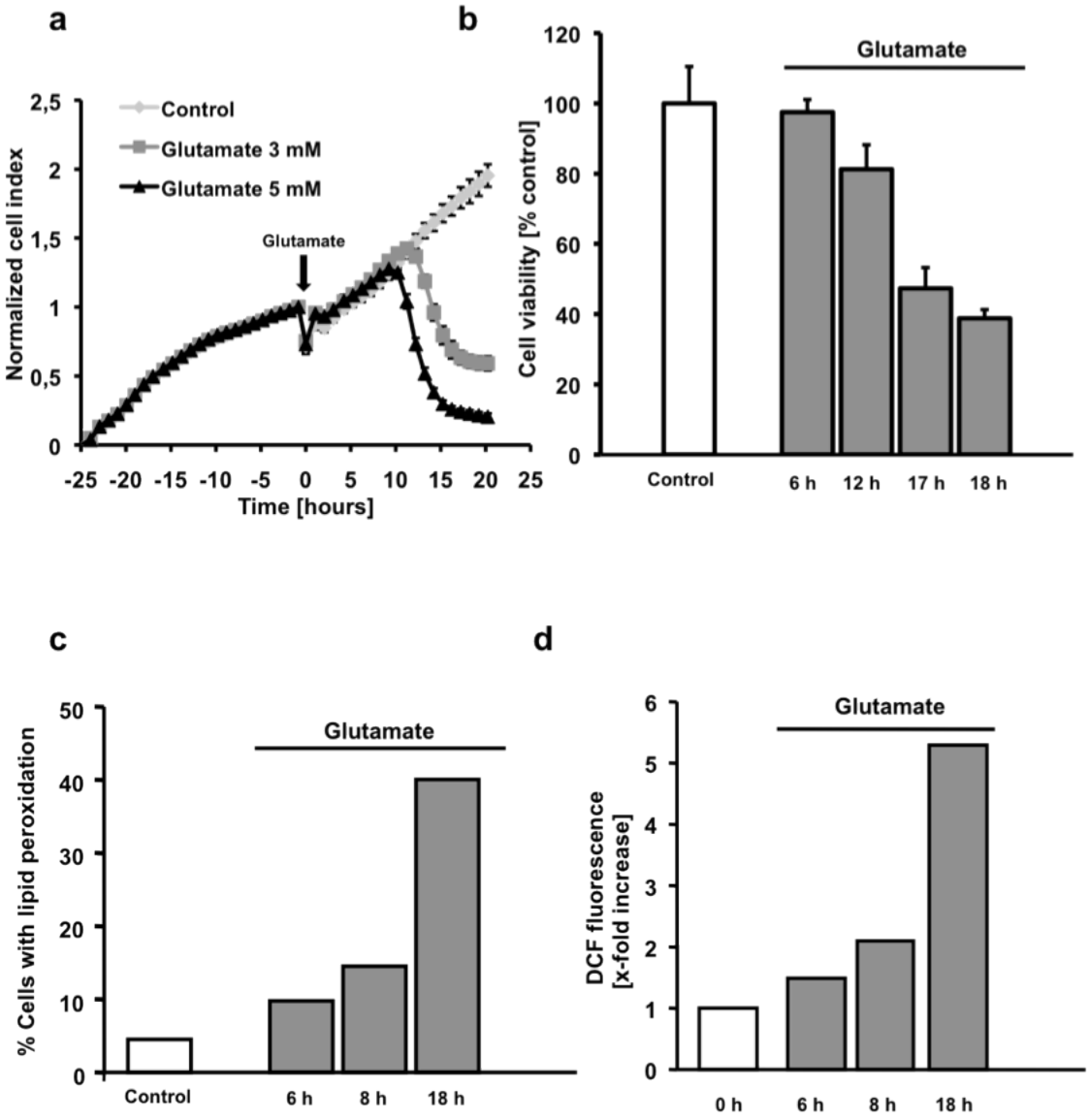

Figure 5: Glutamate leads to a time-dependent damage in HT-22 cells. (a) HT-22 cells were seeded in 96 well E-plates with a density of 4500 cells/well. Attaching of cells and cell proliferation were observed for 48 h after seeding and for further 24 h after onset of the exposure to glutamate (5 mM). Addition of glutamate is indicated by time point "0 h" in the graph. Cell death became detectable 9 – 10 h after the onset of the glutamate challenge. After initiation of cell death the HT-22 cells died within 3 – 5 h (n=8). **(b)** HT-22 cells were treated with glutamate (5 mM) for 6, 12, 17 and 18 h. Cell viability was detected by the MTT assay (n=8). **(c)** Glutamate induces the production of lipid peroxides. Glutamate treatment was performed for 6 – 18 h. After addition of 2 µM BODIPY 581/591 C11 for 60 min, fluorescence was quantified by FACS analysis. Following glutamate exposure, a twofold increase in the percentage of cells with lipid peroxidation was determined after 6 to 8 h, and a second more pronounced increase was detected after 18 h (n=3). **(d)** Glutamate was added to the cells at a concentration of 3 mM. ROS levels were detected by Dichlorodihydrofluoresceine-diacetate (DCF) and quantified by FACS analysis (n=3). Glutamate induced a biphasic increase in ROS formation.

In order to evaluate the importance of the detected ROS accumulation for cell death induced by glutamate in the HT-22 neurons the antioxidants N-Acetyl-L-cysteine (NAC, 5 – 20 mM), ascorbic acid (0.5 and 1 mM) and Trolox (50 + 100 µM) were added together with glutamate (5 mM). Cell viability was determined using the MTT assay 15 hours after the glutamate challenge. All antioxidants significantly reduced glutamate-induced damage in HT-22 cells (Figure 6a, 6b, 6c). This data further supported the proposed role of increased ROS formation in glutamate-mediated cell death in the immortalized hippocampal neurons.

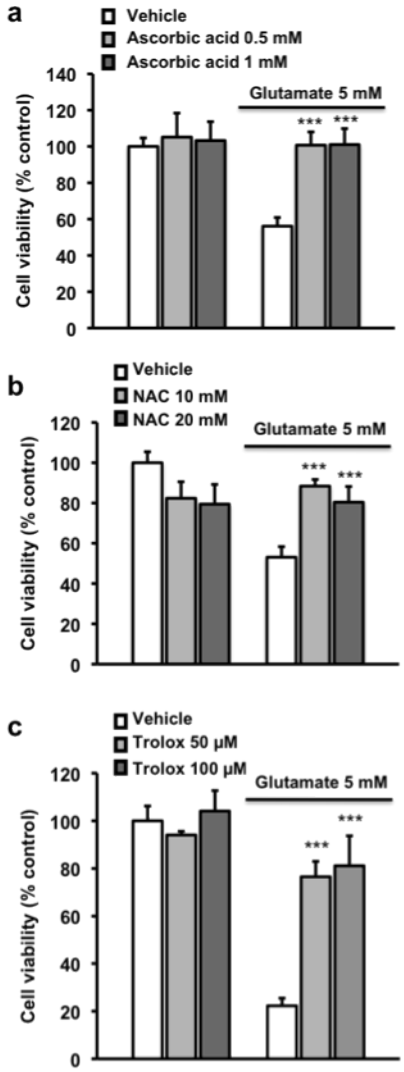

Figure 6: Antioxidants significantly reduce glutamate toxicity in HT-22 cells. (**a - c**) HT-22 cells were exposed to glutamate (5 mM). The antioxidants L-ascorbic acid (**a**, 0.5 – 1 mM), NAC (**b**, 10 - 20 mM) and Trolox (**c**, 50 - 100 µM) were added to the cells together with glutamate. Cellular survival was determined 16 hours after the glutamate challenge using the MTT assay (n=8). All experiments were repeated 3 times and the results are presented as the mean ± S.D. *** P<0.001 compared with glutamate-treated cells (ANOVA, Scheffé-test).

3.2. Extracellular calcium contributes to glutamate-induced cell death in HT-22 cells

The previous results demonstrate a key role for ROS formation in glutamate-induced cell death in HT-22 cells.

In primary neurons calcium dysregulation is known to be a central mechanism caused by glutamate exposure. As HT-22 cells do not express ionotropic glutamate receptors [138] it was interesting to characterize the HT-22 cell model in further detail by analyzing the role of calcium dysregulation in HT-22 cells.

The cells were treated with glutamate (3 mM) and the calcium chelators ethylenediaminetetraacetic acid (EDTA, 200 μM - 1mM) and 1,2-Bis(2-aminophenoxy)ethane-N,N,N′,N′-tetraacetic acid tetrakis(acetoxymethyl ester) (BAPTA-AM, 10 + 20 μM). EDTA functions as a chelator of extracellular calcium whereas BAPTA-AM preferentially reduces intracellular calcium levels. Both calcium chelators were applied together with glutamate and cell viability was measured using the MTT assay at 14 – 16 h after the treatment. Interestingly, EDTA could significantly reduce glutamate-induced cell death in HT-22 cells whereas BAPTA-AM failed to protect the cells but even significantly reduced cell viability (Figure 7a, b). The data show that disruption of the calcium homeostasis is involved in glutamate toxicity in HT-22 cells. In addition, the results indicate that the extracellular calcium is of importance for glutamate toxicity in HT-22 cells whereas release of calcium from intracellular stores may be less important for glutamate-induced cell death. It is also important to note that higher levels of EDTA (2 mM) induced cellular death showing that calcium is important for cellular signaling and survival.

The protective effect of EDTA, however, is not as intense as the strong protection of antioxidants showing again the key role of ROS formation in glutamate-induced cell death. The role of calcium dysregulation in HT-22 cells as demonstrated by these findings links this model system to excitotoxicity in primary neurons.

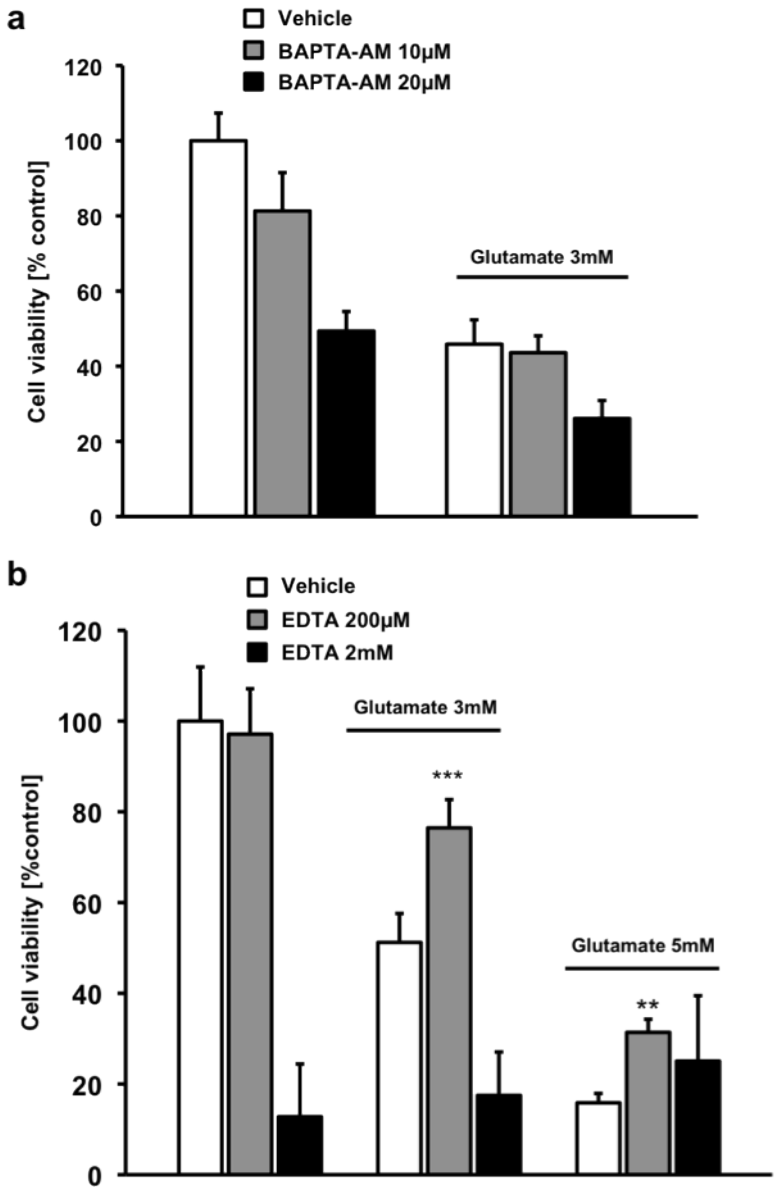

Figure 7: Glutamate causes disruption of calcium homeostasis in HT-22 cells. (**a**) The intracellular calcium chelator BAPTA-AM failed to protect HT-22 cells against glutamate toxicity (3 mM). (**b**) EDTA (200 µM) significantly reduced glutamate-induced cell death (n=8). All experiments were at least repeated 3 times and all data are provided as mean ± S.D. ** *P*<0.01, *** *P*<0.001 compared with glutamate-treated cells (ANOVA, Scheffé test).

3.3. 12/15-lipoxygenases mediates glutamate-induced cell death in HT-22 neurons

The measurements of lipid peroxidation using the BODIPY fluorophore indicated that the formation of lipid peroxides plays a major role in glutamate-induced death in the HT-22 cells. Such formation of lipid peroxides derives from enzymatic and non-enzymatic processing of membrane lipids and is mediated through formation of arachidonic acid (AA), e.g. by phospholipase A_2 (PLA_2). The later stages of lipid peroxide formation may involve different enzymatic pathways since the main substrate AA can be metabolized by cyclooxygenases (COX) or lipoxygenases (LOX). It is known that 12/15-LOX, 5-LOX and also COX-1 and COX-2 are present in the brain [22]. In order to analyze the potential role of COX and LOX in HT-22 cells, glutamate treatment was combined with different small molecule inhibitors of 5-LOX, 12/15-LOX and COX-1/2.

To study the role of COX-1 and COX-2 in HT-22 cells the COX-1/2 inhibitor indomethacin (5 – 100 µM) was added together with glutamate. Cell viability was detected by the MTT assay at 16 hours after the onset of glutamate exposure. Indomethacin failed to protect the HT-22 cells against glutamate toxicity suggesting that enhanced COX activity is not the essential source of ROS production and lipid peroxidation in HT-22 cells exposed to glutamate (Figure 8a).

The 5-LOX was also detected in the brain and was found to be involved in different mechanisms as for example in inflammatory processes [22]. The selective 5-LOX inhibitors YS121 (0.41 µM + 4.1 µM) and C06 (0.065 µM + 0.65 µM) were used to test the involvement of 5-LOX in glutamate-induced cell death in HT-22 cells. Both inhibitors were added one hour prior to glutamate and 16 hours later cell viability was detected using the MTT assay. Both compounds did not provide protection of the cells against glutamate challenge (Figure 8b, 8c) indicating that 5-LOX activation does not mediate ROS formation and glutamate toxicity in HT-22 cells.

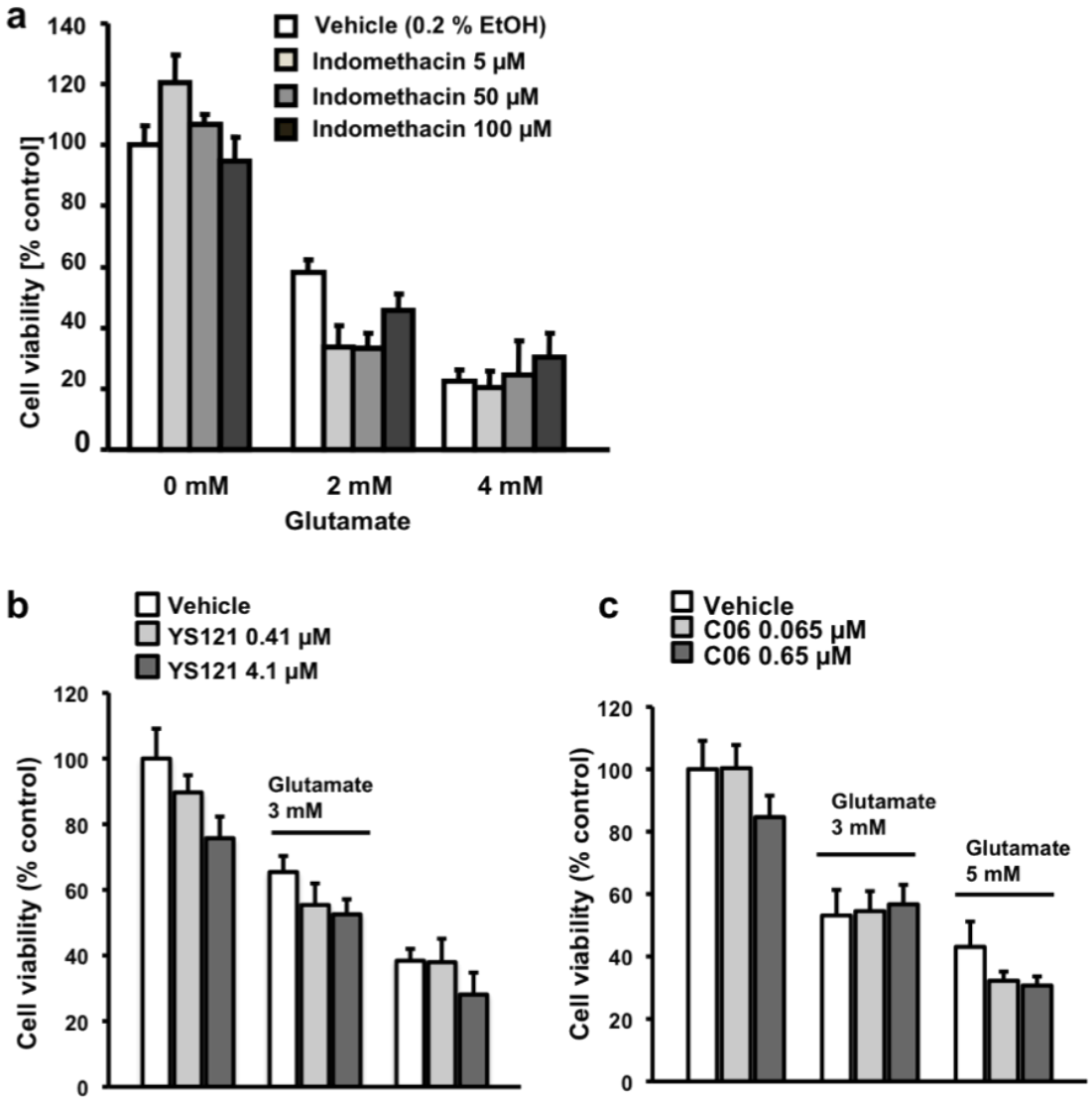

Figure 8: Neither COX nor 5-LOX prevent glutamate-induced cell death. HT-22 cells were challenged with glutamate (2 – 5 mM). (**a**) The COX1/2 inhibitor indomethacin (5 µM, 50 µM and 100 µM) failed to protect the cells against glutamate toxicity. Cell viability was detected by MTT assay (n=8). (**b + c**) The selective 5-LOX inhibitors YS121 (**b**, 0.41 µM - 4.1 µM) and CO6 (**c**, 0.065 µM - 0.65 µM) did not attenuate glutamate induced cell death. Cell viability was analyzed using the MTT assay (n=8). All experiments were repeated 3 times and the results indicate the mean ± S.D.

The small molecule inhibitors PD146176 and AA861 inhibit the 12/15-LOX, which is known to be the most abundant LOX in the brain. Both inhibitors were added to the HT-22 cells at different concentrations one hour before adding glutamate (4 – 5 mM). The glutamate-induced damage was detected using the MTT assay and also by real time impedance measurements and annexin V/propidium iodide (PI) staining. The cells were analyzed at 16 hours after the exposure to glutamate

according to the different protocols. PD146176 (0.1 - 0.5 µM) significantly reduced glutamate toxicity measured by the MTT assay (Figure 9a) and also significantly reduced the number of annexin V/PI-positive cells after the glutamate treatment (Figure 9b). These findings were supported by the impedance measurements showing that 12/15-LOX inhibition by PD146176 prevented the glutamate-induced decrease of the cell index (Figure 9c).

12/15-LOX inhibition by AA861 also prevented glutamate toxicity (Figure 9d) confirming the protective effect of 12/15-LOX inhibition in glutamate-induced oxidative stress in HT-22 neurons.

In summary, these results clearly showed that 12/15-LOX inhibitors protected HT-22 cells against glutamate toxicity whereas neither COX nor 5-LOX were involved in this model of cell death through oxytosis.

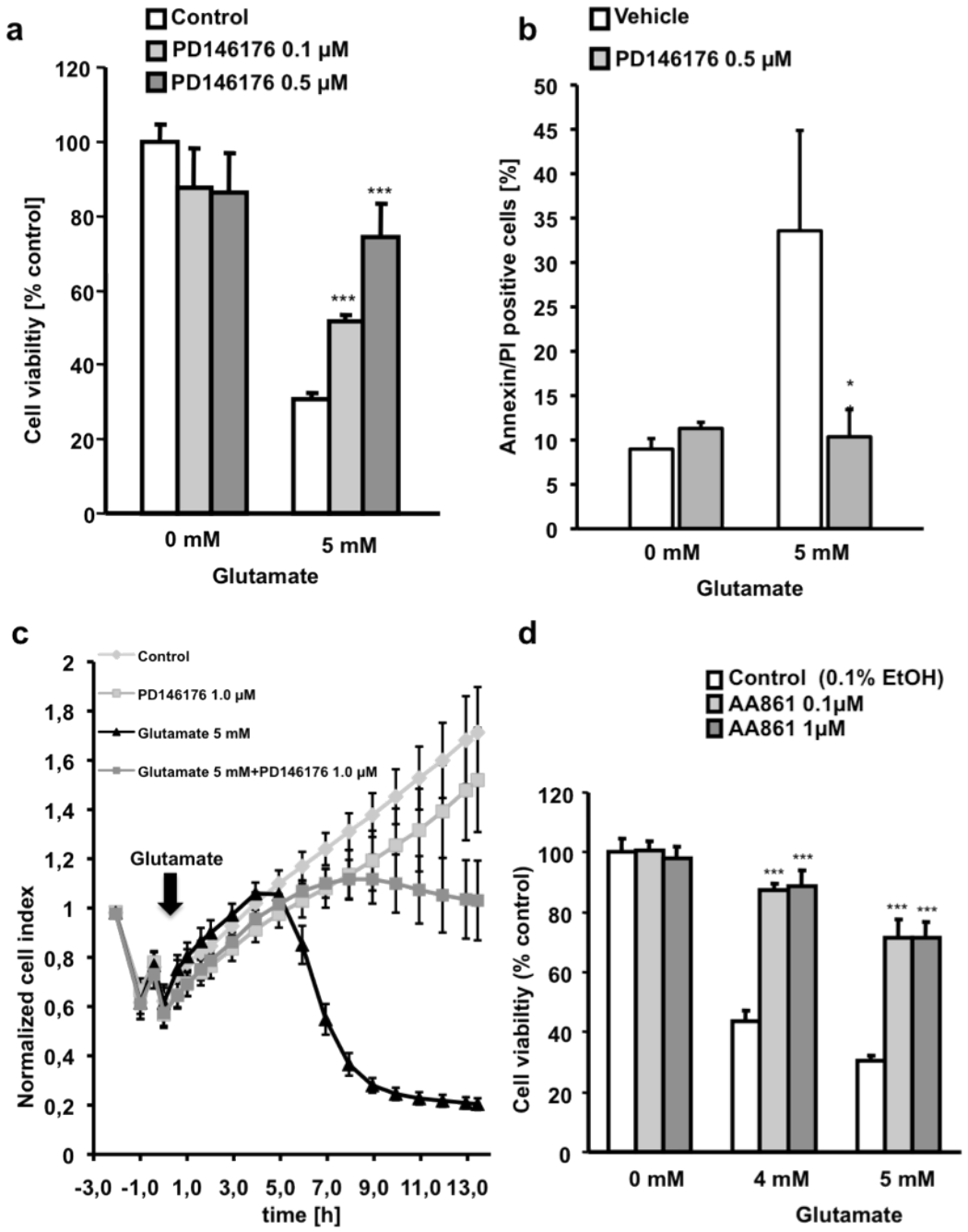

Figure 9: 12/15-LOX-inhibitors protect HT-22-cells against glutamate induced cell death. (**a**) The 12/15-LOX inhibitor PD146176 was applied 1 h before exposure to glutamate (5 mM) at concentrations of 0.1 and 0.5 µM (n=8). MTT assay was used to determine cell viability 18 h after onset of glutamate treatment. (**b**) PD146176 significantly reduced the annexin-V/propidium iodide positive cells compared to glutamate treated cells. Cells were pretreated with the 12/15-LOX inhibitor PD146176 (0.5 µM) 1 h before glutamate challenge (5 mM). Cells were stained with annexin-V and propidium iodide and detected with FACS analysis (n=4). (**c**) HT-22 cells were seeded in 96 well E-plates with a density of 4500 cells/well. Cells were pretreated with PD146176 for 1 h and treated with glutamate 5 mM at 24 h after the seeding. The time point of glutamate addition is marked as "0 h" in the graph (n=8). (**d**) The LOX inhibitor AA861 (0.1 - 1 µM) was applied 1 h before glutamate treatment at concentrations of 0.1 and 1 µM (n=8). All experiments were repeated 3 times and the results indicate the mean ± S.D. * P<0.05, *** P<0.001 compared with glutamate-treated cells (ANOVA, Scheffé-test).

In order to evaluate the involvement of 12/15-LOX in the formation of ROS after exposure to glutamate, lipid peroxidation was measured in HT-22 cells treated with the 12/15-LOX inhibitors PD146176 and AA861 prior to glutamate treatment. Two different time points (8 h and 17 h) were investigated representing both, the early and late stages of the cell death cascade. Owing to the pronounced cellular damage occurring at 17 h the cells were unsuitable for FACS analysis at this time point when exposed to 3 mM glutamate. Therefore, the concentration used for studying the later time point had to be reduced to 2 mM, whereas 3 mM of glutamate were used for the 8 h time point. The 12/15-LOX-inhibitors PD146176 and AA861 prevented the first glutamate-induced increase in lipid peroxidation after 6 to 8 h (Figure 10a). In addition, 12/15-LOX inhibition significantly attenuated the boost of lipid peroxides detected at 17 h after onset of glutamate treatment indicating that 12/15-LOX activation is an essential source of ROS production and lipid peroxidation in HT-22 cells (Figure 10b).

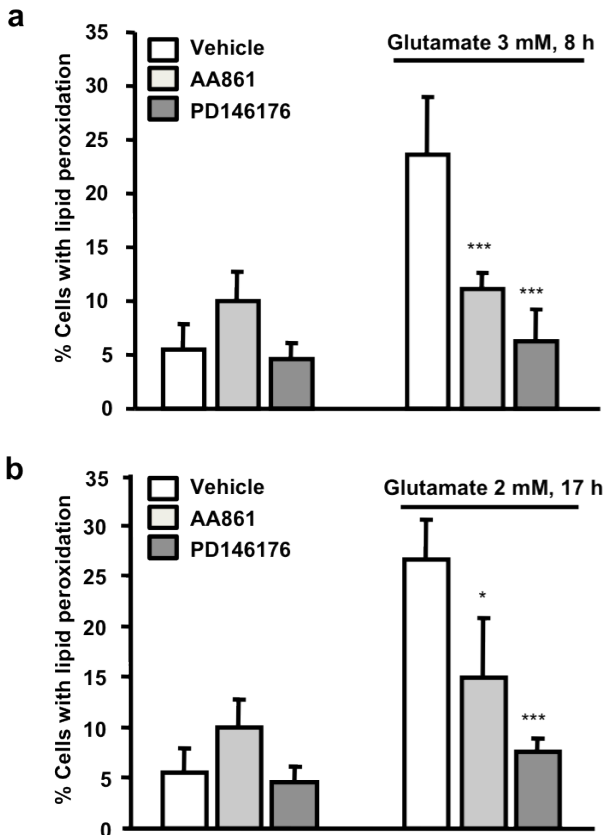

Figure 10: 12/15-LOX inhibitors prevent lipidperoxide formation in HT-cells exposed to glutamate. Lipid peroxidation was detected 8 h (**a**) and up to 17 h (**b**) after onset of glutamate exposure by FACS analysis after staining of the cells with BODIPY C11 (Ex = 488nm, Em = 530nm, 613nm). The 12/15-LOX inhibitors AA861 (0.1 µM) or PD146176 (0.5 µM) were added 1 h before the glutamate challenge (2 – 5 mM) (n=3). The experiments were repeated 3 times and the results indicate the mean ± S.D. ** P<0.01, *** P<0.001 compared with glutamate-treated cells (ANOVA, Scheffé-test).

Since the previous results suggested a key role of 12/15-LOX in glutamate-induced oxidative stress in HT-22 cells, the next steps of the study included a detailed analysis of the underlying mechanism. For the potential therapeutic application of this principle of neuroprotection the protective time window is of utter importance and thus needs to be defined.

To address this question the 12/15-LOX-inhibitor PD146176 was added at different time points between 2 h and 15 h after onset of the glutamate treatment. Cell viability was detected by the MTT assay at 17 hours after the exposure to glutamate. HT-22 cells were protected against glutamate toxicity even when PD146176 was added up to 8 h after the glutamate challenge indicating a prolonged therapeutic time window. Nonetheless, beyond that time point glutamate-induced cell death may have proceeded too far to be rescued by LOX inhibition (Figure 11a). Similar results were obtained with the antioxidant Trolox, which also proved to be protective up to 8 h after the glutamate challenge (Figure 11b). Altogether, these findings stress the significance of ROS in glutamate dependent cell death in HT-22 cells and reveal an 8 h time window for protective intervention when targeting the 12/15-LOX. In terms of therapeutic feasibility this rather prolonged time window of 8 h renders the 12/15-LOX an interesting target to prevent delayed neuronal death that occurs, for example after cerebral ischemia.

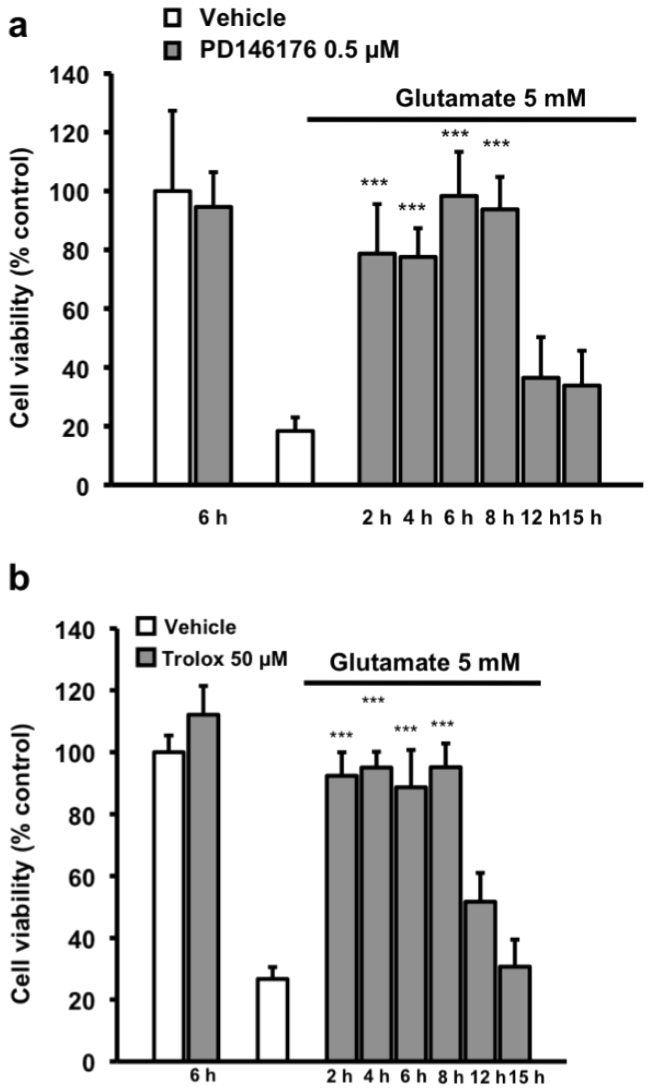

Figure 11: Time window of protection against glutamate toxicity for PD146176 and Trolox. (**a**) The 12/15-LOX inhibitor PD146176 protects HT-22-cells when applied up to 8 h after glutamate treatment. PD146176 (0.5 µM) was added at time points between 2 and 15 h after onset of glutamate treatment (5 mM). MTT assay was used to determine cell viability 18 h after onset of glutamate exposure (n=8). (**b**) Trolox protects HT-22 cells against glutamate toxicity when applied up to 8 h after glutamate challenge. Cells were treated with Trolox (50 µM) at time points between 2 and 15 h after glutamate (5 mM) challenge. Cell viability was detected by MTT assay (n=8). All experiments were repeated 3 times and the results indicate the mean ± S.D. *** $P<0.001$ compared with glutamate-treated cells (ANOVA, Scheffé-test).

3.4. 12/15-LOX mediates cell death in primary neurons

In primary neurons glutamate induces excitotoxicity via massive calcium influx through NMDA receptors. Consequently, cell death mechanisms are different in primary neurons compared to HT-22 cells, since pronounced increases in intracellular calcium levels trigger cell death pathways in primary neurons exposed

to glutamate, whereas calcium influx plays a minor role for glutamate toxicity in HT-22 cells. Nevertheless, formation of ROS is a major feature involved in glutamate toxicity in primary neurons downstream of initial calcium overload of the cells. Therefore, PD146176 was also tested in primary neuronal cultures to examine the role of 12/15-LOX activation in this model system of glutamate-induced excitotoxicity.

Primary cortical cultures were treated on day 6 – 10 after the preparation. At this time point the neurons express NMDA receptors and are highly sensitive to glutamate.

In primary cortical neurons PD146176 (0.5 - 1 μM) was added 1 h before the glutamate exposure (20 μM). Cell viability was evaluated 18 - 24 hours after glutamate treatment by DAPI staining of the nuclei and subsequent quantification of pyknotic nuclei.

The 12/15-LOX inhibitors significantly reduced the glutamate-induced cell death in primary neuronal cells (Figure 12a).

In addition, primary cortical neurons were prepared from Alox-15 mice (12/15-LOX knockout mice, 12/15-LOX is encoded by the *Alox15* gene). This genetic approach was used to confirm the involvement of 12/15-LOX activity in excitotoxicity thereby also validating the previous results obtained with the pharmacological substances. Neurons from wild type mice were used as controls in these experiments. Neuronal cultures obtained from wt and Alox-15 mice were treated with glutamate (20 μM) on day 7 – 10 after the preparation. The cell viability was evaluated by quantification of DAPI-stained pyknotic nuclei. Cortical neuronal cultures from Alox15-mice showed significantly reduced cell death after glutamate challenge compared to cells obtained from wild type mice (Figure 12b). These results demonstrated that activation of 12/15-LOX plays an important role in glutamate induced excitotoxic cell death in primary neuronal cells.

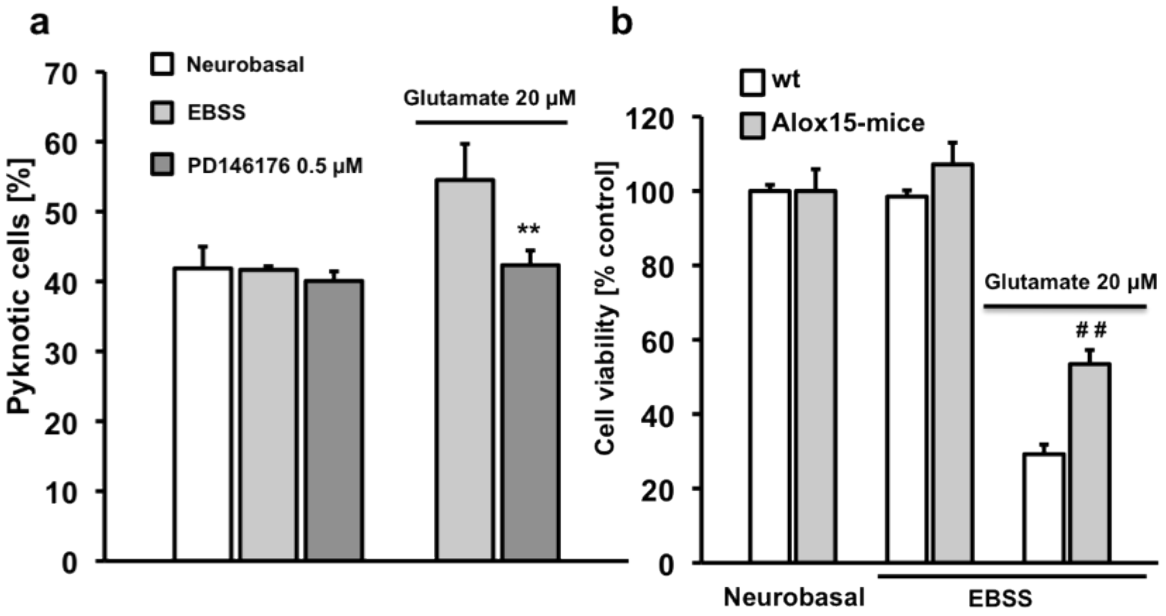

Figure 12: 12/15-LOX inhibition protects primary neurons against glutamate-induced excitotoxicity. (**a**) Primary cortical neurons were damaged with glutamate (20 µM) and pretreated with PD146176 for 1 h. PD146176 (0.5 µM) significantly reduced glutamate-induced cell death. (**b**) Primary cortical neurons obtained from Alox-15 mice and wild type neurons were treated with glutamate (20 µM). Alox-15 neurons showed significantly reduced damage compared to wild type neurons. All data are provided as mean ± S.D. ** *P*<0.01, compared to glutamate-treated cells and ## *P*<0.01 compared to glutamate-treated wild type neurons (ANOVA, Scheffé test).

3.5. 12/15-LOX inhibition prevents calcium dysregulation in primary cortical neurons

Excitotoxicity is known to induce cell death after glutamate stimulation of NMDA receptors in primary neurons. The addition of glutamate causes a rapid increase in intracellular calcium concentration followed by delayed calcium dysregulation with fatal consequences for the neuronal cell.

In order to investigate the effect of 12/15-LOX on glutamate-induced disruption of calcium homeostasis in primary neurons, calcium levels were determined in cortical neuronal cultures using fluorescence measurements.

Primary cortical neurons were pretreated with PD146176 (0.5 µM) and stained with calcium detecting fluorescence dyes (Fura-2 or Fluo-4 AM) on day 6 after the preparation. After adding glutamate the increases in intracellular calcium

concentrations were detected by fluorescence measurements. Fluo-4 AM was used to measure calcium levels in primary cortical cultures with a plate reader (96 well-plate, FluoStar, BMG Labtech, Offenburg, Germany). These experiments showed that glutamate induced a significant increase in fluorescence intensity, i.e. pronounced increases in intracellular calcium levels. PD146176 clearly attenuated the glutamate-induced calcium influx in the neuronal cultures suggesting that 12/15-LOX activation was involved in mechanisms of glutamate-induced excitotoxicity (Figure 13a).

For further analysis single neurons were stained with Fura-2 (5 µM) and analyzed with a fluorescence microscope allowing the detection of calcium dysregulation in single neurons. Exposure to glutamate caused a fast calcium increase as well as a delayed calcium deregulation. Cells pretreated with PD146176 (0.5 µM) before the exposure to glutamate, showed significantly reduced intracellular calcium levels compared to cells treated with glutamate alone (Figure 13b).

Both methods detected a significantly reduced intracellular calcium increase after pretreatment with the 12/15-LOX inhibitor. These data suggest that 12/15-LOX is involved in the regulation of the calcium homeostasis in primary neurons exposed to toxic concentrations of glutamate.

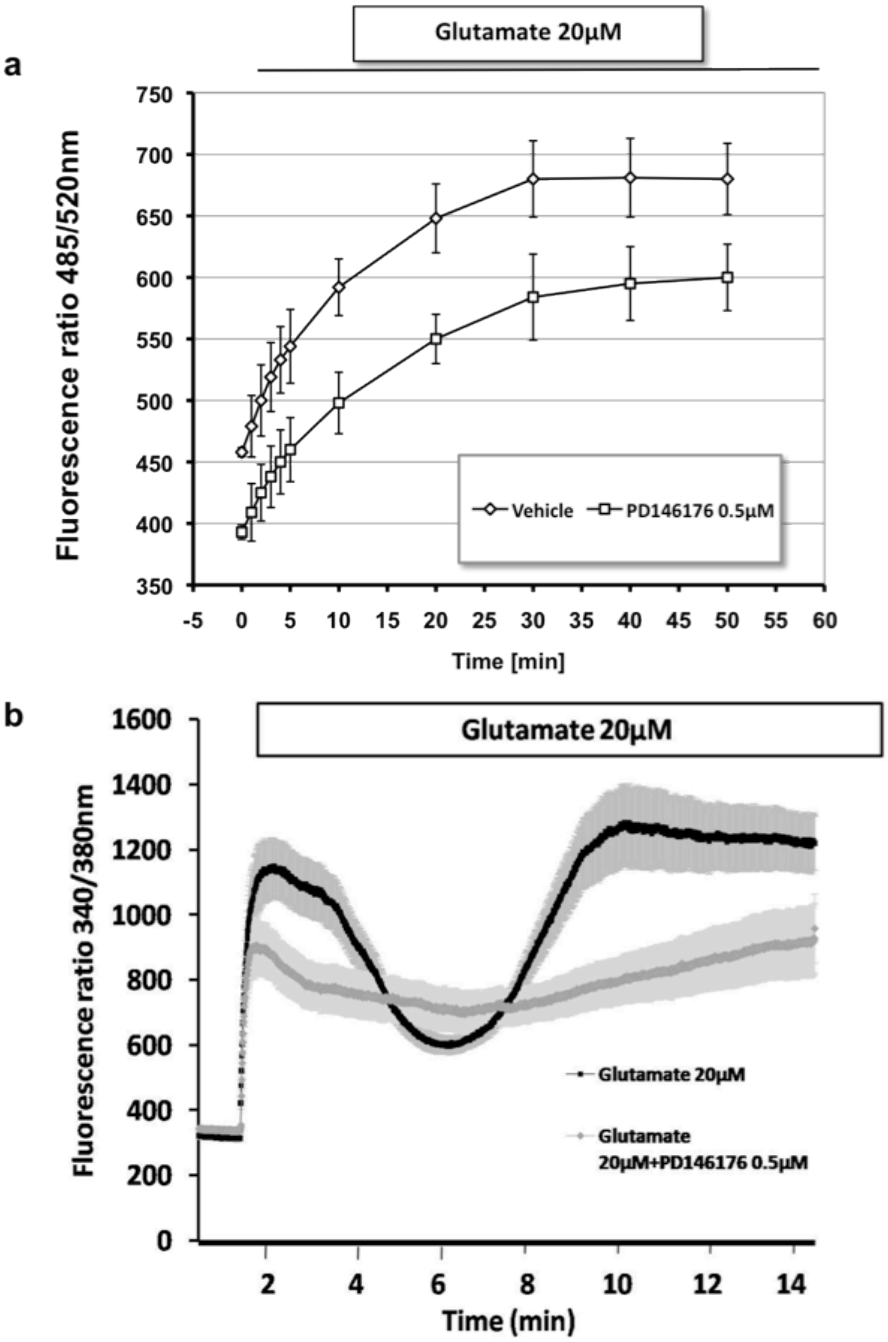

Figure 13: PD146176 significantly reduces glutamate-induced disruption of calcium homeostasis in primary neurons. (**a**) Primary cortical neurons were seeded in 96 well-plates and were stained with Fluo-4 AM for 1 h at 37 °C at day 6 after the preparation. Pluronic® F-127 (0.02% in the final solution) and Probenecid (2.5 mM) were added according to the manufacturer's protocol to allow the penetration of the dye into the cells and to prevent leakage, respectively. PD146176 (0.5 µM) was added 1 h prior to the glutamate treatment. Glutamate (20 µM, final concentration in the well) was injected into each well with a plate reader coupled to an injection pump (FluoStar, BMG Labtech, Offenburg, Germany). (**b**) Primary cortical neurons were seeded on cover slips and stained with Fura-2 (5 µM) at day 6 after the preparation (1 h at 37 °C). PD146176 (0.5 µM) was added 1 h prior to the addition of glutamate (20 µM). Single cells were analyzed with a fluorescence microscope detecting the increase of intracellular calcium in single neurons. The experiments were at least repeated 3 times and all data are provided as mean ± S.D.

3.6. PD146176 reduces cell death after oxygen glucose deprivation in vitro and reduces brain infarction after MCAO in vivo

Cerebral ischemia causes severe and persistent brain damage and thus a detrimental disease with a high mortality rate. To date, tissue plasminogen activator (tPA) is the only available therapy in patients suffering from ischemic stroke. However, the number of stroke patients eligible for tPA treatment is very limited for safety reasons and, thus, the vast majority of patients do not receive any therapy targeting the cause of ischemia or mechanisms of infarct development.

Oxygen glucose deprivation (OGD) was used here as an in vitro model for cerebral ischemia to investigate the role of 12/15-LOX activation in delayed neuronal death. In order to validate the OGD model the highly potent and selective non-competitive NMDA glutamate receptor antagonist MK-801 (Sigma-Aldrich, Taufkirchen, Germany) was used, which is known to reduce neuronal damage after OGD and middle cerebral artery occlusion. Primary cortical neurons were treated with MK-801 (10 µM) 1 hour prior to OGD and were exposed to OGD for 4 hours. After 24 h of reperfusion the cells were analyzed by DAPI staining and quantification of pyknotic nuclei. MK-801 significantly reduced neuronal damage after OGD showing that the OGD protocol is valid (Figure 14a).

For investigation of the role of 12/15-LOX activation for delayed neuronal death after OGD, primary neuronal cultures were treated with PD146176 (0.5 µM) or AA861 (0.1 µM) 1 h before deprivation of oxygen and glucose. Cell viability was evaluated again by DAPI staining and counting of the pyknotic nuclei at 24 hours after reperfusion. 12/15-LOX inhibition significantly reduced cellular death induced by OGD in primary neurons indicating that 12/15-LOX activation is involved in ischemic neuronal death (Figure 14b).

This hypothesis was further addressed in a model of transient middle cerebral artery occlusion (MCAO) in mice to test the effect of 12/15-LOX inhibition in vivo. These experiments were performed by Uta Mamrak und Nicole Terpolilli at the Ludwig-Maximilians-Universität, Munich, Germany. The C57BL/6 mice obtained intraperitoneal injections of two different doses of PD146176 (0.4 and 4 mg/kg) 1 h before the induction of MCAO. The infarct volume in the brains was analyzed 24

hours after reperfusion. Pretreatment with PD146176 (4 mg/kg) significantly reduced the infarct volume in mouse brains suggesting 12/15-LOX as mediators of acute brain damage after MCAO (Figure 14c).

In addition, the neuroscore was evaluated in the mice at 1 and 24 hours after reperfusion. The neuroscore is used to judge about the motor activity of the animals. Mice pretreated with PD146176 (4 mg/kg) had a significantly improved neuroscore at 1 hour and 24 hours after reperfusion (Figure 14d). These results indicate that 12/15-LOX activation also participates in ischemic brain damage and might restore motor function.

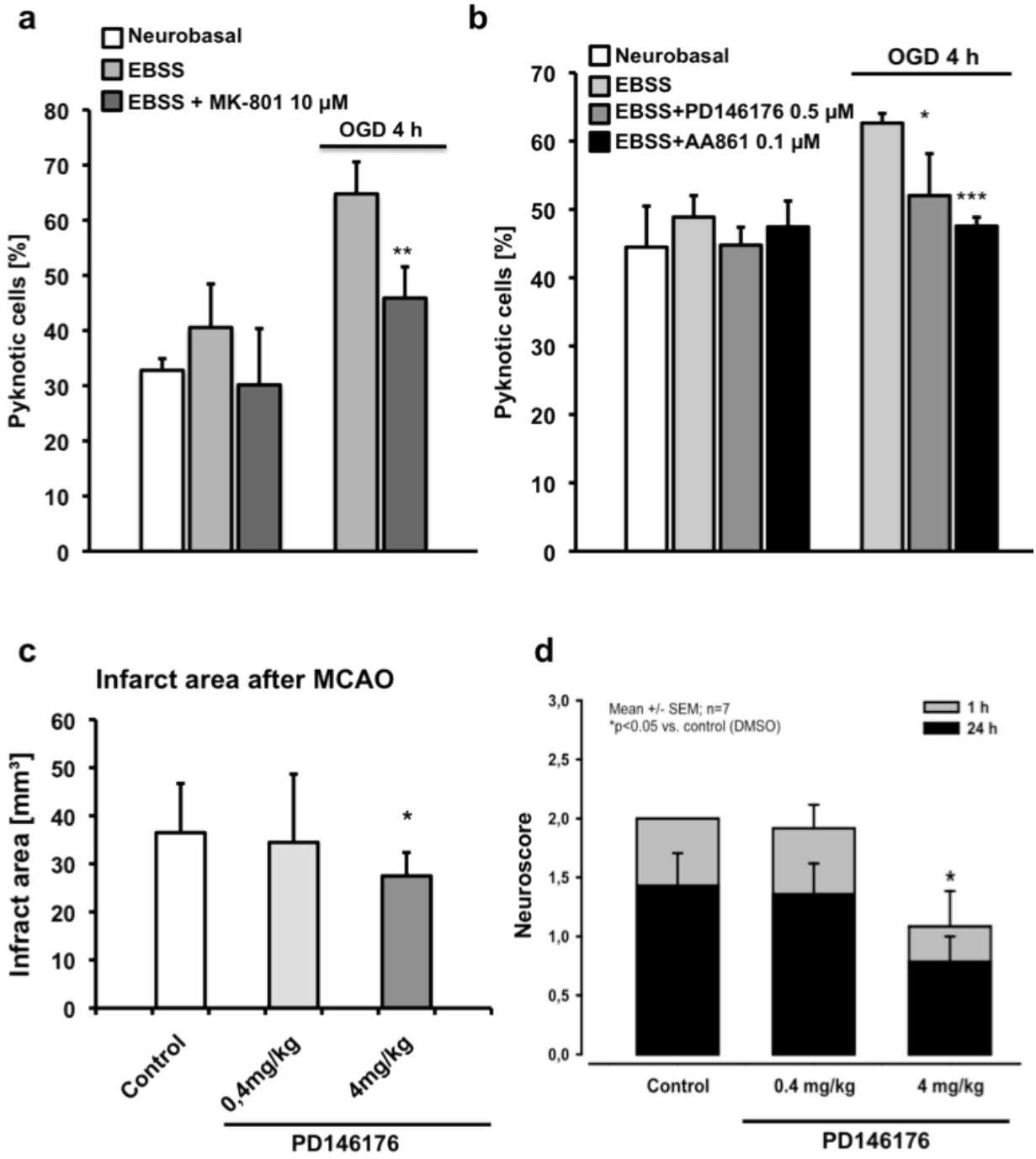

Figure 14: PD146176 reduces damage after OGD and MCAO in primary neurons. (**a**) For validation of the OGD model MK-801 (10 µM) was added to primary cortical neurons 1 hour before the induction of OGD (4 h). MK-801 significantly reduced OGD-induced cell death. (**b**) Primary cortical neurons were exposed to 4 h of OGD. 12/15-LOX inhibition (PD146176 0.5 µM, AA861 0.1 µM) significantly reduced cell death compared to controls. (**a, b**) Cell viability was evaluated by DAPI staining and counting of not less than 200 cells per sample. The experiments were at least repeated 3 times and all data are provided as mean ± S.D. *** P<0.001, ** P<0.01, * P<0.05 compared with glutamate-treated cells (ANOVA, Scheffé-test). (**c, d**) C57BL/6 mice were treated with PD146176 (0.4 mg/kg and 4 mg/kg) before the induction of MCAO. (**c**) The infarct area was calculated 24 hours after reperfusion. (**d**) The neuroscore was determined at 1 and 24 hours after reperfusion in order to analyze the motor activity of the animals. Data are provided as mean ± S.D. * P<0.05 (Mann-Whitney-U-test)

3.7. The role of 12/15-LOX in different models of oxidative stress

The previous results suggested 12/15-LOX activation as key mediator of glutamate-induced oxidative stress in HT-22 cells as well as in primary neurons.
Next, the role of 12/15-LOX activation was investigated in other well-accepted models of oxidative stress in neurons in order to elucidate, whether LOX activity is a general mechanism of neuronal cell death induced by various different oxidative stimuli. To this end, several prominent models of oxidative stress were analyzed to address the potential involvement of 12/15-LOX activity. HT-22 neurons were exposed to radical donors like glucose oxidase (GO) and H_2O_2 as well as to HNE (4-Hydroxynonenal), iron (II) sulfate and nitrogen monoxide (NO)-donors.

3.7.1. 12/15-LOX inhibition does not prevent neuronal death induced by radical donors

Radical donors are commonly used in models of lethal oxidative stress in neuronal cells and were applied in several studies on mechanisms of neurodegenerative diseases [139, 140]. On the basis of the previous findings in glutamate toxicity, it was interesting to analyze the role of 12/15-LOX activation in other settings of oxidative stress.
The radical donors glucose oxidase (GO) and H_2O_2 induced concentration- and time-dependent cell death in HT-22 cells (Figure 15a, 15b). It is important to note that GO induces a continuous release of H_2O_2 whereas H_2O_2 causes high levels of ROS immediately after the treatment. Therefore, the treatment with GO may be more physiological than the addition of H_2O_2.

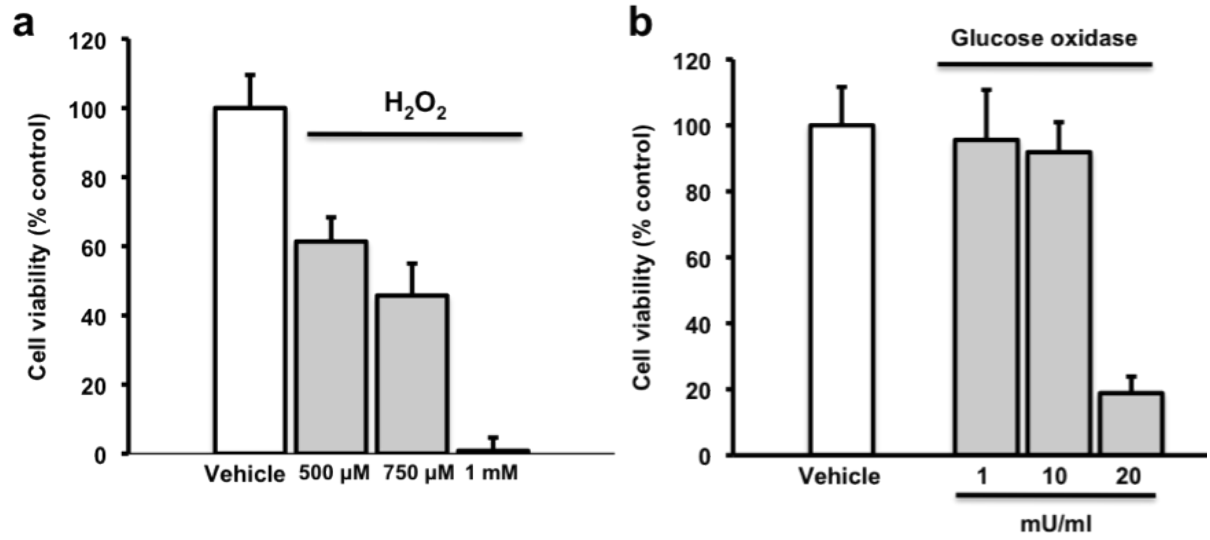

Figure 15: H_2O_2 and glucose oxidase induce cell death in HT-22 cells. HT-22 cells were treated with (**a**) H_2O_2 (500 µM – 1 mM) and (**b**) glucose oxidase (1 – 20 mU/ml). Cell death was evaluated by MTT assay at 14 – 16 h after the onset of the treatment (n=8). Cells died in a concentration- and time-dependent manner. The experiments were repeated 3 times and the results are presented as mean ± S.D.

To determine the potential role of 12/15-LOX in GO- and H_2O_2-induced cell death HT-22 cells were pretreated with PD146176 (0.5 µM) for one hour before incubation with H_2O_2 (500 – 700 µM) or glucose oxidase (10 – 20 mU). Cell viability was evaluated using the MTT assay at 14 h after the treatment showing that 12/15-LOX inhibition could not prevent cell death induced by radical donors (Figure 16a, 16b).

Radical scavengers like NAC (5 – 20 mM,) however, protected HT-22 cells against H_2O_2 induced cell death (Figure 16c).

Overall, these data show that glutamate-induced cell death and the associated oxytosis are not comparable with damage induced by radical donors and that 12/15-LOX activation may not play a major role in cell death of HT-22 cells exposed to radical donors.

In addition, these data confirm previous data [141] showing that PD146176 has no antioxidant properties per se, also confirming that the protective effects against glutamate toxicity were achieved through its activity as a 12/15-LOX inhibitor and not as a radical scavenger.

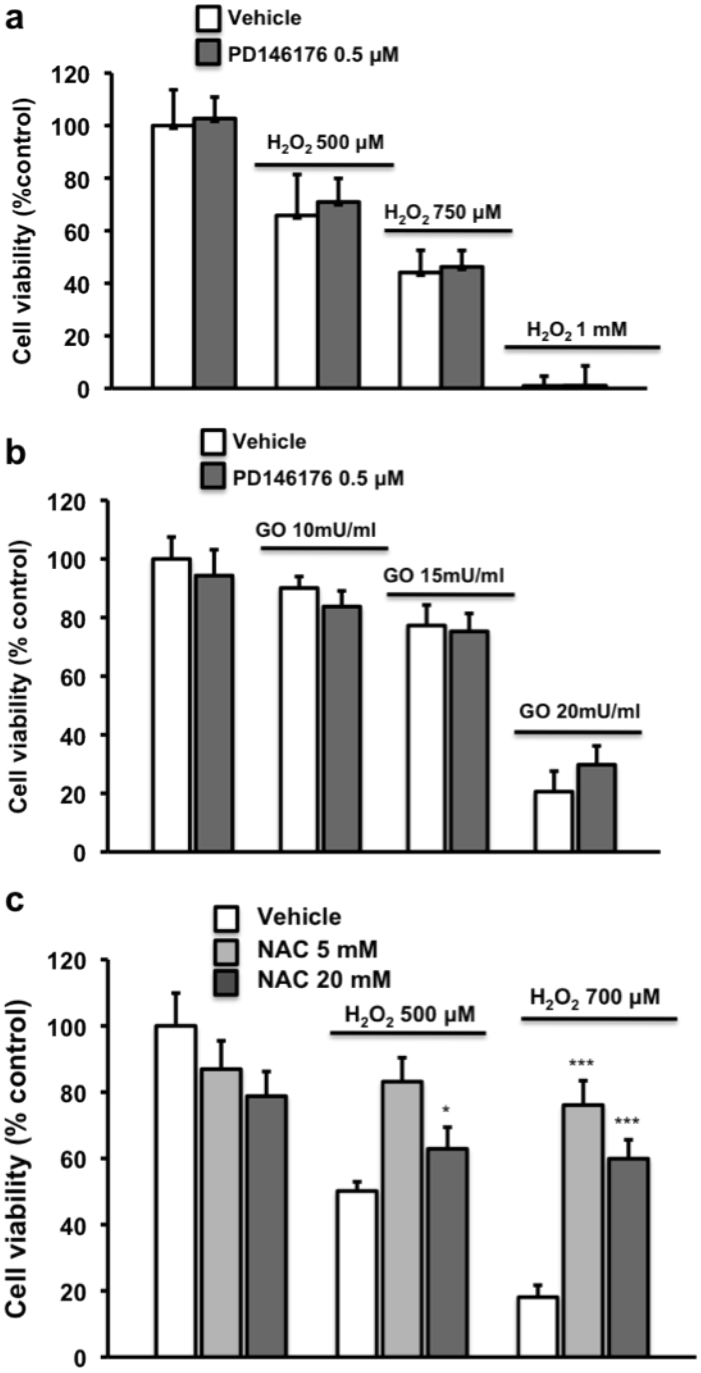

Figure 16: 12/15-LOX inhibition does not prevent radical donor-induced cell death. (**a**) H_2O_2 (500 – 700 µM) and (**b**) glucose oxidase (10 – 20 mU) were added to HT-22 cells 1 hour after pretreatment with PD146176 (0.5 µM). After 16 hours cell death was evaluated using the MTT assay (n=8). (**c**) HT-22 cells were treated with the antioxidant NAC (5 + 20 mM) and H_2O_2 for 16 hours. Cell viability was detected with the MTT assay (n=8). All experiments were repeated 3 times and the results are presented as the mean ± S.D. * $P<0.05$, *** $P<0.001$ compared with glutamate-treated cells (ANOVA, Scheffé-test).

3.7.2. Iron toxicity is not prevented by 12/15-LOX inhibition

It has been proposed that accumulation of iron (Fe^{2+}) and iron dependent formation of ROS through the Fenton reaction, are involved in neuronal cell death in neurodegenerative disorders. For example, in Alzheimer's Disease iron levels are increased in the brain and may thus contribute to the increase in ROS levels [142].

In order to analyze the role of 12/15-LOX in Fe^{2+}-induced oxidative stress iron sulfate solution (2 - 10 mM) was applied to HT-22 cells. The addition of iron sulfate induced the formation of Fe^{2+} and subsequent increase in ROS thereby causing time- and concentration-dependent cell death (Figure 17a).

The radical scavenger N-acetylcysteine (NAC, 5 – 20 mM) was added together with iron sulfate whereas PD146176 (0.5 μM) was added 1 hour before the damage with iron sulfate (2 – 5 mM). Cell viability was evaluated using the MTT assay. Interestingly, neither the antioxidant NAC (Figure 17b) nor the 12/15-LOX inhibitor (Figure 17c) protected the HT-22 cells against Fe^{2+}-induced toxicity.

These results show that cell death induced by Fe^{2+} is independent of 12/15-LOX activation and therefore following different mechanisms than glutamate-induced cell death. The fact that also the antioxidant NAC did not prevent iron toxicity indicates that iron causes cell death mechanisms that are either independent of ROS production or at least cannot be blocked by NAC either.

In addition, it is important to note that the results obtained with the MTT assay may cause the impression that NAC induced cell death itself but regarding the morphology of the cells, NAC only reduces the proliferation of the HT-22 cells.

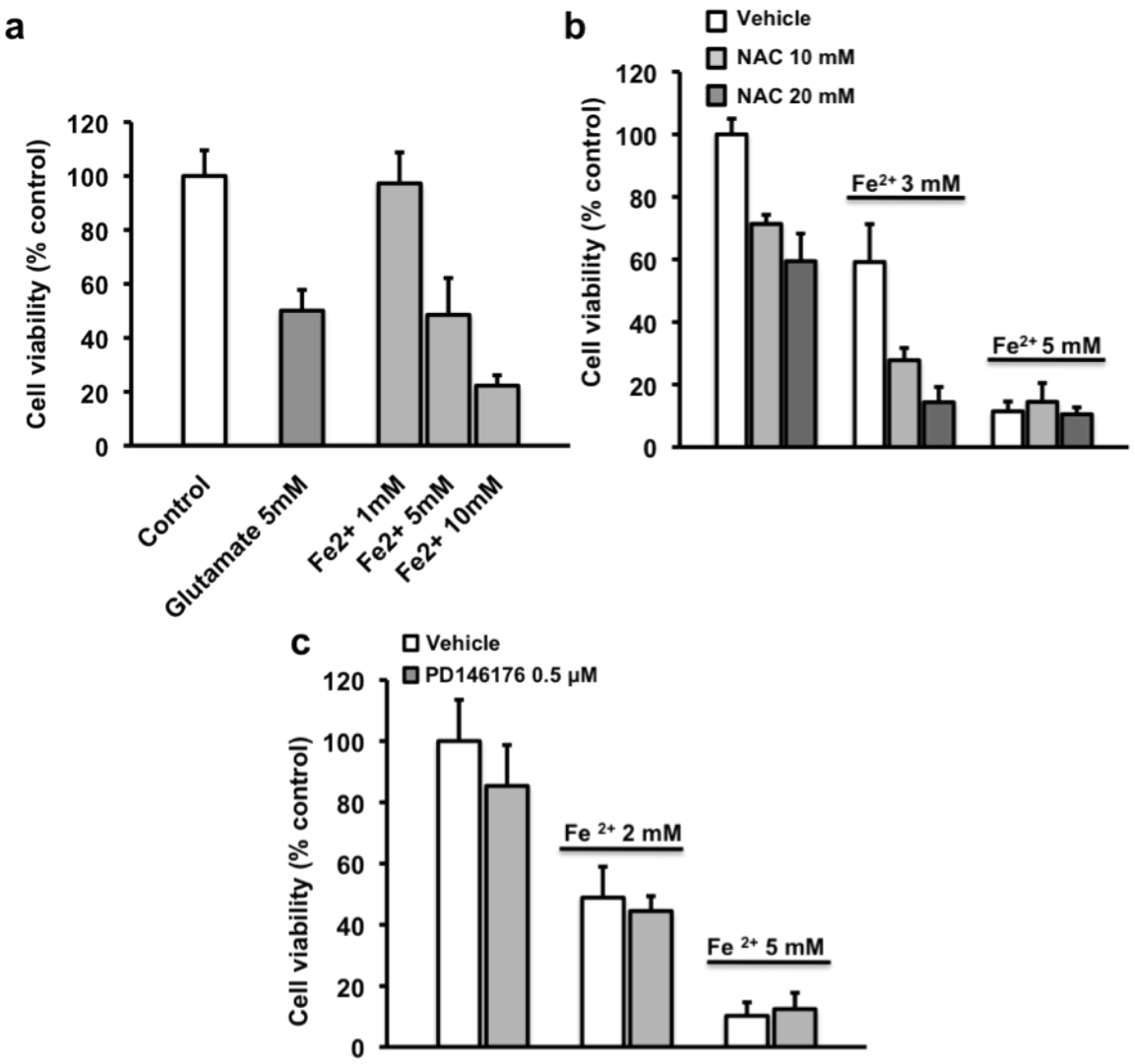

Figure 17: Fe^{2+} toxicity in HT-22 cells is not prevented by NAC or 12/15-LOX inhibition. (**a**) Iron sulfate (2 – 10 mM) induced cell death in HT-22 cells. (**b**) NAC (10 – 20 mM) and (**c**) PD146176 (0.5 µM) failed to prevent Fe^{2+}-induced cell death (n=8). Cell viability was detected using the MTT assay at 14 – 16 hours after the exposure to iron sulfate. All experiments were repeated 3 times and the results are presented as the mean ± S.D.

3.7.3. HNE induced cell death is not prevented by 12/15-LOX inhibition

4-Hydroxynonenal (HNE) is a toxic second messenger of free radical formation often detected, e.g. in the brain of AD patients, and is therefore also used as a model for oxidative stress to investigate mechanisms of in neurodegeneration.

Peroxidation of cellular membrane lipids or circulating lipoprotein molecules generates highly reactive aldehydes among which one of the most important is 4-hydroxynonenal. HNE levels are elevated in several neurodegenerative diseases and application of HNE to neuronal cultures is widely used as a model system of oxidative stress in neurodegenerative diseases [76, 143, 144].

PD146176 was used to investigate the role of 12/15-LOX activation after HNE treatment in HT-22 cells. HNE induced concentration- and time- dependent cell death in HT-22 neurons (Figure 18a) that could not be reduced by PD146176 (0.5 µM) (Figure 18b). Cell viability was measured using the MTT assay 14 – 16 hours after the exposure to HNE.

These data suggest that 12/15-LOX is not mediating cell death induced by HNE in HT-22 cells. Further, these results indicate that HNE induces different apoptotic death pathways than glutamate in these cells, and that glutamate toxicity does not involve formation of large amounts of HNE.

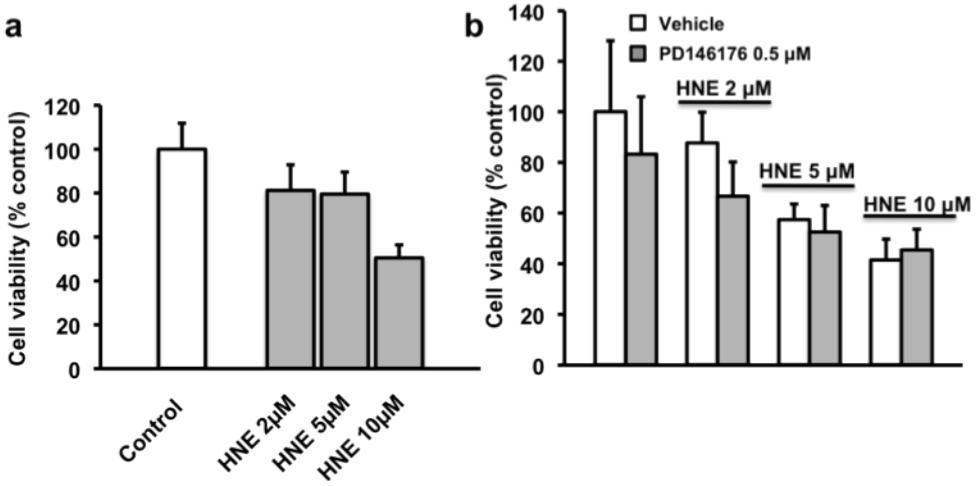

Figure 18: 4-hydroxynonenal (HNE) causes damage in HT-22 cells that is independent of 12/15-LOX activation. (**a**) HNE (2 – 10 µM) induced time- and concentration- dependent cell death in HT-22 cells (n=8). (**b**) The inhibition of 12/15-LOX by PD146176 (0.5 µM) failed to prevent HNE-induced damage (5 + 10 µM) (n=8). Cell viability was detected using the MTT assay. All experiments were repeated 3 times and the results are shown as the mean ± S.D.

3.7.4. NO toxicity and subsequent nitrosylation of proteins is not affected by 12/15-LOX inhibition

Nitrogen monoxide (NO) toxicity has been described to be involved in different neurodegenerative processes associated with enhanced oxidative stress [25, 113, 114, 123, 145]. It has been suggested that NO mediates, for example, the nitrosylation of Drp-1 and other proteins thereby inducing cellular death [107, 123, 124, 146-148]. Therefore, it was interesting to investigate the role of 12/15-LOX activation in NO-mediated cellular death in HT-22 neurons.

Here, the NO-donor DEANONOate (1 - 5 mM) was applied to induce NO toxicity by a fast release of NO. It is important to note that DEANONOate is not very stable suggesting that after the treatment high NO-levels were present which degraded very fast. DEANONOate induced a concentration dependent damage in HT-22 cells that was detected by the MTT assay at 14 hours after the onset of the treatment with DEANONOate (Figure 19a, 19b). In order to analyze the involvement of 12/15-LOX in NO-mediated toxicity PD146176 (0.5 μM) was added 1 h prior to DEANONOate. Cell death was detected again using the MTT assay 14 hours after the DEANONOate challenge. Inhibition of 12/15-LOX failed to prevent cell death induced by DEANONOate (Figure 19b) suggesting that NO-induced cell death does not involve 12/15-LOX activation in HT-22 cells.

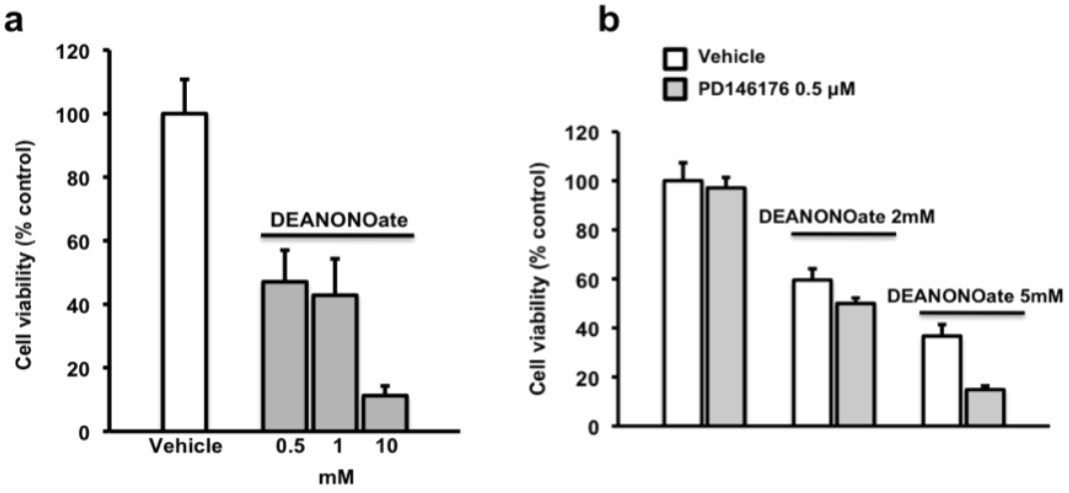

Figure 19: NO toxicity does not involve 12/15-LOX activity. (**a**) The NO-donor DEANONOate (0.5 – 10 mM) reduces cell viability in HT-22 cells in a concentration-dependent manner. (**b**) PD146176 (0.5 μM) was added 1 h prior to DEANONOate (2 – 10 mM). 12/15-LOX inhibition did not prevent DEANONOate-induced cell death (n=8). Cells were analyzed using the MTT assay 14 – 16 h after the onset of the treatment. The experiment was repeated 3 times. The data are presented as mean ± S.D.

In order to examine the role of potential NO release in further detail, the HT-22 cells were treated with sodium nitroprusside (SNP) (20 μM – 20 mM), which induces the formation of NO and CN^-, as well as of Fe^{2+}.

It is important to note that SNP may cause more persistent low levels of NO and also Fe^{2+} and CN^- are continuously released over time in contrast to the addition of DEANONOate or iron sulfate, where the toxic agent is immediately available at the applied concentration (compare 3.7.2). Cell viability was detected by using the MTT assay at 16 hours after SNP application. SNP reduced cell viability in the HT-22 cells in a concentration- and time-dependent manner (Figure 20a). To determine the role of 12/15-LOX after SNP treatment, PD146176 (0.5 μM) was added 1 hour prior to SNP. The MTT assay showed that 12/15-LOX inhibition failed to prevent SNP toxicity (Figure 20b).

These results suggest that cell death induced by NO-donors such as DEANONOate or SNP activate different apoptotic death pathways than glutamate and that 12/15-LOX was not involved in NO-mediated cell death in neuronal HT-22 cells.

In order to examine the mechanism of SNP toxicity in further detail total protein lysates of HT-22 cells were analyzed by western blotting after exposure to SNP and nitrosylation of tyrosine residues was evaluated. The NO-donor DEANONOate was used as positive control in order to confirm the function of the antibody. Interestingly, tyrosine-nitrosylation was not detectable in cells exposed to SNP suggesting that the formation of NO and subsequent tyrosine nitrosylation was not a prominent trigger of cell death in HT-22 cells (Figure 20c). Consequently, SNP toxicity may be mediated predominantly by CN^- or Fe^{2+} formation or may result from additive effects of all three toxic factors.

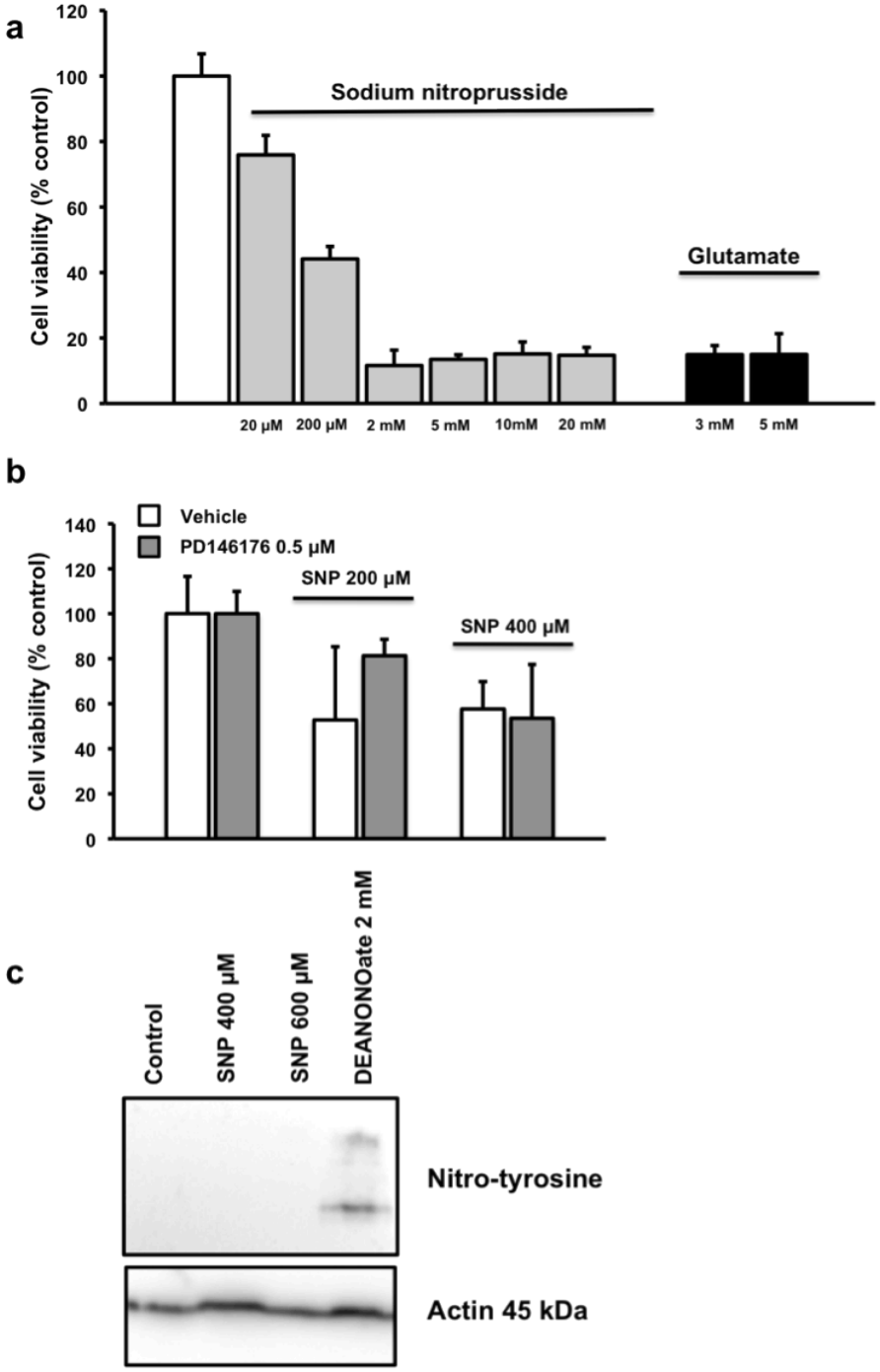

Figure 20: 12/15-LOX inhibition does not prevent SNP-induced cell death. (**a**) SNP (20 µM – 20 mM) induced death in HT-22 cells in a time- and concentration-dependent manner. (**b**) HT-22 cells were pretreated with PD146176 (0.5 µM) for 1 h. 12/15-LOX inhibition failed to prevent SNP-induced cell death (n=8). (**c**) SNP does not induce detectable nitrosylation of tyrosine residues in HT-22 cells. HT-22 cells were treated with SNP (400 - 600 µM) or with DEANONOate (2 mM). Total cell lysates were obtained from the damaged cells 16 h after the exposure to SNP or DEANONOate and analyzed by western blotting. Nitrosylated tyrosine residues were detected using an anti-nitro-tyrosine antibody (New England Biolabs GmbH, Heidelberg, Germany). Cell viability (a + b) was detected by the MTT assay at 14 – 16 h after the exposure to SNP. All experiments were repeated 3 times and the results are presented as the mean ± S.D.

To find out whether NO toxicity is relevant in glutamate induced cell death and contributes to glutamate-induced damage independently of 12/15-LOX activation, the NO synthesis was blocked by Nω-Nitro-L-arginine (L-NNA). L-NNA is a selective inhibitor of the neuronal (nNOS) and the endothelial (eNOS) nitric oxide synthase. The HT-22 cells were treated with glutamate (5 mM) and L-NNA (0.01 and 0.1 mM) for 16 hours. The cell viability was detected by MTT assay showing that the inhibitor of nNOS und eNOS failed to prevent glutamate-induced cell death (Figure 21a). These results indicate that NO-toxicity plays a minor role in HT-22 cells after the glutamate challenge.

To confirm that NO formation after the glutamate challenge is less important in HT-22 cells, total cell lysates were analyzed by western blotting. It is known that NO induces the nitrosylation of proteins which may contribute to subsequent apoptotic processes. Protein nitrosylation was detected using an antibody against nitrosylated tyrosine (New England Biolabs GmbH, Frankfurt am Main, Germany). DEANONOate was used as a positive control to confirm that the antibody worked properly. The analysis did not show nitrosylation of proteins after glutamate induced cell death while DEANONOate induced strong tyrosine nitrosylation (Figure 21b). This analysis confirmed the results obtained with the nNOS/eNOS-inhibitor and showed that glutamate does not induce the formation of NO in HT-22 cells.

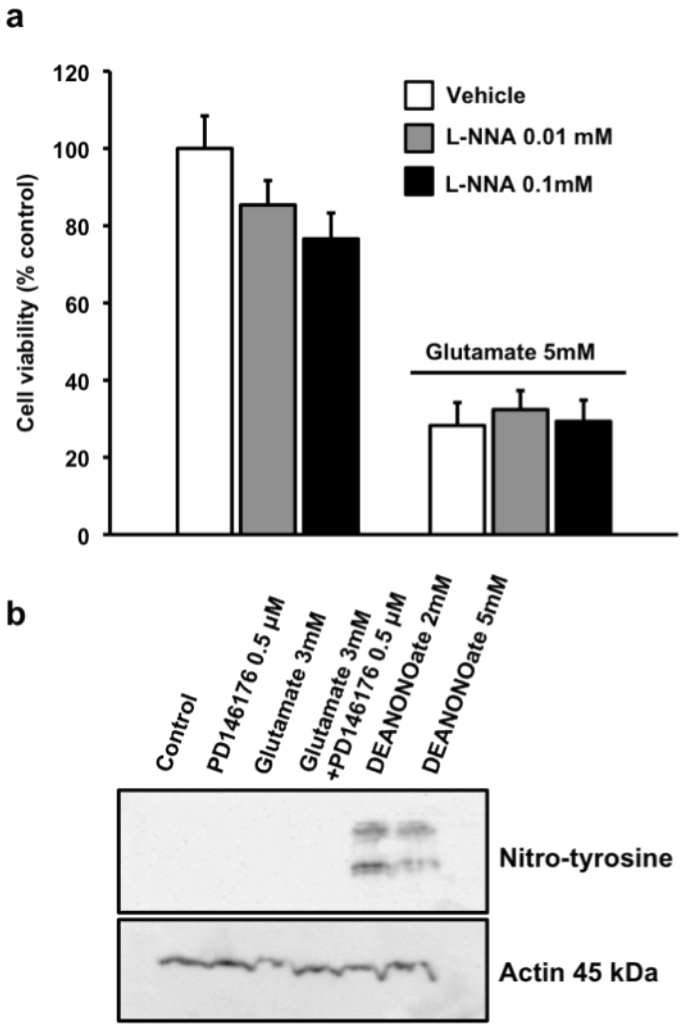

Figure 21: Glutamate does not induce NO-formation in HT-22 cells. (**a**) HT-22 cells were treated with glutamate (5 mM) and the nNOS/eNOS inhibitor L-NNA (0.01, 0.1 mM). The nNOS/eNOS inhibitor did not protect the HT-22 cells against glutamate toxicity (n=8). Cell viability was evaluated using the MTT assay at 14 – 16 h after the onset of glutamate treatment. (**b**) HT-22 cells were treated with PD146176 (0.5 µM) and glutamate (3 mM). The NO-donor DEANONOate (2 + 5 mM) was used as positive control. Total cell lysates of the cells were obtained 14 h after the exposure to glutamate and were analyzed by western blotting. An antibody against nitro-tyrosine (1:1000 in blocking buffer, New England Biolabs GmbH, Frankfurt am Main, Germany) was used to detect tyrosine nitrosylation and an anti-actin antibody (New England Biolabs GmbH, Frankfurt am Main, Germany) was used as loading control (n=3). All experiments were repeated 3 times and the results (**a**) indicate the mean ± S.D.

Overall, the experiments showed that 12/15-LOX activation plays a major role in the formation of ROS after glutamate exposure but not in other models of oxidative stress including exposure of neurons to radical donors, HNE, NO-donors or iron sulfate.

These results further suggest specific cell death mechanisms of oxytosis triggered by glutamate in neurons that involves 12/15-LOX activation. Therefore, this thesis further focused on cell death pathways that were involved downstream of 12/15-LOX activation in neurons exposed to glutamate toxicity.

3.8. Inhibition of Bid protects HT-22 neurons against glutamate-induced oxidative stress

So far, the results obtained in this thesis demonstrated a major role for 12/15-LOX in glutamate-induced lipid peroxidation and cell death. However, it was unclear how the 12/15-LOX dependent bi-phasic increase in ROS production was linked to downstream signaling pathways of programmed cell death. Very recent reports on the role of 12/15-LOX suggested a mitochondrial activity of 12/15-LOX [149] indicating that LOX may induce mitochondrial demise directly at the mitochondrial membrane. Thus, further investigations in this study focused on the link between 12/15-LOX and mitochondrial pathways of neuronal cell death in HT-22 cells.

It is known that mitochondria are important organelles in cell death mechanisms because they can release pro-apoptotic proteins and produce large amounts of ROS. The protective effect of the 12/15-LOX inhibitors included inhibition of the first increase in ROS after the glutamate challenge but failed to protect from further damage when applied after 8-10 h, i.e. the time point of the secondary more pronounced increase in ROS. This suggested that cell death pathways initially triggered by 12/15-LOX activity reached a ‘point of no return’ because other cell death messengers and, for example, production of ROS in mitochondria took over to execute cell death independent of 12/15-LOX activity. To identify key elements of these secondary events and the mode of mitochondrial death pathways were thus the next aims.

One possible candidate that may link increased ROS production and mitochondrial dysfunction in HT-22 cells is the pro-apoptotic Bcl-2 family protein Bid.

Bid plays an important role in glutamate induced cell death in HT-22 cells [26] and also in primary neurons [131, 150]. The selective Bid inhibitor BI-6C9 [151] significantly reduced glutamate induced cell death in HT-22 cells (Figure 22) as well as in primary neurons [150] and prevented mitochondrial demise [26] suggesting Bid as a key molecule in glutamate-induced neuronal cell death. Consequently, the following experiments addressed the potential link between Bid and 12/15-LOX in glutamate-induced neuronal damage in HT-22 neurons.

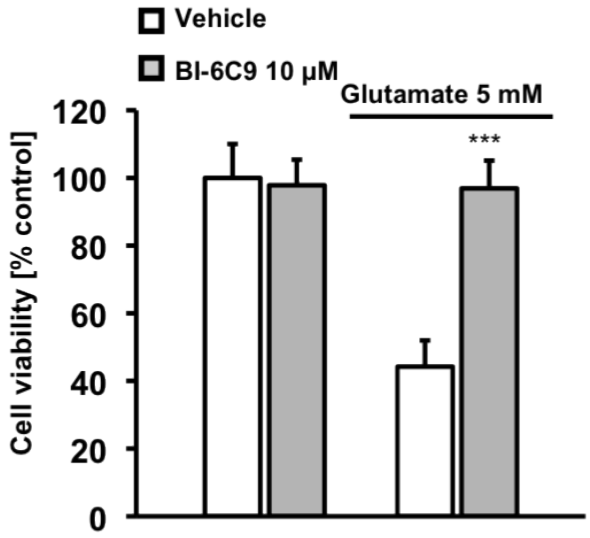

Figure 22: Bid inhibition protects HT-22 cells against glutamate-induced cell death. HT-22 cells were treated with glutamate (5 mM) and the small molecular Bid inhibitor BI-6C9 (10 µM). BI-6C9 prevented glutamate-induced cellular death. Cell viability was detected by using the MTT assay (n=8). The experiment was repeated 3 times and the results are presented as the mean ± S.D. *** P<0.001 compared with glutamate-treated cells (ANOVA, Scheffé test).

To find out more about the potential link of the Bid protein and the 12/15-LOX, HT-22 cells were transfected with a vector, which causes the expression of the cytotoxic truncated Bid (tBid), which induces cellular death within 24 h. The cells were treated with PD146176 (0.5 µM) or AA861 (0.1 µM) one hour before the transfection and cell viability was detected using the MTT assay 14 hours after the treatment. Notably, inhibition of 12/15-LOX could not prevent tBid induced cell death (Figure 23a) suggesting that Bid activation occurs downstream of 12/15-LOX activity. Clearly, 12/15-LOX activity does not contribute to mitochondrial pathways

downstream of tBid toxicity. In addition, the vitamin E analog Trolox failed to prevent tBid induced toxicity (Figure 23b) confirming the note that Bid-mediated cell death did not require the formation of ROS but may involve other apoptotic pathways.

As shown earlier in this study, increasing lipid peroxidation has been detected at different time points after glutamate treatment. Now, both, increased ROS formation and Bid activity have been identified as key mechanisms in glutamate-induced neurotoxicity, with Bid acting independent of 12/15-LOX.

Thus it was next interesting to examine if Bid inhibition could also block the detected increases in ROS in a similar manner as 12/15-LOX inhibition.

Lipid peroxidation was determined after the glutamate challenge in the presence or absence of the Bid inhibitor BI-6C9 using the BODIPY assay and subsequent FACS analysis.

Interestingly, inhibition of Bid activation failed to reduce the increase of lipid peroxidation 6 - 8 h after glutamate challenge. In contrast, BI-6C9 significantly reduced the secondary increase in lipid peroxidation as determined 17 h after the glutamate treatment (Figure 23c, 23 d). Comparing these results with the data showing that 12/15-LOX inhibition also reduced the first increase in lipid peroxidation (6 – 8 h) these data confirmed the suggestion that the activation of 12/15-LOX occurs upstream of Bid activation in HT-22 cells. The first increase in ROS seems is to be attributed to the activation of 12/15-LOX and is thus affected by 12/15-LOX inhibitors but not by Bid inhibition.

The secondary formation of ROS after 16 – 18 h is much stronger than the first increase and appears to be a consequence of mitochondrial damage and the subsequent production of large amounts of ROS in the mitochondria.

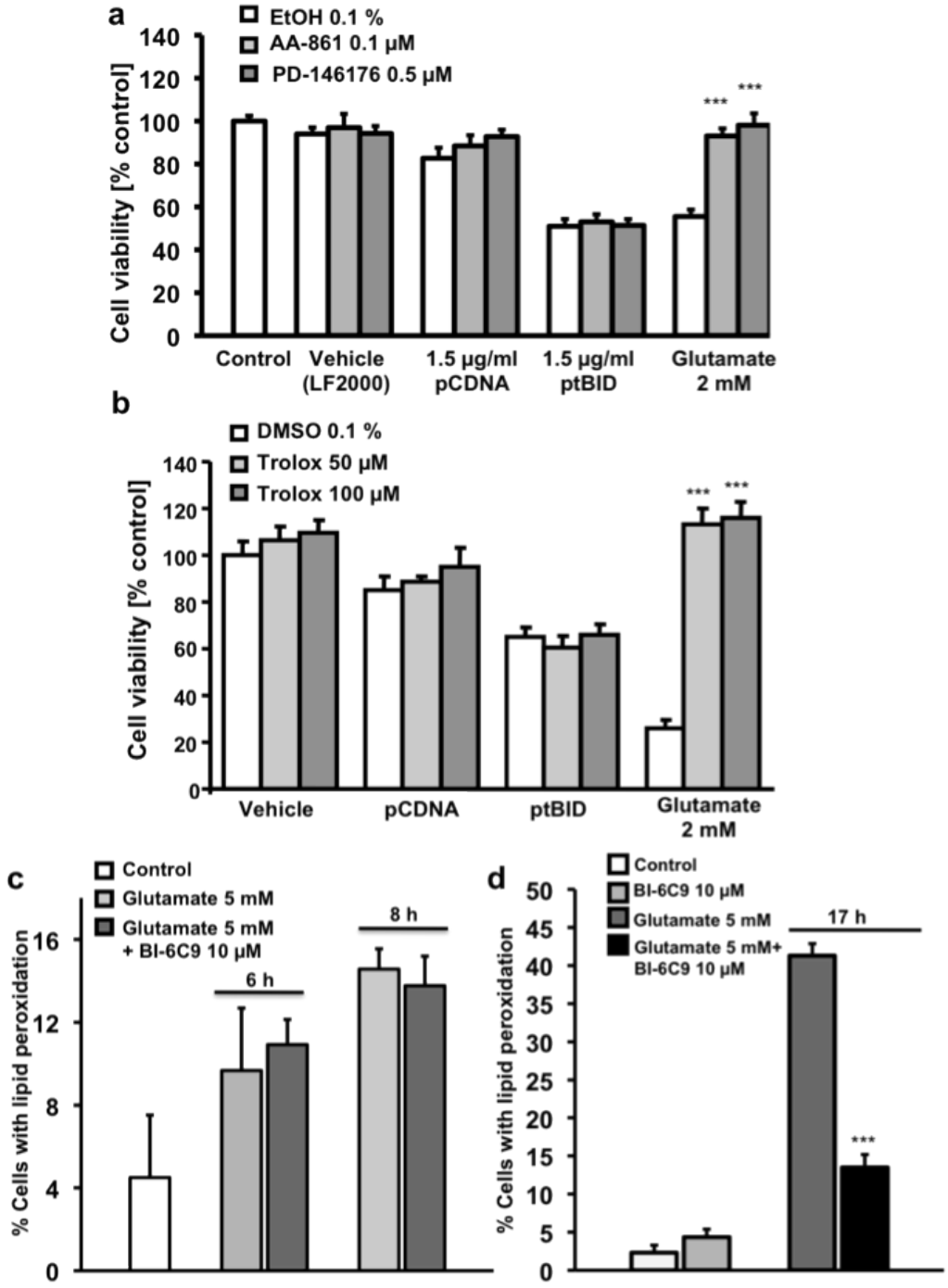

Figure 23: 12/15-LOX activation triggers glutamate-induced oxytosis, upstream but not downstream of Bid. (**a**) PD146176 (0.5 µM) or AA861 (0.1 µM) were added to HT-22 cells before the transfection with a tBid expression vector (ptBid). In addition, the cells were damaged with glutamate (2 mM) to control the sensitivity of the cells. Cell death was detected by using MTT assay 14 h after the transfection (n=8). (**b**) The vitamin E analog Trolox (50, 100 µM) was applied prior to the transfection of HT-22 cells with ptBid or exposure to glutamate (2 mM). MTT assay was used to determine cell viability 14 h later (n=8). (c + d) Lipid peroxidation was detected (**c**) 6 - 8 h and (**d**) up to 17 h after onset of glutamate exposure by FACS analysis after staining cells with BODIPY C11 (Ex = 488nm, Em = 530nm, 613nm). The Bid inhibitor BI-6C9 was present in the medium 1 h before and during the glutamate challenge (n=3). All experiments were repeated 3 times and the results are reported as mean ± S.D. *** P<0.001 compared with glutamate-treated cells (ANOVA, Scheffé test).

3.9. NADPH oxidase activation mediates mitochondrial demise in HT-22 neurons

The previous results suggested a critical role of Bid-mediated mitochondrial demise and the subsequent pronounced increases in ROS during glutamate-induced oxidative stress in HT-22 cells. Previous studies suggested that NADPH oxidase activation can also mediate mitochondrial damage in neuronal cell death, in particular when triggered by ATP depletion and downstream of Bid-mediated mitochondrial damage [152-157].

NADPH oxidase (NOX), is a cytosolic enzyme that catalyzes the transfer of an electron from NADPH to molecular oxygen and induces the formation of superoxide. Therefore, NOX may be a source of the enhanced ROS formation in the second phase of glutamate-induced oxytosis.

In order to analyze the role of the NADPH oxidase in HT-22 neurons and especially its possible link to mitochondrial demise and the secondary increase in ROS the NOX inhibitor DPI (Diphenyleneiodonium chloride, Enzo Life Science, Lörrach, Germany) was applied.

HT-22 cells were pretreated for one hour with DPI and exposed to glutamate (5 mM) for 14 – 16 hours. Cell death was detected using different methods. In addition to MTT assays (Figure 24a) and detection of annexin V/propidium iodide (PI) staining (Figure 24b), impedance measurements (Figure 24c) were performed using the xCELLigence system (Roche Applied Science, Penzberg, Germany). The results showed that DPI (0.1 µM) protected the cells significantly against glutamate-induced cell death suggesting that activation of the NADPH oxidase was involved in glutamate-induced neuronal cell death in HT-22 cells.

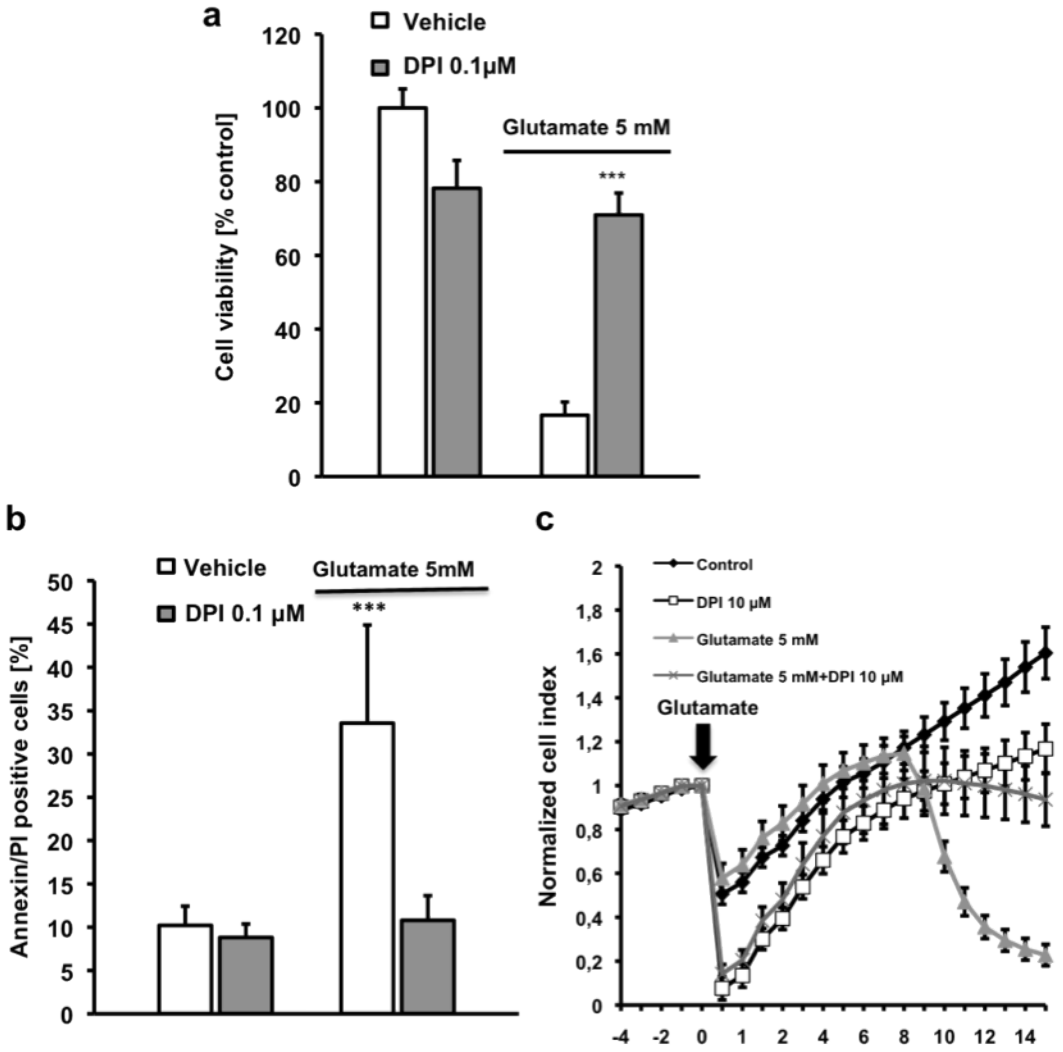

Figure 24: NOX inhibition prevents glutamate-induced cell death. The NOX inhibitor DPI (0.1 µM) was added 1 hour prior to the glutamate treatment (5 mM). Cell viability was evaluated with (**a**) the MTT assay, (**b**) annexin V/PI staining and (**c**) impedance measurements (c). The time point of the addition of glutamate is marked as "0 h" in the xCELLigence-graph. All experiments were repeated 3 times and the results are presented as the mean ± S.D. * *P*<0.05, ** *P*<0.01, *** *P*<0.001 compared with glutamate-treated cells (ANOVA, Scheffé-test).

As DPI protected HT-22 cells against glutamate toxicity, it was interesting to examine the time-dependent role of NADPH oxidase in neuronal oxidative stress. Therefore, DPI was added at different time points between 2 h and 15 h after onset of the glutamate treatment. HT-22 cells were protected against glutamate toxicity even when DPI was added up to 8 h after the glutamate challenge indicating that beyond that time point glutamate-induced cell death proceeded too far for protection by NOX inhibition (Figure 25).

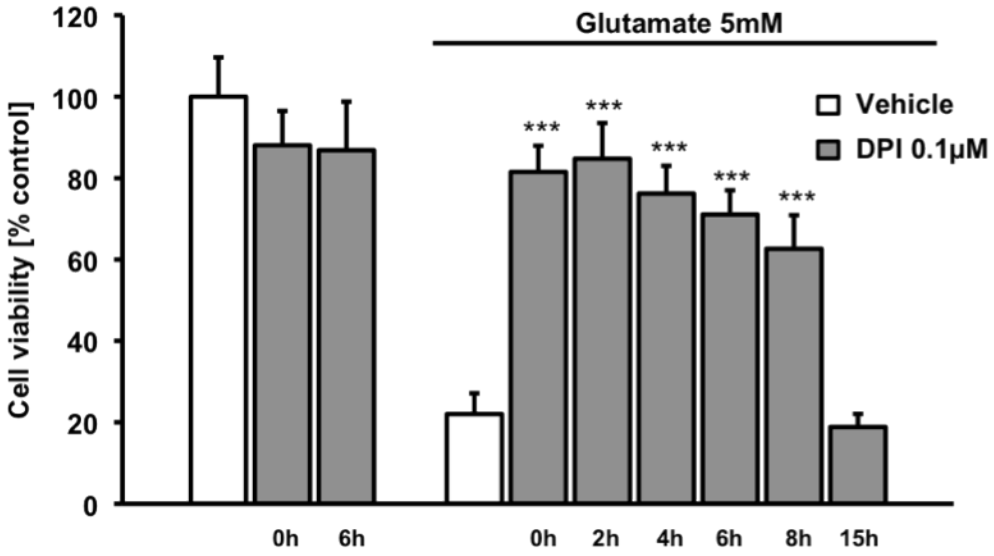

Figure 25: The NOX inhibitor DPI protects HT-22-cells when applied up to 8 h after glutamate treatment. DPI (0.1 µM) was added 2 – 15 h after glutamate challenge. Inhibition of the NADPH oxidase protected the cells even if DPI was added 8 h after glutamate-induced damage (n=8). Cell viability was detected by the MTT assay at 17 h after the onset of the treatment. The experiment was repeated 3 times and the results are presented as the mean ± S.D. *** P<0.001 compared with glutamate-treated cells (ANOVA, Scheffé-test).

Since previous studies suggested a link of NADPH oxidase to mitochondrial demise the effect of NOX inhibition on mitochondria was further analyzed by monitoring the effect of DPI on mitochondrial morphology and ATP levels.

For the investigation of mitochondrial morphology, the HT-22 cells were transfected with a plasmid inducing the expression of a green-fluorescent protein targeted to mitochondria (mitoGFP). The cells were analyzed using a fluorescence microscope (DMI 6000 B, Leica, Wetzlar, Germany; connected to a CCD camera DFC 360 FX, Leica, Wetzlar, Germany) for the quantification of mitochondrial morphology. For the quantification three different categories of mitochondrial morphology were defined (category 1: tubulin-like, category 2: intermediate, category 3: fragmented) and analyzed in at least 200 cells per condition.

Interestingly, DPI reduced glutamate-induced mitochondrial fragmentation after glutamate challenge (Figure 26a) suggesting a link between mitochondrial demise and NOX activity in HT-22 cells.

In order to explore the effect of glutamate-induced NOX activation on mitochondrial function ATP-levels were detected in the cells, because mitochondrial damage

results in loss of ATP production in the cells (ViaLight MDA Plus-Kit, Lonza, Verviers, Belgium). Concomitant with the cytoprotective effect, the NOX inhibitor DPI restored ATP levels in HT-22 cells and thus prevented the loss of energy associated with glutamate toxicity (Figure 26b). These results indicated a role for NADPH oxidase in glutamate-induced cell death in HT-22 cells and identified NOX as an important mediator of mitochondrial damage.

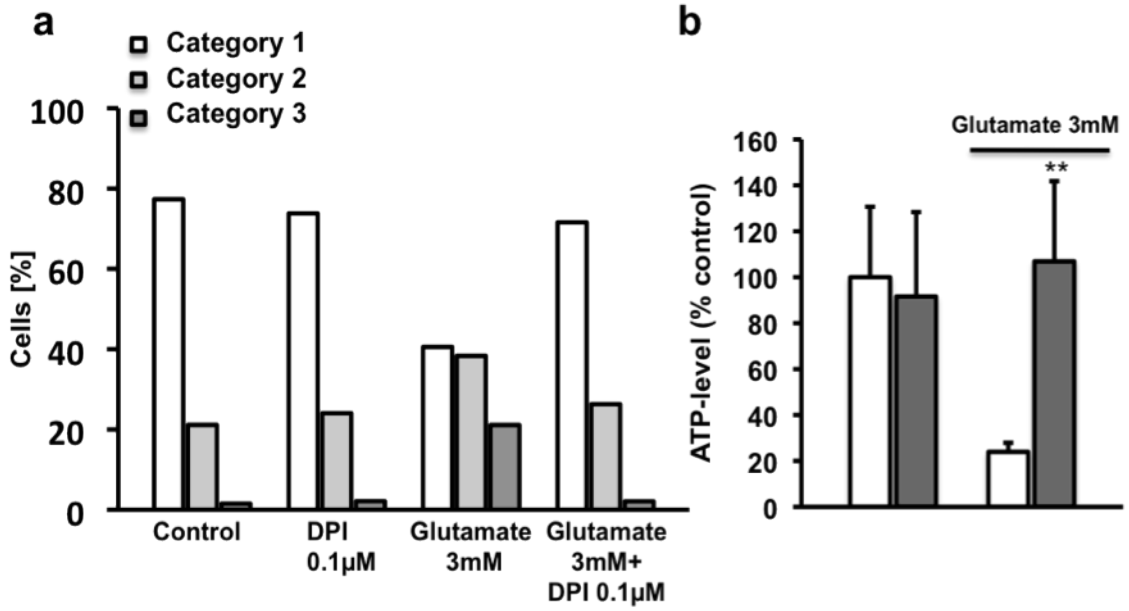

Figure 26: NADPH oxidase inhibition preserves mitochondrial morphology and energy-metabolism. (**a**) HT-22 cells were transfected with mitoGFP and damaged with glutamate (3 mM) 24 h after the transfection. The NOX inhibitor DPI was added 1 h prior to glutamate. 16 h after the addition of glutamate mitochondrial morphology was evaluated (category 1: tubulin-like, category 2: intermediate, category 3: fragmented) (n=3). (**b**) ATP-levels were determined by luminescens measurements after glutamate challenge. DPI prevented the glutamate-induced loss of ATP (n=8). All experiments were repeated 3 times and the results are presented as the mean ± S.D. ** *P*<0.01 compared with glutamate-treated cells (ANOVA, Scheffé-test).

For more detailed investigation on the role of NOX in glutamate-induced neuronal death the link between NOX and other important pro-apoptotic proteins was analyzed. In particular, the mechanistic link between Bid activation and NOX activity was investigated because of the key role for Bid activation in mitochondrial damage after induction of glutamate toxicity.

The HT-22 cells were transfected with a tBid expression vector 24 h after the seeding and pretreated with DPI (0.1 and 10 μM) one hour before the transfection. Cell viability was evaluated using the MTT assay at 14 hours after the transfection.

It is interesting to note that DPI failed to prevent tBid-induced toxicity (Figure 27) indicating that NOX activation occurred upstream of Bid activation.

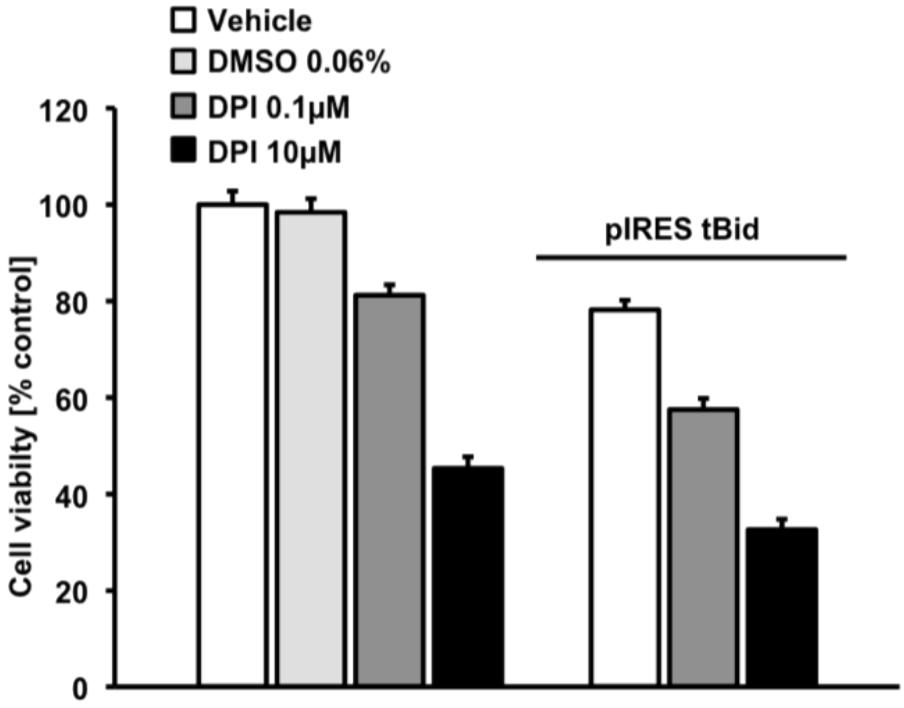

Figure 27: DPI failed to prevent tBid induced cell death. HT-22 cells were pretreated with DPI (0.1 μM) and transfected with the pIRES tBid vector 24 h after the seeding. After 12 h cell viability was evaluated with the MTT assay (n=4). The experiment was repeated 3 times. The data are presented as mean ± S.D.

In summary, these results showed a key role of NADPH oxidase in glutamate-induced cell death in HT-22 cells and suggested a link of NOX to mitochondrial demise.

3.10. Inhibition of 12/15-LOX inhibits mitochondrial demise, the subsequent loss of ATP and preserves mitochondrial morphology

The previous results suggested a link between 12/15-LOX and Bid activation and mitochondrial damage in HT-22 cells exposed to glutamate.

Mitochondria play a key role in cell death induced by oxidative stress and mitochondrial fusion and fission processes are known to be involved in neurodegenerative processes and cell viability [31, 54, 55]. Functional breakdown of mitochondria leads to loss of ATP, increased ROS production and release of pro-apoptotic proteins from the organelles. Consequently, the mitochondrial demise represents a crucial step in neuronal death.

Here, pathological changes in mitochondria were assessed in further detail to elucidate the intrinsic pathways involved in glutamate toxicity in HT-22 cells.

Loss of energy is known as key mediator of neuronal cell death because neurons depend on high levels of energy. For further determination of the mitochondrial 12/15-LOX activity and the link to Bid activation, ATP levels were measured in HT-22 cells after the glutamate challenge.

Glutamate (5 mM) induced a strong loss of ATP in HT-22 cells suggesting glutamate-induced mitochondrial damage and permeabilization (Figure 28a). The first detectable loss of ATP became obvious between 6 and 12 hours after the exposure to glutamate indicating that the beginning of mitochondrial damage occurs in this time window. To test the effect of 12/15-LOX inhibition on the loss of ATP after glutamate treatment, PD146176 was added one hour before the glutamate challenge. The pretreatment with 12/15-LOX inhibitors completely prevented the loss of ATP in the cells after induction of oxidative stress (Figure 28b) showing that 12/15-LOX inhibition prevented mitochondrial damage and the subsequent ATP loss.

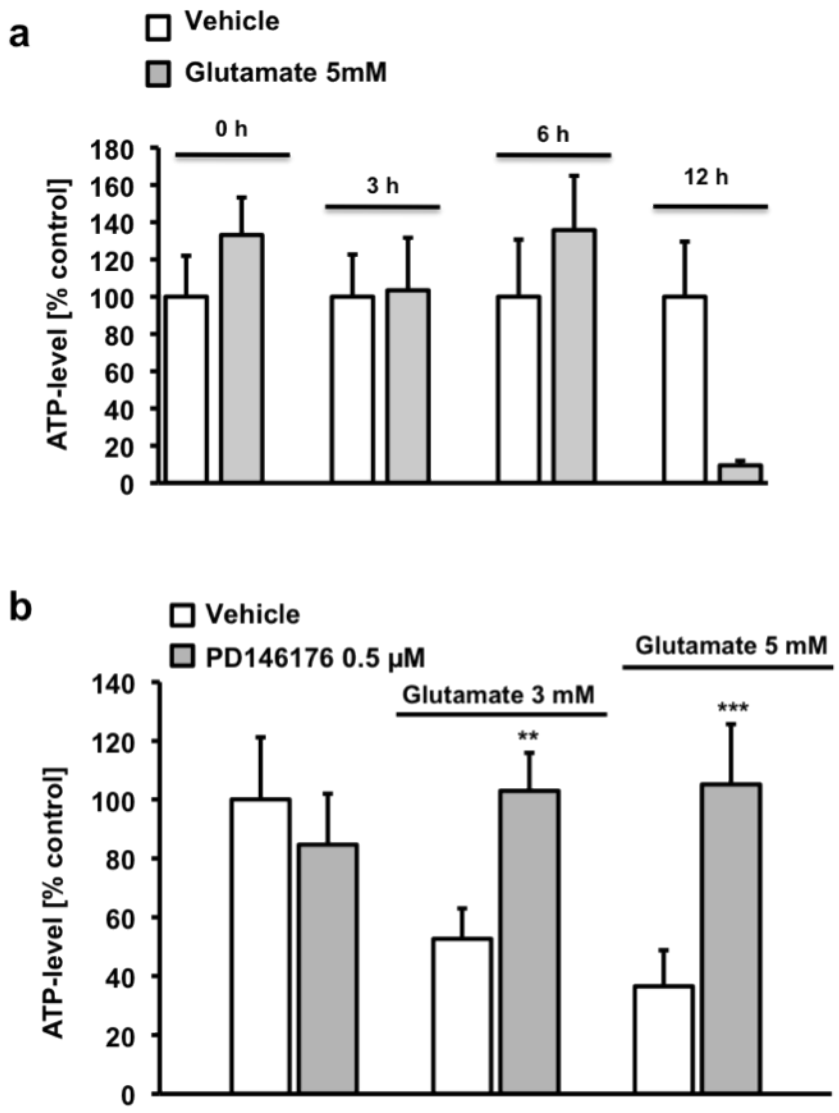

Figure 28: Glutamate induces loss of ATP that is prevented by PD146176. (**a**) ATP-levels were detected at different time-points after glutamate challenge. Glutamate induced a time-dependent loss of ATP in HT-22 neurons. (**b**) PD146176 (0.5 µM) inhibits the loss of ATP after the exposure to glutamate. All experiments were repeated 3 times and the results represent the mean ± S.D. ** $P<0.01$, *** $P<0.001$ compared with glutamate-treated cells (ANOVA, Scheffé-test).

These results suggested that 12/15-LOX activation leads to mitochondrial damage after exposure to glutamate in HT-22 neurons. In order to understand the effects on mitochondria, the next steps included analysis of the mitochondrial morphology and the mitochondrial membrane potential.

For this purpose HT-22 cells were transfected with a vector inducing the expression of mitoGFP. The vector leads to the expression of a green fluorescent protein in mitochondria and allows the observation of mitochondrial morphology. Under

standard growth conditions, HT-22 cells contain elongated mitochondria whereas glutamate treatment induced pronounced mitochondrial fragmentation. 12/15-LOX inhibition reduced glutamate-induced fragmentation and increased the percentage of elongated mitochondria (Figure 29a, 29b) showing again that 12/15-LOX is a key mediator of mitochondrial damage and metabolism.

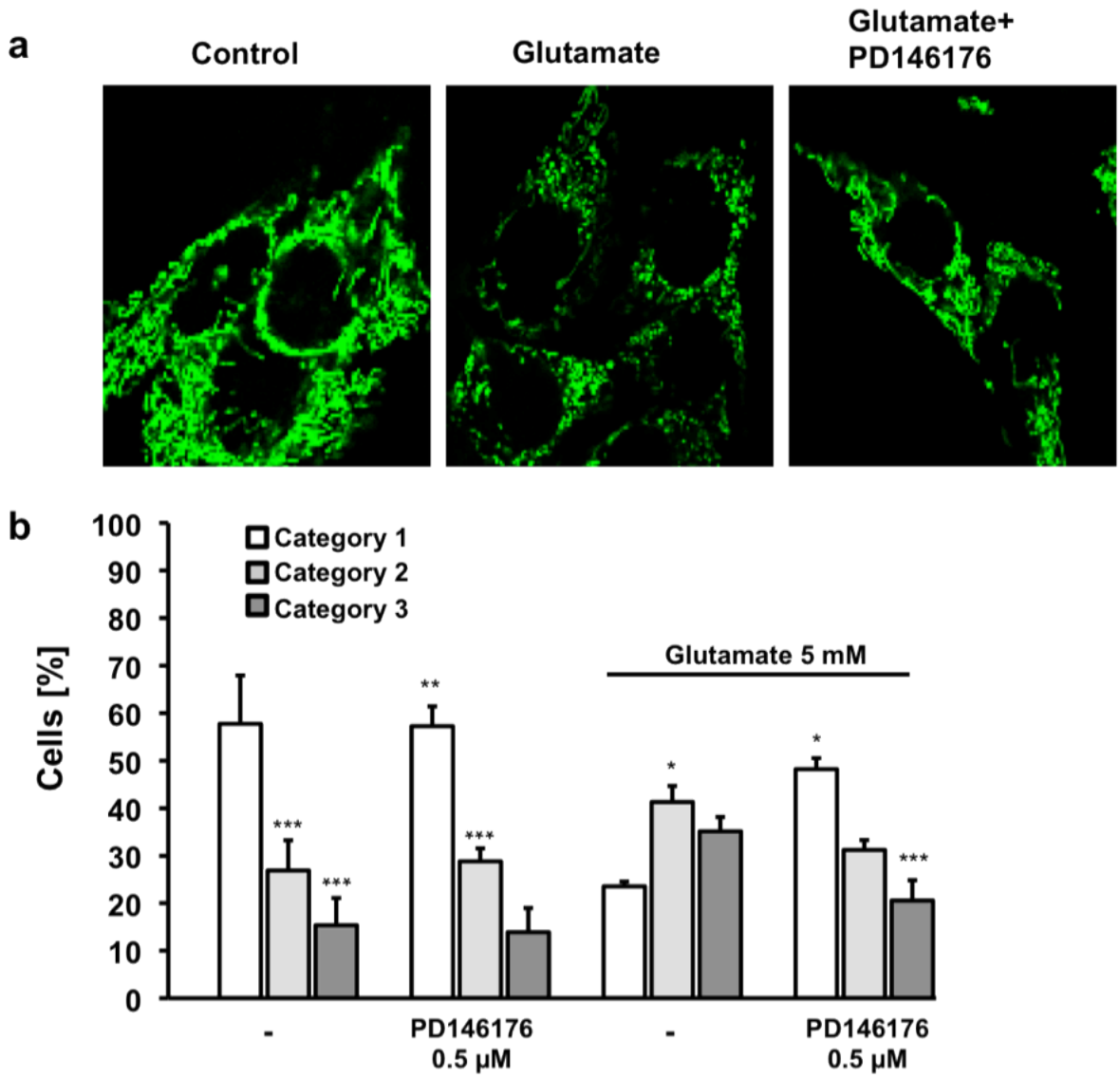

Figure 29: The 12/15-LOX inhibitor PD146176 (0.5 µM) prevents glutamate-induced mitochondrial fragmentation. (**a**) HT-22 cells were transfected with mitoGFP using Lipofectamine 2000 and seeded in ibidi slides. Twenty-four hours later the cells were damaged with glutamate 5 mM (n=4). (**b**) Mitochondrial morphology was analyzed by fluorescence microscopy and classified into 3 categories indicating the status of fission and fusion (category 1: tubulin-like, category 2: intermediate, category 3: fragmented) (n=4). All experiments were repeated 3 times and the results represent the mean ± S.D. * $P<0.05$, *** $P<0.001$ compared with glutamate-treated cells (ANOVA, Scheffé-test).

In addition, the mitochondrial membrane potential was analyzed using the fluorescent dye JC-1 (2 µM). The loss of mitochondrial membrane potential is detected by a loss of red fluorescence that can be measured by FACS analysis. Carbonyl cyanide m- chlorophenylhydrazone (CCCP, 50 µM) that induces a fast and strong mitochondrial depolarization was used as positive control. The cells were examined 16 hours after glutamate challenge. Glutamate (2 mM) caused a loss of mitochondrial membrane potential as shown by the reduced number of cells with red fluorescence. PD146176 significantly reduced the glutamate-induced loss of mitochondrial membrane potential (Figure 30a, 30b). These data confirmed that 12/15-LOX inhibition prevented mitochondrial damage thereby rescuing the HT-22 neurons from glutamate toxicity.

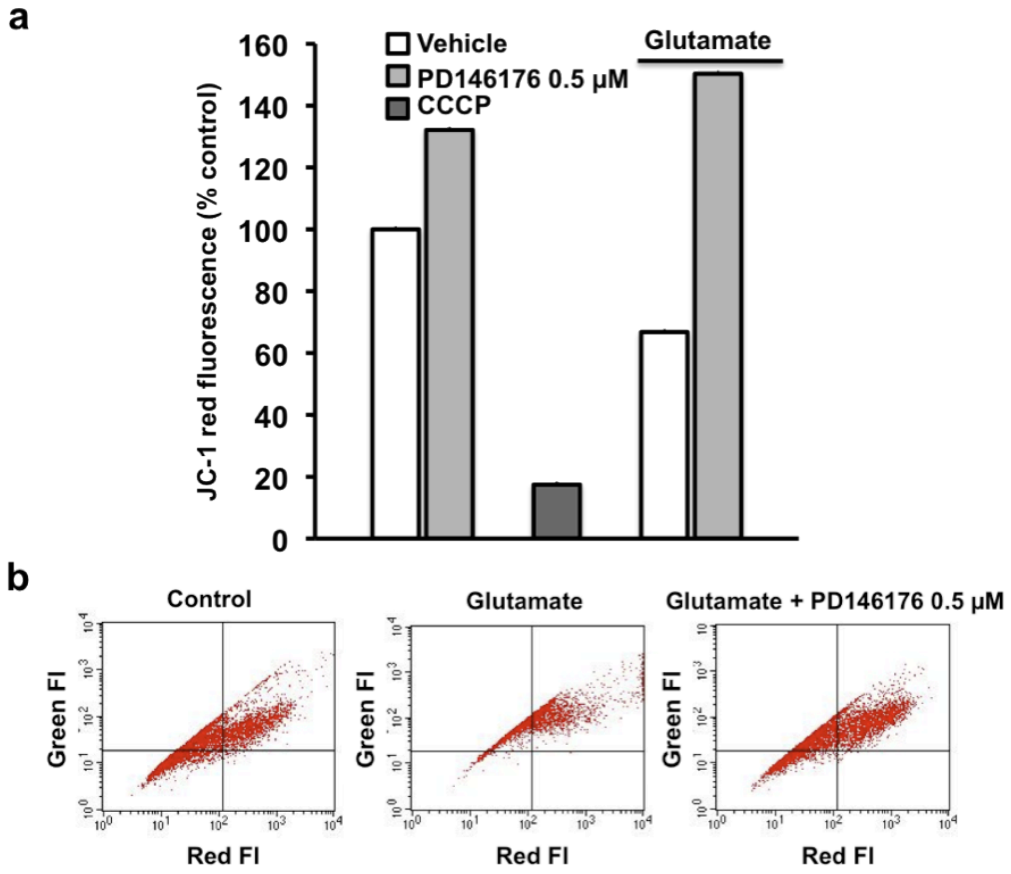

Figure 30: 12/15-LOX inhibition prevents the disruption of the mitochondrial membrane potential. (**a, b**) The mitochondrial membrane potential was measured using the JC-1 fluorescent dye. HT-22 cell were treated with glutamate (2 mM) and pretreated with PD146176 (0.5 µM). Sixteen hours later the cells were stained with JC-1 (2 µM) and analyzed by FACS measurements. CCCP (50 µM) was used as positive control to induce loss of the mitochondrial membrane potential. The green fluorescence (green Fl) indicates the loading of the cells with the dye whereas the red fluorescence (red Fl) is only detectable in cells with an intact mitochondrial membrane potential. Glutamate induced a loss of red fluorescence that could be prevented by PD146176 (n=3).

In summary, 12/15-LOX influenced mitochondrial morphology, energy metabolism and also mitochondrial membrane potential thereby protecting the cells against glutamate toxicity.

In order to further explore the potential role of 12/15-LOX on the mitochondrial level the cells were treated with rotenone (10 – 100 μM). Rotenone inhibits the mitochondrial electron transport chain at complex I and induces pronounced damage in HT-22 cells (Figure 31a, 31b). It was interesting to explore the effect of 12/15-LOX inhibition on rotenone-induced damage to see whether 12/15-LOX may mediate cell death downstream of complex I inhibition.

Cell viability was measured by the MTT assay at 16 hours after onset of the treatment with rotenone. It is interesting to note that PD146176, added one hour prior to rotenone, failed to protect the cells against complex I inhibition (Figure 31a). These data suggested that glutamate and 12/15-LOX do not mediate cell death by inhibition of the complex I of the mitochondrial respiratory chain. Interestingly, the vitamin E analog Trolox also failed to prevent rotenone induced cell death in HT-22 cells (Figure 31b) showing that the formation of ROS may not play a major role in mediating cell death after complex I inhibition. In conclusion, the fact that neither antioxidants nor 12/15-LOX inhibitors could interact with rotenone toxicity suggested that complex I inhibition is of minor relevance in HT-22 cells after glutamate treatment and that neither LOX activity nor ROS formation alone mediated death induced by complex I inhibition.

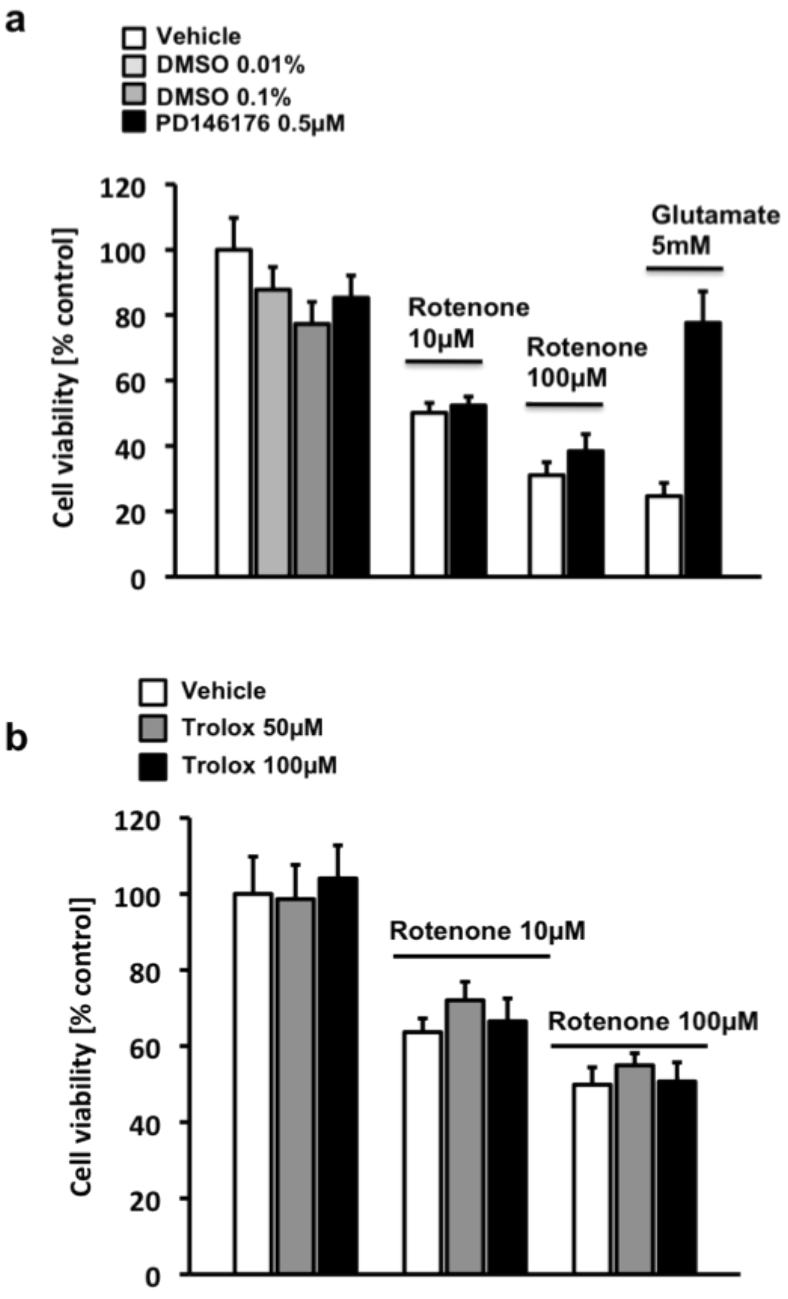

Figure 31: Neither PD146176 nor Trolox protect HT-22 cells against rotenone toxicity. The complex I inhibitor rotenone (10 – 100 µM) induced cell death in HT-22 cells that could not be prevented by addition of (**a**) PD146176 (0.5 µM) or (**b**) Trolox (50 + 100 µM) (n=8). Cell viability was detected by the MTT assay at 16 hours after the exposure to rotenone. All experiments were at least repeated 3 times and all data are provided as mean ± S.D.

3.11. Inhibition of 12/15-LOX prevents AIF translocation to the nucleus

It has been shown that the translocation of the apoptosis-inducing factor (AIF) from the mitochondria to the nucleus is a crucial step in glutamate induced cell death in HT-22 cells and primary neurons [26, 158, 159]. The release of AIF from the mitochondria is triggered by different mediators, like e.g. Bid or Bax, and causes DNA degradation and cell death. In order to examine the link between 12/15-LOX activation in neuronal cell death and the execution of mitochondrial death pathways at low ATP levels the effect of PD146176 on glutamate-induced AIF translocation was addressed.

The HT-22 cells were seeded in ibidi slides and treated with PD146176 (0.5 µM) and glutamate (5 mM). After 12 hours the cells were fixed with PFA (4%) and stained using a primary antibody against AIF (Santa Cruz Biotechnology, Inc, Heidelberg, Germany) and a biotinylated secondary antibody (Vector Labs, Axxora, Loerrach, Germany), which was linked to streptavidin oregon green (Invitrogen, Karlsruhe, Germany) for detection using a confocal fluorescent laser scanning microscope (Carl Zeiss AG, Jena, Germany). The nuclei were stained with DAPI to control the translocation to the nucleus. Glutamate induced detectable AIF translocation to the nucleus that was prevented by 12/15-LOX inhibition (Figure 32a).

For confirmation of the results obtained with immunostainings nuclear extracts of HT-22 cells were examined by western blot. The cells were damaged for 12 hours with glutamate and PD146176 was used again to inhibit 12/15-LOX activation. After 12 hours nuclear and cytosolic extracts were prepared which were analyzed after western blotting using an anti-AIF antibody (Santa Cruz Biotechnology, Inc, Heidelberg, Germany). Translocation of AIF could be detected in the cells treated with glutamate whereas PD146176 significantly reduced the amount of AIF in the nucleus despite the exposure to glutamate (Figure 32b).

Overall, these results show that the activation of 12/15-LOX mediates mitochondrial damage and the translocation of AIF to the nucleus showing again the key role of 12/15-LOX as a trigger mechanism in glutamate-induced neuronal death.

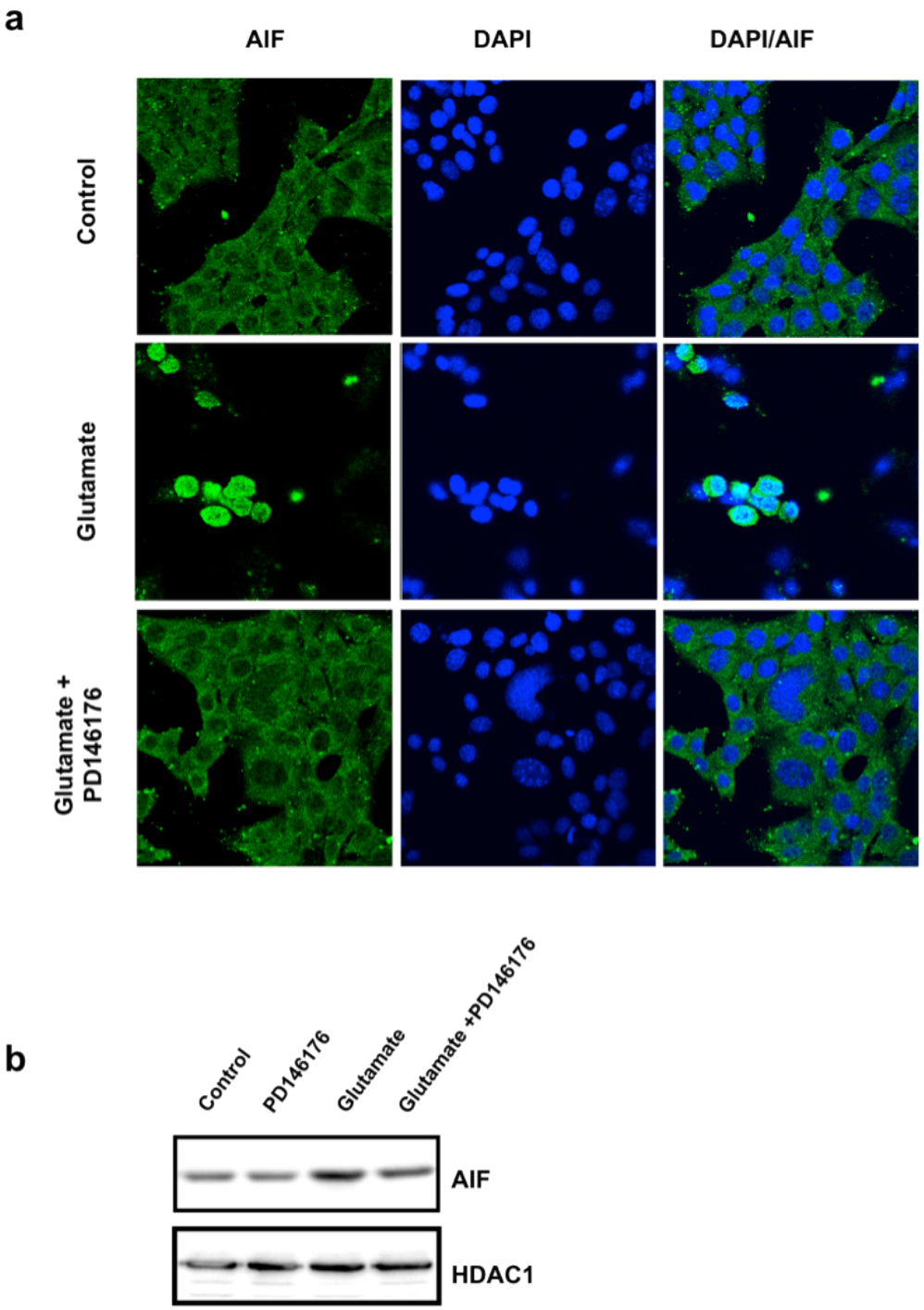

Figure 32: PD146176 prevents AIF translocation to the nucleus. (**a**) HT-22-cells were treated with glutamate (5 mM) 24 h after seeding. PD146176 (0.5 µM) was applied 1 h prior to glutamate. Cells were fixed and immunostained 12 h after the treatment. Nuclei were stained with DAPI. Pictures were taken with a confocal microscope (Carl Zeiss AG, Jena, Germany). The 12/15-LOX inhibitor prevented glutamate-induced translocation of AIF to the nucleus. (**b**) HT-22 cells were damaged with glutamate and treated with PD146176 as indicated. After 12 h nuclear extracts were obtained for western blot analysis of AIF. HDAC1 served as a loading control (n=3). Both experiments were repeated 3 times.

4. Discussion

The aim of this study was to analyze the role of 12/15-lipoxygenases in glutamate-induced neuronal cell death. The involvement of 12/15-LOX was characterized in immortalized mouse hippocampal HT-22 neurons and in primary neuronal cultures. In addition to glutamate toxicity that induced oxidative stress and increases in intracellular calcium levels in HT-22 cells and primary neurons, the role of 12/15-LOX was also addressed in other models of oxidative stress including application of H_2O_2, Fe(II)-salts, 4-HNE and NO-donors.

The results obtained here suggested a key role for 12/15-LOX in glutamate-induced neuronal cell death showing that inhibition of 12/15-LOX significantly reduced oxidative stress and protected HT-22 cells and primary neurons against glutamate toxicity. In addition, neuronal cultures obtained from Alox15-mice (12/15-LOX knock-out mice) showed less neuronal damage after the glutamate challenge compared to cells obtained from wild type mice. Furthermore, PD146176, a potent and selective inhibitor of 12/15-LOX, prevented the glutamate-induced loss of ATP, preserved the mitochondrial membrane potential and mitochondrial morphology and inhibited AIF translocation from the mitochondria to the nucleus.

However, 12/15-LOX inhibition failed to prevent tBid-induced cell death in HT-22 cells indicating that 12/15-LOX activation triggers pathways of mitochondrial death signaling upstream of Bid activation. Additionally, the study revealed that PD146176 attenuated the deregulation of intracellular calcium and prevented cell death after OGD in primary neurons in vitro and significantly reduced infarct size after MCAO in vivo.

In conclusion, these data suggest that the findings on a major role of 12/15-LOX as a key trigger of lethal oxidative stress induced by glutamate in HT-22 immortalized neurons were relevant for mechanisms of delayed neuronal death in models of cerebral ischemia. Therefore, 12/15-LOX and the associated downstream mediators of mitochondrial damage and cell death are promising targets for novel neuroprotective strategies in neurodegenerative diseases.

4.1. Glutamate in HT-22 cells: 12/15-LOX mediated cell death

HT-22 cells do not express ionotropic glutamate receptors such as NMDA receptors or AMPA/Kainate receptors. Therefore, glutamate cannot induce rapid calcium influx and exitotoxicity in HT-22 cells but mediates cellular death by inhibition of cystine import and subsequent GSH depletion.

In a recent study the functional loss of glutathione peroxidase 4 (GPx4) was identified as the underlying mechanism that links reduced glutathione levels to oxidative cell death [160]. In addition, it was unraveled that loss of GPx4 sparks 12/15-LOX-derived lipid peroxidation and subsequent execution of caspase-independent cell death by mitochondrial release of AIF in fibroblasts [160].

In HT-22 cells glutamate blocks the glutamate-cystine antiporter (xc-transporter) and causes a lack of cysteine in the cell, which is required for glutathione (GSH) formation [28, 29]. GSH is an important antioxidative system that also regulates the activity of GPx4 and thus indirectly the activity of 12/15-LOX. According to recent findings in fibroblasts and primary neurons, reduced GSH levels cause reduced GPx4 activity and subsequent activation of 12/15-LOX. This may also apply in HT-22 neurons, since also in these cells glutamate-induced GSH depletion was followed by an increase in lipid peroxidation, which is attributable to 12/15-LOX activation.

The present study further revealed a secondary more pronounced burst of ROS levels, which was associated with mitochondrial damage (Figure 5). Pharmacological inhibitors of 12/15-LOX significantly protected HT-22 cells against glutamate-induced cell death, indicating a key role of 12/15-LOX activation as a primary trigger of cell death in the HT-22 cell model of glutamate toxicity (Figure 9, 10).

This is further supported by findings showing that glutamate triggered LOX-dependent lipid peroxidation that occurred upstream of essential steps of glutamate-induced cell death in HT-22 cells.

Since ROS can originate from different sources in the cell this study analyzed not only the role of 12/15-LOX but also the role of 5-LOX as well as of COX and NADPH oxidase (3.3 + 3.9).

This thesis showed that neither 5-LOX nor COX are involved in the formation of ROS in HT-22 cells because selective inhibitors of both enzymes failed to protect the cells against glutamate-induced cell death (Figure 8) whereas 12/15-LOX inhibition was highly protective. These findings further supported the key role 12/15-LOX as trigger of glutamate-induced cell death in HT-22 cells.

It is important to note that the calcium chelator EDTA significantly reduced cell death after glutamate challenge (Figure 7) indicating that disruption of calcium homeostasis plays a role in HT-22 cells. Supporting these findings Tan et al. reported elevated calcium levels after glutamate treatment in HT-22 cells [30]. However, EDTA failed to completely prevent glutamate-induced damage, in particular at high concentrations of glutamate, suggesting that Ca^{2+} influx contributed to cell death but was dispensable and less important than pronounced lipid peroxidation.

In summary, these data connect the HT-22 cell model to glutamate-induced excitotoxicity in primary neurons as they highlight two trigger mechanisms of cell death, i.e. increased production of ROS and elevated levels of intracellular calcium that these two models have in common.

It has been shown that the activation of the pro-apoptotic Bcl-2 protein Bid is required for induction of damage and depolarization of mitochondria in HT-22 cells [26, 150]. Others have shown that after activation and translocation to mitochondria Bid interacts with the Bcl-2 family member Bax and induces the formation of a mitochondrial pore and the subsequent breakdown of the mitochondrial membrane potential indicating the important role of the Bid protein in neuronal demise [31, 34].

In addition, it is known that Bid activation and the subsequent mitochondrial damage induce translocation of AIF (apoptosis inducing factor) from the mitochondria to the nucleus. The translocation of AIF is known to be a crucial step in caspase-independent apoptosis in HT-22 cells [26].

Taken together, these data suggested that Bid activation and the subsequent AIF translocation are key mediators of neuronal cell death in HT-22 cells. In addition, this thesis now showed that 12/15-LOX activation is important in oxidative stress-induced cell death in HT-22 cells and that 12/15-LOX dependent mechanisms of cell death are linked to Bid activation and AIF translocation (Figure 23, 32).

4.2. 12/15-LOX-dependent Bid activation

Since 12/15-LOX inhibition was highly protective in glutamate-induced neuronal cell death the pro-apoptotic pathways, which are connected to 12/15-LOX activation, were analyzed in further detail with special interest in the connection between 12/15-LOX activation and the important pro-apoptotic proteins Bid and AIF. The importance of Bid activation and AIF translocation in HT-22 cells as major steps in neuronal damage was confirmed in this thesis which now links GSH depletion, 12/15-LOX activation and these key events of intrinsic death signaling [26, 150].

Bid has been revealed as key mediator of cell death in different paradigms of neurodegeneration, including model systems of oxidative stress and excitotoxicity in vitro, and cerebral ischemia and brain trauma in vivo [38, 40, 161].

Accordingly, Bid knockout mice developed significantly reduced brain damage after cerebral ischemia and brain trauma [37]. Similar results were obtained in cultured neurons from Bid-deficient mice when exposed to oxygen glucose deprivation (OGD) [38]. Further, small molecule inhibitors of Bid provided protective effects against glutamate-induced excitotoxicity or OGD in cultured primary neurons [150]. The selective Bid inhibitor BI-6C9 [151] also prevented mitochondrial demise [150], AIF release and cell death in HT-22 cells exposed to oxidative stress induced by glutamate or amyloid-beta peptide [26, 131]. All of these different paradigms of lethal stress induced activation of Bid, which translocated to the mitochondria where it mediated mitochondrial membrane permeabilization and release of death inducing proteins such as cytochrome c or AIF. Therefore, Bid activation is a common feature of death signaling that can significantly amplify deadly stress signals through involvement of mitochondrial mechanisms in the execution of cell death.

Both, 12/15-LOX- and Bid-inhibition, were able to protect the HT-22 cells up to control level against glutamate toxicity (Figure 9, 22) strengthening the importance of the two proteins and their possible link in the cascade of cell death signaling.

Measurement of lipidperoxides using the fluorescent dye BODIPY showed that inhibition of 12/15-LOX could prevent the first increase in lipidperoxides as well as the secondary burst after mitochondrial damage (Figure 10). In contrast, the selective Bid inhibitor BI-6C9 reduced only the secondary burst of ROS (16 – 18h)

and did not influence the first ROS formation (6 – 8h) suggesting that Bid activation occurs downstream of 12/15-LOX activity (Figure 23).

Indeed, the proposed timing of transition from moderate to severe oxidative stress fits well with the timing of Bid translocation to mitochondria and indicators of mitochondrial damage such as loss of mitochondrial membrane potential and subsequent release of AIF as determined in previous work [26].

Of note, 12/15-LOX inhibition as well as antioxidants and NADPH oxidase inhibitors failed to prevent tBid-induced damage (Figure 23, Figure 27) whereas the Bid inhibitor BI-6C9 prevented tBid toxicity [26]. These results confirmed the proposed time course of 12/15-LOX activation and subsequent Bid activity. Further, these data clearly suggest that 12/15-LOX activity and further ROS formation is not essential for the further damage of mitochondria and execution of cell death downstream of Bid. Thus, the observed secondary burst of ROS indicates the 'point of no return', i.e. fatal damage to the mitochondria that cannot be reversed by antioxidants or inhibitors of 12/15-LOX.

It is important to note that previous studies showed similar effects on mitochondria and AIF-dependent cell death in HT-22 cells for both, mitochondrial translocation of full length Bid after the glutamate challenge and over-expression of tBid [26]. Consequently, the transfection with a tBid-expressing vector is a potential model for Bid-induced toxicity and was therefore used in this study.

Previous studies showed that Bid cleavage could not be detected after exposure to glutamate in HT-22 cells as well as in primary neurons, suggesting that full length Bid translocated to the mitochondria and/or only a small part of Bid was cleaved to tBid [26, 52]. This is in line with reports that suggested activation and mitochondrial translocation of full length Bid prior to Bid cleavage and execution of mitochondrial death pathways [162]. It is important to note that the Bid inhibitor BI-6C9 prevented the translocation of full length Bid and tBid to mitochondria and the according detrimental effects on mitochondria, suggesting that the effects of both forms of activated Bid on mitochondria are comparable.

The exact mechanisms of Bid activation in the present model system are currently unknown and matter of ongoing studies.

In summary, these data strongly suggest that activation of 12/15-LOX and formation of ROS initiated cell death mechanisms after glutamate treatment, whereas activation of Bid, mitochondrial damage and the boost of ROS are hallmarks of

downstream mechanisms that cannot be blocked by 12/15-LOX inhibitors or radical scavengers. These findings also contrast recent reports from studies in isolated mitochondria suggesting a function of activated 12/15-LOX at the mitochondrial membrane [149]. The present findings clearly indicate that in whole cells, 12/15-LOX may function as a trigger for other mediators of mitochondrial damage whereas 12/15-LOX may play only a minor role once these mediators induced damage at the mitochondria.
These assumptions are supported by experiments showing that cell death induced by the complex I inhibitor rotenone was neither prevented by 12/15-LOX inhibition nor by the antioxidant Trolox in HT-22 neurons (Figure 31).

In particular, the present findings suggest a transition phase where Bid acts as a crucial link between the 12/15-LOX-dependent initial increases in lipid peroxidation and the following mitochondrial damage. This conclusion is supported by previous studies where the small molecule Bid inhibitor BI-6C9 or Bid siRNA prevented mitochondrial damage, AIF translocation and cell death in neurons [26]. Moreover, the therapeutic time window of 8-10 h identified in previous studies for the Bid inhibitor [26] is in accordance with the ‘point of no return’ and the associated secondary boost of oxidative stress revealed in the present study. Here, the LOX inhibitor PD146176 and the antioxidant Trolox showed a similar therapeutic time window of approximately 8 h after onset of the glutamate challenge (Figure 11). This supports the view that accumulating oxidative stress leads to Bid-mediated mitochondrial damage, which marks the execution phase of cell death that cannot be blocked, by LOX inhibitors or radical scavengers targeting the initiation phase.
In summary, the present study shows an important role for Bid acting as a key link between early ROS formation by 12/15-LOX and downstream mitochondrial damage that executes cell death after glutamate challenge in neuronal cells.

4.3. 12/15-LOX activation mediates AIF-translocation

The translocation of AIF from mitochondria to the nucleus is a key feature of caspase-independent neuronal death as shown previously in models of glutamate

toxicity, oxygen glucose deprivation and axonal stretch injury [26, 163]. In addition, previous studies showed that AIF-mediated cell death is dominant in HT-22 cells while activation of caspases occurs only at very late time-points after glutamate challenge [26]. Further, inhibition of caspase activity did not prevent glutamate-induced death in HT-22 cells indicating a minor role of these proteases in the current model system of oxytosis [26].

It has been demonstrated that AIF knockdown with siRNA is protective in HT-22 cells after glutamate challenge [26]. In addition, Hq mice, which express only about 20% AIF, in comparison to wild type mice, exhibit protection against different pro-apoptotic stimuli like MCAO or glutamate-induced excitotoxicity [164][158]. There is not much known about the process of mitochondrial AIF release and nuclear translocation but others proposed that AIF, which is localized at the inner membrane of the mitochondrial intermembrane space, has to be cleaved before its translocation [165, 166]. Possible candidates for the proteolytic cleavage of AIF are for example calpains [46]. Calpains belong to the family of calcium-dependent, non-lysosomal cysteine proteases that mediate processes such as cell cycle progression, cell mobility and cell-type specific functions like long-term potentiation in neurons.

Additionally, inhibition of poly (ADP-ribose) polymerase 1 (PARP-1) attenuated damage of HT-22 cells after glutamate challenge (Landshamer, “Role of Bid and AIF in glutamate-induced neuronal cell death“, dissertation 2007). Others have shown before that PARP-1 inhibition was also protective in OGD or MCAO in mice [158]. Furthermore, PARP-1 can cause depletion of NAD^+ suggesting that mitochondrial NAD^+ depletion connect PARP-1 activation to the release of AIF [167].

In addition, mitochondrial translocation of the BH3-only death agonists Bid, Bim or BNIP3 have been associated with AIF translocation in neurons supporting the important role of AIF and the activation of pro-apoptotic Bcl-2 proteins in neuronal demise [26, 158, 168, 169].

These data show the important role of AIF-induced caspase-independent cell death in HT-22 cells as well as in primary neurons therefore the role of AIF was explored in further detail in this study.

In this thesis HT-22 cells were stained for AIF using an anti-AIF antibody (Santa Cruz Biotechnology, Inc., Heidelberg, Germany) to explore if 12/15-LOX inhibition can prevent translocation of AIF to the nucleus and to investigate the potential link between 12/15-LOX activation and AIF translocation. In order to confirm the results nuclear and cytosolic extracts of HT-22 cells were analyzed by western blotting. Both experiments showed that the 12/15-LOX inhibitor PD146176 prevented AIF translocation to the nucleus after glutamate-induced damage (Figure 32a, 32b). Overall, these data suggest that 12/15-LOX activation mediate subsequent AIF translocation. This demonstrates again the important role of 12/15-LOX activation in neuronal damage.

Regarding the results obtained from analysis of tBid toxicity in HT-22 cells (see 4.2) these results suggest a potential link between 12/15-LOX, Bid activation and the translocation of AIF from the mitochondria to the nucleus.

4.4. 12/15-LOX activation and mitochondrial demise

This thesis revealed a link between 12/15-LOX and the activation of Bid and AIF, which indirectly suggests a strong effect of 12/15-LOX on mitochondrial death pathways. A role for 12/15-LOX as an upstream trigger of mitochondrial execution mechanisms of cell death was further supported by analysis of mitochondrial morphology, mitochondrial membrane potential and loss of ATP after glutamate challenge (Figure 28, 29, 30). Mitochondria are crucial organelles of every cell as they are the primary source of energy and perform decisive tasks in the process of cell differentiation and are involved in the synthesis of neurotransmitters and the maintenance of ion homeostasis.

Mitochondria are dynamic organelles that undergo permanent fission and fusion under physiological conditions. In damaged neurons however, this dynamic process is disturbed leading to excessive fragmentation of mitochondria and thereby promoting cell death progression [61, 123, 170]. Although the mechanisms controlling mitochondrial morphology under pathological conditions are only partly known, increasing evidence suggests a potential role for oxidative stress and impaired bioenergetics as potential triggers of mitochondrial fission in the cell death

program [150]. The present study demonstrates that glutamate-induced cell death is associated with mitochondrial fragmentation in HT-22 cells (Figure 29). Inhibition of 12/15-LOX prevented glutamate-induced disruption of the mitochondrial morphology, blocked loss of ATP after glutamate challenge and preserved the mitochondrial membrane potential (Figure 28, 29, 30). These data suggest that activation of 12/15-LOX is an important upstream stimulus of glutamate-induced neurotoxicity resulting in enhanced mitochondrial fission, loss of mitochondrial integrity, loss of energy (ATP) and progression of AIF-dependent cell death.

4.5. 12/15-LOX in primary neurons

Further studies have shown a key role of 12/15-LOX in different models of neuronal cell death [133, 134]. Recent work in models of cerebral ischemia exposed LOX as a potential target for neuroprotective strategies in stroke treatment. In these studies, genetic 12/15-LOX deletion significantly reduced the infarct size in a mouse model of transient cerebral ischemia as compared to wild type mice, and similar protective effects against ischemic brain damage were achieved by treating wild type mice with the LOX inhibitor baicalein [133]. It is important to note that baicalein is supposed to inhibit 12/15-LOX but it has been shown that it also has antioxidant properties, which may partly contribute to the protective effects achieved in vitro and in vivo where baicalein was applied in very high doses. Consequently, in the present study the selective 12/15-LOX inhibitor PD146176 was chosen for the experiments.

The present thesis demonstrated a protective effect of 12/15-LOX inhibition in glutamate-induced excitotoxicity as well as in oxygen glucose deprivation. In addition, this study showed that glutamate-induced toxicity was significantly reduced in neuronal cultures obtained from 12/15-LOX-knockout mice compared to wild type cultures confirming the key role of 12/15-LOX activity in oxidative stress induced neuronal cell death. Further, PD146176 also significantly reduced the infarct volume after MCAO and improved the neuroscore of the treated mice showing that 12/15-LOX inhibition reduced ischemic brain damage and improved motor activity after ischemia.

Disruption of calcium homeostasis occurs after glutamate-induced excitotoxicity in primary neurons. Excitotoxicity is supposed as a pathological mechanism of neuronal death in different neurodegenerative diseases like Alzheimer's Disease, Parkinson's Disease and also contributes to infarct development after acute brain damage by trauma or ischemia [171, 172]. Glutamate induced a fast calcium increase and a secondary delayed calcium deregulation in primary cortical neurons that was influenced by 12/15-LOX inhibition. The 12/15-LOX inhibitor PD146176 did not prevent the initial short increase in $[Ca^{2+}]_i$ after glutamate exposure but significantly attenuated the secondary sustained increase in intracellular calcium levels and concurrently reduced cellular death. These findings support the conclusion that the 12/15-LOX inhibitors interfered with delayed downstream execution mechanisms of glutamate neurotoxicity, such as ROS formation, sustained increases in $[Ca^{2+}]_i$ and mitochondrial damage. Others have postulated before a direct interaction of 12/15-LOX with calcium channels that would explain the effect of 12/15-LOX activation on calcium homeostasis [173].

Thus, lipoxygenases are promising targets for therapeutic strategies against glutamate-mediated death signaling that may occur in the presence or absence of glutamate receptor ion channels.

4.6. The role of NADPH oxidase (NOX) in HT-22 neurons

Activation of the neuronal glutamate receptors initiates several downstream events, including cation influx, activation of nitric oxide synthase and formation of superoxide [174-176]. Superoxide functions as an inter-cellular messenger in long-term potentiation [177, 178] and participates in redox inhibition of glutamate receptor function [179]. However, superoxide can also promote neuronal death when glutamate receptor activation is sustained [174, 180]. A possible source of superoxide and lipidperoxides, is NADPH oxidase (NOX). NOX is a cytoplasmic enzyme that transfers an electron from NADPH to molecular oxygen to generate superoxide. NOX was originally described in neutrophils, but has subsequently

been identified in many other cell types including neurons [153, 181]. Neurons express the NOX2 isoform of NADPH oxidase and may also express the NOX1 and NOX4 isoforms [153].

Others have shown that inhibition of NOX prevents NMDA toxicity in neurons and suggested NOX as the major source for superoxides in neurons [154].

This study evaluated the role of NOX in HT-22 cells and the involvement of NOX in the induction of ROS formation and the induction of mitochondrial demise.

The NOX inhibitor diphenyleneiodonium chloride (DPI) protected HT-22 cells against glutamate-induced cell death even when it was applied up to 8 hours after the exposure to glutamate (Figure 24, 25). In addition, DPI preserved the mitochondrial morphology (Figure 26a), suggesting that NOX also contributed to glutamate-induced mitochondrial damage. NOX inhibition also prevented the loss of ATP after glutamate challenge (Figure 26b) confirming the effect of NOX on mitochondria. This finding supplemented recent reports indicating that NOX activation links NMDA-receptor mediated increases in $[Ca]_i$ levels and ROS formation [154].

This thesis suggests that NOX activity is also involved in glutamate-induced ROS formation and cell death in the absence of NMDA-receptors. Loss of ATP, arachidonic acid formation or elevated intracellular calcium levels, among others [182], can also activate NOX.

Therefore, the observed slight changes in calcium concentration, loss of ATP or formation of arachidonic acid may induce NOX activation in HT-22 cells exposed to glutamate. It is, however, important to note that the exact mechanisms of NOX activation and of NOX-mediated cellular damage in HT-22 cells are not known, yet.

Others have suggested an activation of PARP-1 after the exposure to glutamate, which leads to a decrease of NAD^+, and therefore might induce Bid-mediated AIF translocation [157]. NOX is expressed in the cytosol and its activation can also induce PARP-1 mediated NAD^+ depletion [156] suggesting that therefore the cytosolic protein Bid becomes activated and can mediate subsequent AIF translocation. This hypothesis explains the protective effect of the NADPH oxidase inhibitor DPI in HT-22 cells as well as the fact that DPI did not prevent tBid-induced cell death (Figure 24, 27).

4.7. NO in HT-22 cells

Several studies have implicated nitric oxide (NO) as a key mediator of neurodegeneration in numerous neurodegenerative diseases including Parkinson's Disease, Alzheimer's Disease, Huntington's Disease, and ischemic brain injury [102-105, 183, 184]. On the other hand, NO mediates different physiological functions like dilation of blood vessels and elimination of pathogens. NO toxicity primarily occurs after its conversion into highly reactive and toxic molecules that react with proteins, DNA, and lipids to alter their function and thereby induce cellular death [101].

In the present study, the role of NO production in HT-22 cells was analyzed in further detail. NO-toxicity was induced by the NO-donor DEANONOate (2 – 5 mM) and by sodium nitroprusside (SNP), which induces NO-release as well as the formation of CN^- and Fe^{2+}. Inhibition of 12/15-LOX failed to protect HT-22 cells against toxicity induced by DEANONOate (Figure 19b) as well as cell death induced by SNP (Figure 20b) demonstrating that both substances cause neuronal cell death independently of 12/15-LOX activity. DEANONOate leads to a fast but short-term increase in NO-concentrations while SNP induces a continuous, endogenous production of NO, CN^- and Fe^{2+}. Consequently, these results suggest different mechanisms of cell death for a fast and short lasting increase of NO, compared to a continuous NO production associated with additional stress stimuli. In fact, the cell death induced by SNP appears to be more complex than the damage induced by direct addition of NO-donors like DEANONOate and it is not possible to indentify the final trigger of cell death after SNP treatment in HT-22 cells. Previous studies showed that the CN^-, that functions as mitochondrial toxin and induces oxidative stress, is released prior to the formation of NO and Fe^{2+} and therefore CN^- may be the most important stress stimulus after exposure to SNP. However, it is also important to note that SNP induced glutathione depletion and upregulation of NFκB in neuronal cells [185] suggesting GSH depletion as an additional mechanism for SNP toxicity in HT-22 cells. Nevertheless, GSH depletion seems to be not the most important trigger of SNP toxicity because 12/15-LOX inhibitors failed to prevent SNP toxicity and because it has been elucidated before that decreased GSH levels mediate 12/15-LOX activation.

Interestingly, preliminary data showed that SNP does not induce nitrosylation of tyrosine residues in HT-22 cells suggesting that NO is not the major trigger of SNP-induced cellular damage (Figure 20c).

Furthermore, this study analyzed whether NO is released after glutamate challenge in HT-22 cells and analyzed the role of NO production and protein nitrosylation after glutamate treatment in the HT-22 model system. For this purpose, total cellular protein extracts were analyzed with western blotting and tyrosine-nitrosylation was detected using an anti-nitro tyrosine antibody (New England Biolabs GmbH, Heidelberg, Germany). Interestingly, there was no nitrosylation of tyrosine residues detectable after the exposure to glutamate showing that NO-toxicity is less important in glutamate-induced oxidative stress in HT-22 cells (Figure 21).

4.8. The role of 12/15-LOX in other models of oxidative stress

In this study several well-accepted models of oxidative stress that had been previously used in other studies of neurodegenerative diseases were tested in HT-22 cells to analyze the role of 12/15-LOX [139, 140, 186]. Radical donors like glucose oxidase (GO) and H_2O_2, iron sulfate and HNE, which induces lipidperoxide formation, were used to investigate whether activation of 12/15-LOX occurs also in these model systems of oxidative stress. Inhibition of 12/15-LOX failed to prevent cell death induced by the radical donors glucose oxidase and H_2O_2. These results showed that cell death occurring after the exposure to radical donors differs from glutamate-induced apoptotic cascades and is not mediated by 12/15-LOX activation. On the other hand, the antioxidant NAC was able to prevent cell death induced by radical donors and glutamate (Figure 6b, 16c).

Taken together, these results confirmed the key role of ROS production after glutamate challenge and demonstrated that the mechanisms, occurring in HT-22 cells after glutamate challenge, differ from those after treatment with radical donors.

In addition, it is important to note that the direct addition of H_2O_2 does not reflect physiological H_2O_2 formation. The treatment with GO may better mimic continuous release of H_2O_2 but both model systems are currently under debate concerning their suitability for research on mechanisms of neurodegeneration.

Moreover, HNE was used to induce cellular damage in HT-22 cells. HNE is known to be both, a marker and mediator of oxidative stress, and a possible contributor to Alzheimer's Disease and atherosclerosis, an inhibitor of growth modulating factor and a signaling molecule in the induction of apoptosis [187-189].
Peroxidation of cellular membrane lipids, or circulating lipoprotein molecules generate highly reactive aldehydes among which one of the most important is HNE. HNE was used in several studies on neurodegenerative diseases for induction of neuronal demise. This thesis analyzed the effect of HNE in HT-22 cells and examined the role of 12/15-LOX after the exposure to HNE. 12/15-LOX inhibition failed to prevent HNE-induced damage demonstrating that HNE-mediated cellular damage is independent of 12/15-LOX-activation (Figure 18).
Furthermore, iron sulfate was used to induce Fe^{2+}-toxicity and subsequent ROS production in HT-22 cells. It is known that Fe^{2+}-levels in the brain are increased in several neurodegenerative diseases and that Fe^{2+}-formation contributes to neuronal oxidative stress [142]. Therefore, induction of neuronal death with iron sulfate has been used in different studies on neurodegeneration, before. Interestingly, iron sulfate-induced cell death was not attenuated by 12/15-LOX inhibition and not by the antioxidant NAC (Figure 17b, 17c) showing that Fe^{2+}-induced toxicity does not depend on 12/15-LOX activation and is not only mediated by ROS formation but may also induce other pro-apoptotic mechanisms.

In summary, the results obtained for all different models of oxidative stress demonstrate that glutamate induces a very specialized form of oxidative stress that is not comparable to cell death induced by radical donors, HNE or NO.
The activation of 12/15-LOX is apparently linked specifically to glutamate-induced oxidative stress and does not occur in the other tested models of oxidative stress.
It is important to note, however, that the addition of glutamate reflects pathological conditions much better than the other models showing again the suitability of HT-22 cells as model for neurodegenerative processes induced by oxidative stress.

Overall, this thesis identified 12/15-LOX as a key trigger in glutamate neurotoxicity, in particular for glutamate-induced oxidative stress that is initiated by glutathione depletion, significantly amplified by Bid-dependent mitochondrial damage, and executed through mitochondrial AIF release to the nucleus. The delineated sequences of glutamate-induced cell death signaling in HT-22 cells (Figure 33) are highly relevant for neurodegenerative diseases and acute neurological disorders such as ischemic stroke, since glutamate toxicity and downstream mitochondrial death pathways have been identified as key features of neuronal death in related experimental models in vitro and in vivo. Thus, targeting 12/15-LOX is proposed as a potential therapeutic target for neuroprotective strategies in neurological diseases where glutamate-induced neuronal death is prominent.

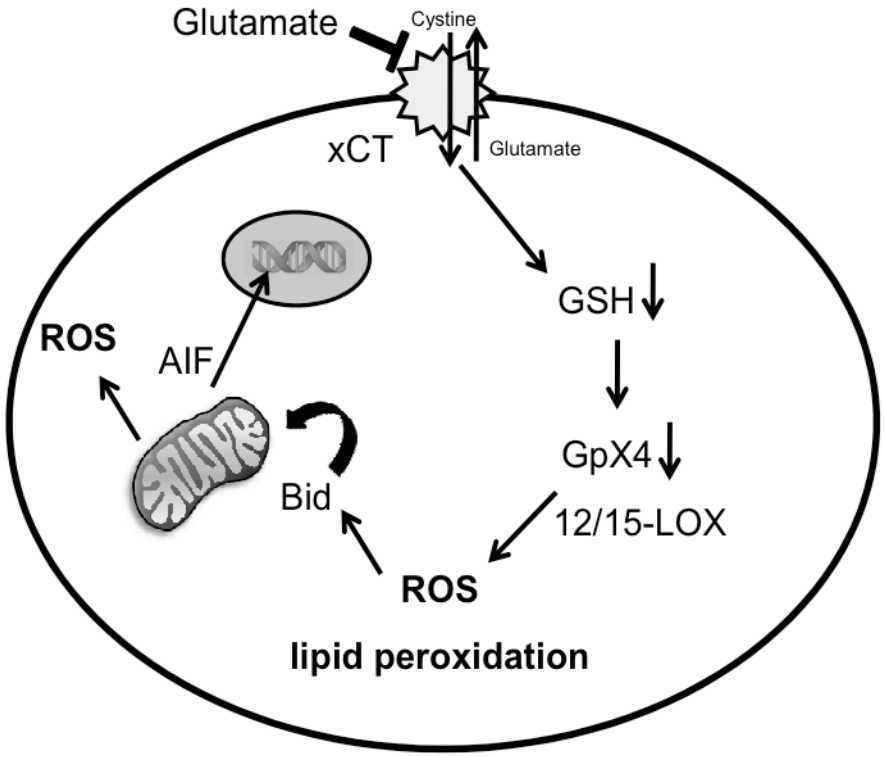

Figure 33: Proposed mechanism of glutamate-induced oxidative stress in HT-22 cells. Glutamate inhibits the Xc- transporter and thereby triggers glutathione depletion. Consequently, the activity of glutathione peroxidase-4 (GPx4) is reduced, while 12/15-LOX activity increases. 12/15-LOX activation induces a first increase in ROS and the translocation of Bid to the mitochondria where activated Bid induces mitochondrial fragmentation and mitochondrial membrane permeabilization. This results in reduced ATP production, pronounced increases in ROS production and, finally, release of pro-apoptotic proteins like AIF from the mitochondria. Upon mitochondrial release, AIF immediately translocates to the nucleus where it causes DNA damage and cell death independent of ATP and caspase activity.

5. Summary

Oxidative stress has been established as a key trigger of neuronal dysfunction and death in age-related neurodegenerative diseases and in delayed neuronal death after acute brain injury by ischemic stroke or brain trauma. Despite increasing knowledge on the toxicity of reactive oxygen species (ROS) and oxidized reaction products that may further accelerate neuronal cell death, the major sources of ROS formation and the mechanisms involved in cell death signaling triggered by oxidative stress in neurons are poorly defined. Therefore, major aims of this study included the characterization of key enzymes that contribute to the formation of ROS and key factors of the downstream signaling pathways that may amplify the oxidative cellular stress thereby causing irreversible damage and death in neurons.
Major parts of the study were performed in a model of glutamate toxicity in immortalized hippocampal HT-22 neurons, since glutamate selectively induced oxidative stress through glutathione depletion in these cells. To verify the relevance of the findings in HT-22 cells for post-mitotic neurons, further experiments included models of glutamate-induced excitotoxicity and oxygen-glucose deprivation primary embryonic neurons in vitro and in a mouse model of cerebral ischemia in vivo.

The findings of these studies revealed that 12/15-lipoxygenases (LOX), but neither 5-LOX nor COX activation, mediated glutamate-induced lipid peroxidation and oxidative cellular death (oxytosis) in HT-22 cells. Pharmacological inhibition of 12/15-LOX protected HT-22 cells as well as primary neurons against glutamate toxicity. This protective effect included significantly reduced ROS formation and attenuated deregulation of the intracellular calcium homeostasis in the cultured neurons. Moreover, the 12/15 LOX inhibitor PD146176 reduced neuronal cell death after OGD in primary neurons in vitro, and significantly reduced the infarct volume after MCAO in vivo.
Further experiments addressing the involved signaling pathways linked, for the first time, 12/15-LOX activation and key mediators of mitochondrial death pathways. In particular, the selective 12/15-LOX inhibitor PD146176 reduced mitochondrial fragmentation and ATP depletion after exposure to glutamate in HT-22 cells. Most interestingly, this study identified the pro-apoptotic Bcl-2 protein Bid as a key link

between 12/15-LOX activation, mitochondrial demise and the translocation of the mitochondrial protein AIF to the nucleus. In fact, mitochondrial transactivation of Bid downstream of 12/15-LOX activation was exposed as the key step for the mitochondrial damage that resulted in a second burst of lipid peroxidation and marked the ‘point of no return’ in the glutamate-induced death cascade.

In summary, the glutamate-induced cell death mechanisms in HT-22 cells are highly relevant for neurodegenerative diseases and acute neurological disorders.

Thus, 12/15-LOX is proposed as a potential therapeutic target for neuroprotective strategies in neurological disorders.

6. Zusammenfassung

Oxidativer Stress spielt bei der Entstehung neurodegenerativer Erkrankungen und neuronalem Zelltod nach traumatischen und ischämischen Hirnschädigungen eine wichtige Rolle. Trotz vermehrter Forschung auf dem Gebiet des oxidativen Stresses ist bis heute nicht bekannt, welche Zelltodmechanismen durch reaktive Sauerstoffspezies (ROS) ausgelöst werden und wie deren Bildung verursacht wird. Folglich sollten in dieser Arbeit Mechanismen genauer untersucht werden, die beim neuronalen Zelltod zur Entstehung von ROS beitragen. Des Weiteren sollten auch die Signalkaskaden näher charakterisiert werden, die durch oxidativen Stress letztlich zum neuronalen Zelltod führen.

Im Rahmen dieser Arbeit wurde vor allem eine neuronale hippokampale Zelllinie (HT-22 Zellen) verwendet, die dadurch gekennzeichnet ist, dass eine Schädigung mit Glutamate zu einem kontinuierlichen Abfall der intrazellulären Glutathionspiegel führt und somit oxidativen Stress induziert. Zusätzlich wurden primäre neuronale Zellkulturen und ein in vivo-Modell der zerebralen Ischämie eingesetzt, um die in HT-22 Zellen erhaltenen Ergebnisse zu bestätigen und auszubauen.

Die Ergebnisse dieser Untersuchung zeigen, dass nach Glutamatschädigung vor allem 12/15-Lipoxygenasen für die Bildung reaktiver Sauerstoffspezies in den neuronalen Zellen verantwortlich sind und somit im Rahmen des glutamatinduzierten oxidativen Stresses eine entscheidende Rolle spielen.

Es konnte dagegen ausgeschlossen werden, dass Cyclooxigenasen (COX) und 5-LOX zur Bildung von ROS nach Glutamatschädigung von HT-22 Zellen beitragen. Durch Hemmung bzw. genetische Deletion der 12/15-LOX konnte sowohl in HT-22 Zellen als auch in primären neuronalen Kulturen eine deutliche protektive Wirkung gegenüber Glutamatschädigung gezeigt werden. Zusätzlich konnten, die nach Glutamatbehandlung auftretenden erhöhten Konzentrationen von reaktiven Sauerstoffspezies durch 12/15-LOX-Inhibition deutlich reduziert werden und auch die glutamatinduzierte Störung der Calciumhomöostase wurde durch den selektiven 12/15-LOX-Inhibitor PD146176 deutlich verringert. PD146176 reduzierte zudem den neuronalen Zelltod nach Sauerstoff-Glucose-Entzug in primären Neuronen und verringerte auch signifikant das Infarktvolumen in einem Schlaganfallmodell in Mäusen.

Weitere Untersuchungen beleuchteten den Zusammenhang zwischen der Aktivierung von 12/15-LOX und mitochondrialer Schädigung, die wiederum durch einen starken Anstieg der reaktiven Sauerstoffspezies gekennzeichnet war. Durch Hemmung der 12/15-LOX wurde sowohl der glutamatinduzierte Abfall der ATP-Spiegel als auch die Fragmentierung der Mitochondrien verhindert. Zusätzlich wurde im Rahmen dieser Studie zum ersten Mal gezeigt, dass die Schädigung von Mitochondrien nach der initialen Aktivierung der 12/15-LOX und Bildung größerer Mengen ROS vor allem durch das proapoptotische Bcl-2 Protein Bid vermittelt wird. Nach diesen Befunden induziert 12/15-LOX-Hemmung über die Aktivierung von Bid die Depolarisation der Mitochondrienmembran und die Translokation des mitochondrialen proapoptotischen Proteins AIF in den Zellkern, wo AIF über die Zerstörung der DNA die Endphase des Zelltods einleitet.

Zusammenfassend konnte in dieser Arbeit dargestellt werden, dass 12/15-LOX über die Bildung von ROS eine wichtige Stellung im glutamatinduzierten oxidativen Stress einnimmt. Nach dem Abfall von Glutathion in der Zelle werden 12/15-Lipoxygenasen aktiviert und bewirken in der Folge eine Aktivierung des cytotoxischen Proteins Bid, dass die Schädigung von Mitochondrien vermittelt. Durch die mitochondriale Schädigung kommt es zum Abfall von ATP-Spiegeln sowie zur Bildung weiterer großer Mengen reaktiver Sauerstoffspezies und zur Freisetzung proapoptotischer Proteine wie AIF aus den Mitochondrien.
Im Rahmen dieser Arbeit konnte daher gezeigt werden, dass 12/15-Lipoxygenasen möglicherweise ein neues Target für die Therapie von neurologischen Erkrankungen sind, bei denen Glutamattoxizität und oxidativer Stress zur Schädigung und zum irreversiblen Verlust von Nervenzellen beitragen.

7. Appendix

7.1. Abbreviations

µ	micro
AA	Arachidonic acid
AD	Alzheimer's Disease
AIF	Apoptosis inducing factor
ALS	Amyotrophic lateral sclerosis
AMPA	2-amino-3-(3-hydroxy-5-methylisoxazol-4-yl)proprionate
ANOVA	Analysis of variance
Apaf-1	Apoptosis protease-activating factor-1
ATP	Adenosinetriphosphate
BAPTA-AM	1,2-Bis(2-aminophenoxy)ethane-N,N,N′,N′-tetraacetic acid tetrakis(acetoxymethyl ester)
BH	Bcl-2 homology
BCA	Bicinchoninic acid
Bcl-2	B-cell lymphoma-2
BODIPY	4,4-difluoro-5-(4- phenyl-1,3-butadienyl) - 4-bora-3a,4a-diaza-s-indacene-3-undecanoic acid
BSO	L-Buthionine-sulfoximine
CAD	caspase-activated deoxyribunuclease
CCCP	Carbonyl cyanide 3-chlorophenylhydrazone
CO_2	Carbon dioxide
COX	Cyclooxygenase

DAPI	4‘‘, 6-diamidino-2-phenylindole dihydrochloride
DCF	Dichlorodihydrofluoresceine-diacetate
DEANONOate	DEA/NO, 2-(N,N-Diethylamino)-diazenolate-2-oxide diethylammonium salt
DHA	Docosahexaenoic acid
DMEM	Dulbecco's Modified Eagle Medium
DMSO	Dimethylsulfoxide
DNA	Desoxyribonucleic acid
DPI	Diphenyleneiodonium chloride
Drp-1	Dynamin-related protein 1
DTT	DL-Dithiothreitol
EBSS	Earl’s balanced salt solution
EBSS w/o glucose	Earl’s balanced salt solution without glucose
EDTA	Ethylenediaminetetraacetic acid
EGTA	Ethylene glycol-bis(2-aminoethylether)-*N,N,N′,N′*-tetraacetic acid
ER	Endoplasmatic reticulum
FACS	Fluorescence-activated cell sorting
FADD	Fas-associated death domain
FasL	Fas-ligand
FCS	Fetal calf serum
GFP	Green fluorescent protein
GO	Glucose oxidase
GpX 4	Glutathione peroxidase 4
Gbr2	Growth-factor-receptor-bound-protein 2

GSH	Glutathione
h	hour
HCl	Hydrochloric acid
HBSS	Hank's balanced salt solution
HEPES	4-(2-Hydroxyethyl)piperazine-1-ethanesulfonic acid
HNE	4-Hydroxynonenal-dimethylacetal
H_2O_2	Hydrogen peroxide
Hq	harlequin
12-HETE	12-hydroxyeicosatetraenoic acid
15-HETE	15-hydroxyeicosatetraenoic acid
ICAD	inhibitor of caspase-activated deoxyribonuclease
IP_3	Inositol triphosphate
JC-1	5,5',6,6'-tetrachloro-1,1',3,3'-tetraethyl-benzimidazolylcarbocyanine iodide
JNK	c-Jun N-terminal kinase
kDa	kilo Dalton
LOX	Lipoxygenase
LTD	Long-term-depression
LTP	Long-term-potentiation
MCA	Middle coronary artery
MCAO	Middle coronary artery occlusion
Mfn-1/-2	Mitofusin-1/-2
MTT	3-(4,5-Dimethylthiazol-2-yl)-2,5-diphenyltetrazolium bromide
mU	Milliunit
N_2	Nitrogen
NAC	N-acetyl-L-cysteine
NADPH(oxidase)/NOX	Nicotinamide adenine dinucleotide phosphate
$NaHCO_3$	Sodium hydrogen carbonate
nm	nanometre

NMDA	N-methyl-D-aspartic acid
NO	Nitrogen monoxide
NO^+	Nitrosium ion
NOS	Nitrogen monooxide synthethase
OGD	Oxygen glucose deprivation
Omi/HtrA2	high temperature requirement protein A2
PARP	Poly(ADP-ribose) polymerase
PBS	Phasphate buffered solution
PD	Parkinson's Disease
PFA	Para formaldehyde
pH	potentia hydrogenii
PHOX	Phagocytic oxidase
PI	Propidium iodide
PVDF	Polyvinylidenfluorid
ROS	Reactive oxygen species
SDS	Sodium dodecyl sulfate
SMAC/DIABLO	Second mitochondria - derived activator of caspase/direct IAP binding protein with low pI
SNF	Sodium nitroprusside
tBid	truncated Bid
TBS	Tris-buffered solution
TBST	Tris-buffered solution with Tween 20
TE	Trypsin-EDTA
TEMED	Tetramethylenethylendiamin
(Cu/Mn/Zn)-SOD	Copper/Manganese/zinc)-superoxide dismutase
wt	wild type
XIAP	X-chromosomal linked inhibitors of apoptosis

7.2. Publications

7.2.1. Original papers

S Landshamer, M Hoehn, N Barth, S Duvezin-Caubet, G Schwake, **S Tobaben**, S Kazhdan, B Becattini, S Zahler, A Vollmar, M Pellecchia, A Reichert, N Plesnila, E Wagner, C Culmsee

Bid-induced release of AIF from mitochondria causes immediate neuronal cell death,

Cell Death Differ. 2008 Oct; 15(10):1553-63

S Tobaben, J Grohm, A Seiler, M Conrad, N Plesnila, C Culmsee

Bid-mediated mitochondrial damage is a key mechanism in glutamate-induced oxidative stress and AIF-dependent cell death in immortalized HT-22 hippocampal neurons.

Cell Death Differ. 2010 Aug 6

S Diemert, J Grohm, **S Tobaben**, A Dolga, C Culmsee

Real-time detection of neuronal cell death by impedance-based analysis using the xCELLigence System.

Application note for Roche Applied Science, 2010 Aug

J Grohm, S-W Kim, U Mamrak, **S Tobaben**, A Cassidy-Stone, J Nunnari, N Plesnila, C Culmsee

Inhibition of Dynamin-related protein 1 (Drp1) prevents mitochondrial fission and provides neuroprotection in vitro and in a mouse model of cerebral ischemia.

Journal of Clinical Investigations, submitted

S Diemert, A Dolga, J Grohm, **S Tobaben**, C Culmsee

Real-time detection of neuronal cell death using the xCELLigence Sytem®.

In preparation

AM Dolga, L Meissner, **S Tobaben**, J Grohm, H Zischka, N Plesnila, C Culmsee
Activation of Kca2.2 channels preserves mitochondrial function and mediates neuronal survival
In preparation

7.2.2. Oral presentations and posters

S Tobaben, M Hoehn, A Dolga, N Plesnila, C Culmsee
12/15-Lipoxygenases mediate Bid-dependent cell death after glutathione depletion in HT-22 neurons. 16th European Cell Death Organisation Euroconference, Bern, Schweiz, 06.09. - 09.09.2008

S Tobaben, M Hoehn, D Dolga, N Plesnila, C Culmsee
12/15-Lipoxygenases play a key role in AIF-dependent cell death after glutathione depletion in HT-22 cells. 50. Jahrestagung der Deutschen Gesellschaft für Experimentelle und Klinische Pharmakologie und Toxikologie, Mainz, Deutschland, 10.03. - 12.03.2009

S Tobaben, A Dolga, J Grohm, N Plesnila, C Culmsee
12/15-lipoxygenases are key regulators of mitochondrial damage and sustained disturbances of calcium homeostasis in glutamate-induced neurotoxicity. 17th European Cell Death Organisation Euroconference, Institut Pasteur, Paris, Frankreich, 23.09. - 25.09.2009

S Tobaben, J Grohm, M Hoehn, N Plesnila, C Culmsee
12/15-Lipoxygenases mediate mitochondrial AIF release and mitochondrial fission upstream of Bid in oxidative stress-induced neuronal cell death. Jahrestagung der Deutschen Pharmazeutischen Gesellschaft, Jena, Deutschland, 28.09. - 01.10.2009

S Tobaben, A Dolga, J Grohm, M Conrad, N Plesnila, C Culmsee
Activation of 12/15-lipoxygenases plays a key role in neuronal cell death induced by oxidative stress. Society for Neuroscience Annual Meeting 2009, Chicago, USA, 17.10. - 21.10.2009

S Tobaben, J Grohm, A Seiler, M Conrad, N Plesnila, C Culmsee
Bid-induced damage of mitochondrial integrity plays a key role in oxytosis.
51. Jahrestagung der Deutschen Gesellschaft für Experimentelle und Klinische Pharmakologie und Toxikologie, Mainz, Deutschland, 23.03. - 25.03.2010

S Tobaben, A Dolga, J Grohm, U Mamrak, M Conrad, N Plesnila, C Culmsee
12/15-lipoxygenases play a key role in AIF mediated neuronal cell death induced by oxidative stress. 6th International Symposium on Neuroprotection and Neurorepair, Rostock, Deutschland, 01.10. - 4.10.2010

8. References

1. Andersen JK. Does neuronal loss in Parkinson's disease involve programmed cell death? *Bioessays* 2001; **23(7)**:640-646.
2. Culmsee C, Landshamer S. Molecular insights into mechanisms of the cell death program: role in the progression of neurodegenerative disorders. *Curr Alzheimer Res* 2006; **3**:269-283.
3. Loo DT, Copani A, Pike CJ, Whittemore ER, Walencewicz AJ, Cotman CW. Apoptosis is induced by beta-amyloid in cultured central nervous system neurons. *Proc Natl Acad Sci U S A* 1993; **90(17)**:7951-7955.
4. Mattson MP. Apoptosis in neurodegenerative disorders. *Nat Rev Mol Cell Biol* 2000; **1(2)**:120-129.
5. Majno G, Joris I. Apoptosis, oncosis, and necrosis. An overview of cell death. *Am J Pathol* 1995; **146(1)**:3-15.
6. Yuan J, Lipinski M, Degterev A. Diversity in the mechanisms of neuronal cell death. *Neuron* 2003; **40(2)**:401-413.
7. Kerr JF, Wyllie AH, Currie AR. Apoptosis: a basic biological phenomenon with wide-ranging implications in tissue kinetics. *Br J Cancer* 1972; **26(4)**:239-257.
8. Dive C, Gregory CD, Phipps DJ, Evans DL, Milner AE, Wyllie AH. Analysis and discrimination of necrosis and apoptosis (programmed cell death) by multiparameter flow cytometry. *Biochim Biophys Acta* 1992; **1133(3)**:275-285.
9. Vaux DL, Korsmeyer SJ. Cell death in development. *Cell* 1999; **96(2)**:245-254.
10. Vandenabeele P, Galluzzi L, Vanden Berghe T, Kroemer G. Molecular mechanisms of necroptosis: an ordered cellular explosion. *Nat Rev Mol Cell Biol* 2010; **11(10)**:700-714.
11. Oppenheim RW. Cell death during development of the nervous system. *Annu Rev Neurosci* 1991; **14**:453-501.
12. Joza N, Pospisilik JA, Hangen E*, et al*. AIF: not just an apoptosis-inducing factor. *Ann N Y Acad Sci* 2009; **1171**:2-11.
13. Mehta SL, Manhas N, Raghubir R. Molecular targets in cerebral ischemia for developing novel therapeutics. *Brain Res Rev* 2007; **54(1)**:34-66.

14. Ankarcrona M, Dypbukt JM, Bonfoco E*, et al*. Glutamate-induced neuronal death: a succession of necrosis or apoptosis depending on mitochondrial function. *Neuron* 1995; **15(4)**:961-973.
15. Mattson MP. Modification of ion homeostasis by lipid peroxidation: roles in neuronal degeneration and adaptive plasticity. *Trends Neurosci* 1998; **21(2)**:53-57.
16. Mattson MP, Keller JN, Begley JG. Evidence for synaptic apoptosis. *Exp Neurol* 1998; **153(1)**:35-48.
17. McKay SE, Purcell AL, Carew TJ. Regulation of synaptic function by neurotrophic factors in vertebrates and invertebrates: implications for development and learning. *Learn Mem* 1999; **6(3)**:193-215.
18. Jenner P, Olanow CW. The pathogenesis of cell death in Parkinson's disease. *Neurology* 2006; **66**:S24-36.
19. Portera-Cailliau C, Price DL, Martin LJ. Non-NMDA and NMDA receptor-mediated excitotoxic neuronal deaths in adult brain are morphologically distinct: further evidence for an apoptosis-necrosis continuum. *J Comp Neurol* 1997; **378(1)**:88-104.
20. Lin MT, Beal MF. Mitochondrial dysfunction and oxidative stress in neurodegenerative diseases. *Nature* 2006; **443(7113)**:787-795.
21. Culmsee C, Krieglstein J. Ischaemic brain damage after stroke: new insights into efficient therapeutic strategies. International Symposium on Neurodegeneration and Neuroprotection. *EMBO Rep* 2007; **8**:129-133.
22. Phillis JW, Horrocks LA, Farooqui AA. Cyclooxygenases, lipoxygenases, and epoxygenases in CNS: their role and involvement in neurological disorders. *Brain Res Rev* 2006; **52(2)**:201-243.
23. Ray DE, Abbott NJ, Chan MW, Romero IA. Increased oxidative metabolism and oxidative stress in m-dinitrobenzene neurotoxicity. *Biochem Soc Trans* 1994; **22(4)**:407S.
24. Roth KA. Caspases, apoptosis, and Alzheimer disease: causation, correlation, and confusion. *J Neuropathol Exp Neurol* 2001; **60(9)**:829-838.
25. Moncada S, Bolanos JP. Nitric oxide, cell bioenergetics and neurodegeneration. *J Neurochem* 2006; **97(6)**:1676-1689.

26. Landshamer S, Hoehn M, Barth N*, et al*. Bid-induced release of AIF from mitochondria causes immediate neuronal cell death. *Cell Death Differ* 2008; **15**:1553-1563.
27. Bannai S. Transport of cystine and cysteine in mammalian cells. *Biochim Biophys Acta* 1984; **779(3)**:289-306.
28. Davis JB, Maher P. Protein kinase C activation inhibits glutamate-induced cytotoxicity in a neuronal cell line. *Brain Res* 1994; **652(1)**:169-173.
29. Sagara Y, Dargusch R, Chambers D, Davis J, Schubert D, Maher P. Cellular mechanisms of resistance to chronic oxidative stress. *Free Radic Biol Med* 1998; **24**:1375-1389.
30. Tan S, Sagara Y, Liu Y, Maher P, Schubert D. The regulation of reactive oxygen species production during programmed cell death. *J Cell Biol* 1998; **141(6)**:1423-1432.
31. Polster BM, Fiskum G. Mitochondrial mechanisms of neural cell apoptosis. *J Neurochem* 2004; **90(6)**:1281-1289.
32. Giam M, Huang DC, Bouillet P. BH3-only proteins and their roles in programmed cell death. *Oncogene* 2008; **27 Suppl 1**:S128-36.
33. Kim R. Unknotting the roles of Bcl-2 and Bcl-xL in cell death. *Biochem Biophys Res Commun* 2005; **333(2)**:336-343.
34. Ward MW, Kogel D, Prehn JH. Neuronal apoptosis: BH3-only proteins the real killers? *J Bioenerg Biomembr* 2004; **36**:295-298.
35. Desagher S, Osen-Sand A, Nichols A*, et al*. Bid-induced conformational change of Bax is responsible for mitochondrial cytochrome c release during apoptosis. *J Cell Biol* 1999; **144(5)**:891-901.
36. Ward MW, Rehm M, Duessmann H, Kacmar S, Concannon CG, Prehn JH. Real time single cell analysis of Bid cleavage and Bid translocation during caspase-dependent and neuronal caspase-independent apoptosis. *J Biol Chem* 2006; **281**:5837-5844.
37. Bermpohl D, You Z, Korsmeyer SJ, Moskowitz MA, Whalen MJ. Traumatic brain injury in mice deficient in Bid: effects on histopathology and functional outcome. *J Cereb Blood Flow Metab* 2006; **26(5)**:625-633.
38. Plesnila N, Zinkel S, Le DA*, et al*. BID mediates neuronal cell death after oxygen/ glucose deprivation and focal cerebral ischemia. *Proc Natl Acad Sci U S A* 2001; **98**:15318-15323.

39. Yin XM, Luo Y, Cao G*, et al*. Bid-mediated mitochondrial pathway is critical to ischemic neuronal apoptosis and focal cerebral ischemia. *J Biol Chem* 2002; **277(44)**:42074-42081.
40. Martin-Villalba A, Herr I, Jeremias I*, et al*. CD95 ligand (Fas-L/APO-1L) and tumor necrosis factor-related apoptosis-inducing ligand mediate ischemia-induced apoptosis in neurons. *J Neurosci* 1999; **19(10)**:3809-3817.
41. Schendel SL, Azimov R, Pawlowski K, Godzik A, Kagan BL, Reed JC. Ion channel activity of the BH3 only Bcl-2 family member, BID. *J Biol Chem* 1999; **274(31)**:21932-21936.
42. Culmsee C, Zhu Y, Krieglstein J, Mattson MP. Evidence for the involvement of Par-4 in ischemic neuron cell death. *J Cereb Blood Flow Metab* 2001; **21(4)**:334-343.
43. Le DA, Wu Y, Huang Z*, et al*. Caspase activation and neuroprotection in caspase-3- deficient mice after in vivo cerebral ischemia and in vitro oxygen glucose deprivation. *Proc Natl Acad Sci U S A* 2002; **99(23)**:15188-15193.
44. Chan SL, Mattson MP. Caspase and calpain substrates: roles in synaptic plasticity and cell death. *J Neurosci Res* 1999; **58(1)**:167-190.
45. Goll DE, Thompson VF, Li H, Wei W, Cong J. The calpain system. *Physiol Rev* 2003; **83(3)**:731-801.
46. Polster BM, Basanez G, Etxebarria A, Hardwick JM, Nicholls DG. Calpain I induces cleavage and release of apoptosis-inducing factor from isolated mitochondria. *J Biol Chem* 2005; **280(8)**:6447-6454.
47. McCollum AT, Jafarifar F, Lynn BC*, et al*. Inhibition of calpain-mediated cell death by a novel peptide inhibitor. *Exp Neurol* 2006; **202(2)**:506-513.
48. Rami A. Ischemic neuronal death in the rat hippocampus: the calpain-calpastatin-caspase hypothesis. *Neurobiol Dis* 2003; **13(2)**:75-88.
49. Zhang WH, Wang X, Narayanan M*, et al*. Fundamental role of the Rip2/caspase-1 pathway in hypoxia and ischemia-induced neuronal cell death. *Proc Natl Acad Sci U S A* 2003; **100(26)**:16012-16017.
50. Ward MW, Rehm M, Duessmann H, Kacmar S, Concannon CG, Prehn JH. Real time single cell analysis of Bid cleavage and Bid translocation during caspase-dependent and neuronal caspase-independent apoptosis. *J Biol Chem* 2006; **281(9)**:5837-5844.

51. Valentijn AJ, Gilmore AP. Translocation of full-length Bid to mitochondria during anoikis. *J Biol Chem* 2004; **279(31)**:32848-32857.
52. Tobaben S, Grohm J, Seiler A, Conrad M, Plesnila N, Culmsee C. Bid-mediated mitochondrial damage is a key mechanism in glutamate-induced oxidative stress and AIF-dependent cell death in immortalized HT-22 hippocampal neurons. *Cell Death Differ* 2010;
53. Eckert A, Keil U, Marques CA*, et al*. Mitochondrial dysfunction, apoptotic cell death, and Alzheimer's disease. *Biochem Pharmacol* 2003; **66(8)**:1627-1634.
54. Regula KM, Ens K, Kirshenbaum LA. Mitochondria-assisted cell suicide: a license to kill. *J Mol Cell Cardiol* 2003; **35(6)**:559-567.
55. Mattson MP, Kroemer G. Mitochondria in cell death: novel targets for neuroprotection and cardioprotection. *Trends Mol Med* 2003; **9**:196-205.
56. Bernardi P, Scorrano L, Colonna R, Petronilli V, Di Lisa F. Mitochondria and cell death. Mechanistic aspects and methodological issues. *Eur J Biochem* 1999; **264(3)**:687-701.
57. Kroemer G, Reed JC. Mitochondrial control of cell death. *Nat Med* 2000; **6(5)**:513-519.
58. Uo T, Kinoshita Y, Morrison RS. Neurons exclusively express N-Bak, a BH3 domain-only Bak isoform that promotes neuronal apoptosis. *J Biol Chem* 2005; **280(10)**:9065-9073.
59. Chen H, Chan DC. Critical dependence of neurons on mitochondrial dynamics. *Curr Opin Cell Biol* 2006; **18(4)**:453-459.
60. Frederick RL, Shaw JM. Moving mitochondria: establishing distribution of an essential organelle. *Traffic* 2007; **8(12)**:1668-1675.
61. Knott AB, Perkins G, Schwarzenbacher R, Bossy-Wetzel E. Mitochondrial fragmentation in neurodegeneration. *Nat Rev Neurosci* 2008; **9**:505-518.
62. Barsoum MJ, Yuan H, Gerencser AA*, et al*. Nitric oxide-induced mitochondrial fission is regulated by dynamin-related GTPases in neurons. *EMBO J* 2006; **25(16)**:3900-3911.
63. Bossy-Wetzel E, Barsoum MJ, Godzik A, Schwarzenbacher R, Lipton SA. Mitochondrial fission in apoptosis, neurodegeneration and aging. *Curr Opin Cell Biol* 2003; **15(6)**:706-716.
64. Youle RJ, Karbowski M. Mitochondrial fission in apoptosis. *Nat Rev Mol Cell Biol* 2005; **6(8)**:657-663.

65. Liang WS, Reiman EM, Valla J*, et al*. Alzheimer's disease is associated with reduced expression of energy metabolism genes in posterior cingulate neurons. *Proc Natl Acad Sci U S A* 2008; **105(11)**:4441-4446.
66. Wang X, Su B, Zheng L, Perry G, Smith MA, Zhu X. The role of abnormal mitochondrial dynamics in the pathogenesis of Alzheimer's disease. *J Neurochem* 2009; **109 Suppl 1**:153-159.
67. Hirashima Y, Farooqui AA, Mills JS, Horrocks LA. Identification and purification of calcium-independent phospholipase A2 from bovine brain cytosol. *J Neurochem* 1992; **59(2)**:708-714.
68. Iadecola C, Alexander M. Cerebral ischemia and inflammation. *Curr Opin Neurol* 2001; **14(1)**:89-94.
69. Akaike A, Kaneko S, Tamura Y*, et al*. Prostaglandin E2 protects cultured cortical neurons against N-methyl-D-aspartate receptor-mediated glutamate cytotoxicity. *Brain Res* 1994; **663(2)**:237-243.
70. Hewett SJ, Uliasz TF, Vidwans AS, Hewett JA. Cyclooxygenase-2 contributes to N-methyl-D-aspartate-mediated neuronal cell death in primary cortical cell culture. *J Pharmacol Exp Ther* 2000; **293(2)**:417-425.
71. Hong S, Gronert K, Devchand PR, Moussignac RL, Serhan CN. Novel docosatrienes and 17S-resolvins generated from docosahexaenoic acid in murine brain, human blood, and glial cells. Autacoids in anti-inflammation. *J Biol Chem* 2003; **278(17)**:14677-14687.
72. Marcheselli VL, Hong S, Lukiw WJ*, et al*. Novel docosanoids inhibit brain ischemia-reperfusion-mediated leukocyte infiltration and pro-inflammatory gene expression. *J Biol Chem* 2003; **278(44)**:43807-43817.
73. Farooqui AA, Ong WY, Horrocks LA. Neuroprotection abilities of cytosolic phospholipase A2 inhibitors in kainic acid-induced neurodegeneration. *Curr Drug Targets Cardiovasc Haematol Disord* 2004; **4(1)**:85-96.
74. Kurzel F, Hagel C, Zapf S, Meissner H, Westphal M, Giese A. Cyclo-oxygenase inhibitors and thromboxane synthase inhibitors differentially regulate migration arrest, growth inhibition and apoptosis in human glioma cells. *Acta Neurochir (Wien)* 2002; **144(1)**:71-87.
75. Maccarrone M, Melino G, Finazzi-Agro A. Lipoxygenases and their involvement in programmed cell death. *Cell Death Differ* 2001; **8(8)**:776-784.

76. Farooqui AA, Horrocks LA. Phospholipase A2-generated lipid mediators in the brain: the good, the bad, and the ugly. *Neuroscientist* 2006; **12(3)**:245-260.
77. Esterbauer H, Schaur RJ, Zollner H. Chemistry and biochemistry of 4-hydroxynonenal, malonaldehyde and related aldehydes. *Free Radic Biol Med* 1991; **11(1)**:81-128.
78. Bazan NG, Marcheselli VL, Cole-Edwards K. Brain response to injury and neurodegeneration: endogenous neuroprotective signaling. *Ann N Y Acad Sci* 2005; **1053**:137-147.
79. Roberts LJn, Fessel JP, Davies SS. The biochemistry of the isoprostane, neuroprostane, and isofuran Pathways of lipid peroxidation. *Brain Pathol* 2005; **15(2)**:143-148.
80. Brash AR. Arachidonic acid as a bioactive molecule. *J Clin Invest* 2001; **107(11)**:1339-1345.
81. Kuhn H, Borchert A. Regulation of enzymatic lipid peroxidation: the interplay of peroxidizing and peroxide reducing enzymes. *Free Radic Biol Med* 2002; **33(2)**:154-172.
82. Shimizu T, Wolfe LS. Arachidonic acid cascade and signal transduction. *J Neurochem* 1990; **55(1)**:1-15.
83. Hambrecht GS, Adesuyi SA, Holt S, Ellis EF. Brain 12-HETE formation in different species, brain regions, and in brain microvessels. *Neurochem Res* 1987; **12(11)**:1029-1033.
84. Watanabe T, Haeggstrom JZ. Rat 12-lipoxygenase: mutations of amino acids implicated in the positional specificity of 15- and 12-lipoxygenases. *Biochem Biophys Res Commun* 1993; **192(3)**:1023-1029.
85. Watanabe T, Medina JF, Haeggstrom JZ, Radmark O, Samuelsson B. Molecular cloning of a 12-lipoxygenase cDNA from rat brain. *Eur J Biochem* 1993; **212(2)**:605-612.
86. Lynch MA, Voss KL. Arachidonic acid increases inositol phospholipid metabolism and glutamate release in synaptosomes prepared from hippocampal tissue. *J Neurochem* 1990; **55**:215-221.
87. Wolfe LS, Pellerin L, Drapeau C, Rostworowski K. Formation of 12-lipoxygenase metabolites in rat cerebral cortical slices: stimulation by calcium ionophore, glutamate and N-methyl-D-aspartate. *J Neural Transm Suppl* 1990; **29**:29-37.

88. Feinmark SJ, Begum R, Tsvetkov E*, et al*. 12-lipoxygenase metabolites of arachidonic acid mediate metabotropic glutamate receptor-dependent long-term depression at hippocampal CA3-CA1 synapses. *J Neurosci* 2003; **23(36)**:11427-11435.
89. Uz T, Dwivedi Y, Qeli A, Peters-Golden M, Pandey G, Manev H. Glucocorticoid receptors are required for up-regulation of neuronal 5-lipoxygenase (5LOX) expression by dexamethasone. *FASEB J* 2001; **15(10)**:1792-1794.
90. Lepley RA, Fitzpatrick FA. Inhibition of mitogen-activated protein kinase kinase blocks activation and redistribution of 5-lipoxygenase in HL-60 cells. *Arch Biochem Biophys* 1996; **331(1)**:141-144.
91. Lepley RA, Muskardin DT, Fitzpatrick FA. Tyrosine kinase activity modulates catalysis and translocation of cellular 5-lipoxygenase. *J Biol Chem* 1996; **271(11)**:6179-6184.
92. Manev R, Manev H. 5-Lipoxygenase as a putative link between cardiovascular and psychiatric disorders. *Crit Rev Neurobiol* 2004; **16**:181-186.
93. Kitagawa K, Matsumoto M, Hori M. Cerebral ischemia in 5-lipoxygenase knockout mice. *Brain Res* 2004; **1004(1-2)**:198-202.
94. Farooqui AA, Horrocks LA. Excitotoxicity and neurological disorders: involvement of membrane phospholipids. *Int Rev Neurobiol* 1994; **36**:267-323.
95. Farooqui AA, Yi Ong W, Lu XR, Halliwell B, Horrocks LA. Neurochemical consequences of kainate-induced toxicity in brain: involvement of arachidonic acid release and prevention of toxicity by phospholipase A(2) inhibitors. *Brain Res Brain Res Rev* 2001; **38(1-2)**:61-78.
96. Wang Q, Yu S, Simonyi A, Sun GY, Sun AY. Kainic acid-mediated excitotoxicity as a model for neurodegeneration. *Mol Neurobiol* 2005; **31(1-3)**:3-16.
97. Sandhya TL, Ong WY, Horrocks LA, Farooqui AA. A light and electron microscopic study of cytoplasmic phospholipase A2 and cyclooxygenase-2 in the hippocampus after kainate lesions. *Brain Res* 1998; **788(1-2)**:223-231.
98. Koistinaho J, Koponen S, Chan PH. Expression of cyclooxygenase-2 mRNA after global ischemia is regulated by AMPA receptors and glucocorticoids. *Stroke* 1999; **30(9)**:1900-5; discussion 1905-6.

99. Pepicelli O, Fedele E, Bonanno G*, et al*. In vivo activation of N-methyl-D-aspartate receptors in the rat hippocampus increases prostaglandin E(2) extracellular levels and triggers lipid peroxidation through cyclooxygenase-mediated mechanisms. *J Neurochem* 2002; **81(5)**:1028-1034.
100. Pepicelli O, Fedele E, Berardi M*, et al*. Cyclo-oxygenase-1 and -2 differently contribute to prostaglandin E2 synthesis and lipid peroxidation after in vivo activation of N-methyl-D-aspartate receptors in rat hippocampus. *J Neurochem* 2005; **93(6)**:1561-1567.
101. Lipton SA, Choi YB, Pan ZH*, et al*. A redox-based mechanism for the neuroprotective and neurodestructive effects of nitric oxide and related nitroso-compounds. *Nature* 1993; **364(6438)**:626-632.
102. Liberatore GT, Jackson-Lewis V, Vukosavic S*, et al*. Inducible nitric oxide synthase stimulates dopaminergic neurodegeneration in the MPTP model of Parkinson disease. *Nat Med* 1999; **5(12)**:1403-1409.
103. Nowicki JP, Duval D, Poignet H, Scatton B. Nitric oxide mediates neuronal death after focal cerebral ischemia in the mouse. *Eur J Pharmacol* 1991; **204**:339-340.
104. Schulz JB, Matthews RT, Muqit MM, Browne SE, Beal MF. Inhibition of neuronal nitric oxide synthase by 7-nitroindazole protects against MPTP-induced neurotoxicity in mice. *J Neurochem* 1995; **64(2)**:936-939.
105. Sultana R, Poon HF, Cai J*, et al*. Identification of nitrated proteins in Alzheimer's disease brain using a redox proteomics approach. *Neurobiol Dis* 2006; **22(1)**:76-87.
106. Murphy S, Simmons ML, Agullo L*, et al*. Synthesis of nitric oxide in CNS glial cells. *Trends Neurosci* 1993; **16(8)**:323-328.
107. Nelson EJ, Connolly J, McArthur P. Nitric oxide and S-nitrosylation: excitotoxic and cell signaling mechanism. *Biol Cell* 2003; **95(1)**:3-8.
108. Ghafourifar P, Richter C. Nitric oxide synthase activity in mitochondria. *FEBS Lett* 1997; **418(3)**:291-296.
109. Hibbs JBJ, Taintor RR, Vavrin Z, Rachlin EM. Nitric oxide: a cytotoxic activated macrophage effector molecule. *Biochem Biophys Res Commun* 1988; **157(1)**:87-94.
110. Choi YB, Tenneti L, Le DA*, et al*. Molecular basis of NMDA receptor-coupled ion channel modulation by S-nitrosylation. *Nat Neurosci* 2000; **3**:15-21.

111. Kim WK, Choi YB, Rayudu PV*, et al*. Attenuation of NMDA receptor activity and neurotoxicity by nitroxyl anion, NO-. *Neuron* 1999; **24(2)**:461-469.
112. Lipton SA, Choi YB, Takahashi H*, et al*. Cysteine regulation of protein function--as exemplified by NMDA-receptor modulation. *Trends Neurosci* 2002; **25**:474-480.
113. Dawson VL, Dawson TM, Bartley DA, Uhl GR, Snyder SH. Mechanisms of nitric oxide-mediated neurotoxicity in primary brain cultures. *J Neurosci* 1993; **13(6)**:2651-2661.
114. Dawson VL, Dawson TM, London ED, Bredt DS, Snyder SH. Nitric oxide mediates glutamate neurotoxicity in primary cortical cultures. *Proc Natl Acad Sci U S A* 1991; **88(14)**:6368-6371.
115. Marks JD, Boriboun C, Wang J. Mitochondrial nitric oxide mediates decreased vulnerability of hippocampal neurons from immature animals to NMDA. *J Neurosci* 2005; **25(28)**:6561-6575.
116. Bolanos JP, Peuchen S, Heales SJ, Land JM, Clark JB. Nitric oxide-mediated inhibition of the mitochondrial respiratory chain in cultured astrocytes. *J Neurochem* 1994; **63(3)**:910-916.
117. Brown GC, Cooper CE. Nanomolar concentrations of nitric oxide reversibly inhibit synaptosomal respiration by competing with oxygen at cytochrome oxidase. *FEBS Lett* 1994; **356(2-3)**:295-298.
118. Cleeter MW, Cooper JM, Darley-Usmar VM, Moncada S, Schapira AH. Reversible inhibition of cytochrome c oxidase, the terminal enzyme of the mitochondrial respiratory chain, by nitric oxide. Implications for neurodegenerative diseases. *FEBS Lett* 1994; **345(1)**:50-54.
119. Bolanos JP, Heales SJ, Land JM, Clark JB. Effect of peroxynitrite on the mitochondrial respiratory chain: differential susceptibility of neurones and astrocytes in primary culture. *J Neurochem* 1995; **64(5)**:1965-1972.
120. Lizasoain I, Moro MA, Knowles RG, Darley-Usmar V, Moncada S. Nitric oxide and peroxynitrite exert distinct effects on mitochondrial respiration which are differentially blocked by glutathione or glucose. *Biochem J* 1996; **314 (Pt 3)**:877-880.
121. Radi R, Rodriguez M, Castro L, Telleri R. Inhibition of mitochondrial electron transport by peroxynitrite. *Arch Biochem Biophys* 1994; **308(1)**:89-95.

122. Knott AB, Bossy-Wetzel E. Impairing the mitochondrial fission and fusion balance: a new mechanism of neurodegeneration. *Ann N Y Acad Sci* 2008; **1147**:283-292.
123. Cho DH, Nakamura T, Fang J*, et al*. S-nitrosylation of Drp1 mediates beta-amyloid-related mitochondrial fission and neuronal injury. *Science* 2009; **324**:102-105.
124. Nakamura T, Cieplak P, Cho DH, Godzik A, Lipton SA. S-nitrosylation of Drp1 links excessive mitochondrial fission to neuronal injury in neurodegeneration. *Mitochondrion* 2010; **10**:573-578.
125. Cuajungco MP, Lees GJ. Nitric oxide generators produce accumulation of chelatable zinc in hippocampal neuronal perikarya. *Brain Res* 1998; **799(1)**:118-129.
126. Frazzini V, Rockabrand E, Mocchegiani E, Sensi SL. Oxidative stress and brain aging: is zinc the link? *Biogerontology* 2006; **7(5-6)**:307-314.
127. Frederickson CJ, Maret W, Cuajungco MP. Zinc and excitotoxic brain injury: a new model. *Neuroscientist* 2004; **10(1)**:18-25.
128. Khanna S, Parinandi NL, Kotha SR*, et al*. Nanomolar vitamin E alpha-tocotrienol inhibits glutamate-induced activation of phospholipase A2 and causes neuroprotection. *J Neurochem* 2010; **112**:1249-1260.
129. Khanna S, Roy S, Ryu H*, et al*. Molecular basis of vitamin E action: tocotrienol modulates 12-lipoxygenase, a key mediator of glutamate-induced neurodegeneration. *J Biol Chem* 2003; **278**:43508-43515.
130. Park HA, Khanna S, Rink C, Gnyawali S, Roy S, Sen CK. Glutathione disulfide induces neural cell death via a 12-lipoxygenase pathway. *Cell Death Differ* 2009; **16(8)**:1167-1179.
131. Culmsee C, Plesnila N. Targeting Bid to prevent programmed cell death in neurons. *Biochem Soc Trans* 2006; **34**:1334-1340.
132. Sastry PS, Rao KS. Apoptosis and the nervous system. *J Neurochem* 2000; **74(1)**:1-20.
133. van Leyen K, Kim HY, Lee SR, Jin G, Arai K, Lo EH. Baicalein and 12/15-lipoxygenase in the ischemic brain. *Stroke* 2006; **37**:3014-3018.
134. van Leyen K, Arai K, Jin G*, et al*. Novel lipoxygenase inhibitors as neuroprotective reagents. *J Neurosci Res* 2008; **86**:904-909.

135. Koeberle A, Rossi A, Zettl H*, et al*. The molecular pharmacology and in vivo activity of 2-(4-chloro-6-(2,3-dimethylphenylamino)pyrimidin-2-ylthio)octanoic acid (YS121), a dual inhibitor of microsomal prostaglandin E2 synthase-1 and 5-lipoxygenase. *J Pharmacol Exp Ther* 2010; **332(3)**:840-848.
136. Werz O, Greiner C, Koeberle A*, et al*. Novel and potent inhibitors of 5-lipoxygenase product synthesis based on the structure of pirinixic acid. *J Med Chem* 2008; **51(17)**:5449-5453.
137. Kazhdan I, Long L, Montellano R, Cavazos DA, Marciniak RA. Targeted gene therapy for breast cancer with truncated Bid. *Cancer Gene Ther* 2006; **13(2)**:141-149.
138. Maher P, Davis JB. The role of monoamine metabolism in oxidative glutamate toxicity. *J Neurosci* 1996; **16(20)**:6394-6401.
139. Cente M, Filipcik P, Pevalova M, Novak M. Expression of a truncated tau protein induces oxidative stress in a rodent model of tauopathy. *Eur J Neurosci* 2006; **24(4)**:1085-1090.
140. Lu WC, Chen CJ, Hsu HC, Hsu HL, Chen L. The adaptor protein SH2B1beta reduces hydrogen peroxide-induced cell death in PC12 cells and hippocampal neurons. *J Mol Signal* 2010; **5**:17.
141. Sendobry SM, Cornicelli JA, Welch K*, et al*. Attenuation of diet-induced atherosclerosis in rabbits with a highly selective 15-lipoxygenase inhibitor lacking significant antioxidant properties. *Br J Pharmacol* 1997; **120(7)**:1199-1206.
142. Altamura S, Muckenthaler MU. Iron toxicity in diseases of aging: Alzheimer's disease, Parkinson's disease and atherosclerosis. *J Alzheimers Dis* 2009; **16(4)**:879-895.
143. Butterfield DA, Bader Lange ML, Sultana R. Involvements of the lipid peroxidation product, HNE, in the pathogenesis and progression of Alzheimer's disease. *Biochim Biophys Acta* 2010; **1801(8)**:924-929.
144. Zarkovic K. 4-hydroxynonenal and neurodegenerative diseases. *Mol Aspects Med* 2003; **24(4-5)**:293-303.
145. Lipton SA. Neuronal protection and destruction by NO. *Cell Death Differ* 1999; **6**:943-951.
146. Nakamura T, Lipton SA. Emerging roles of S-nitrosylation in protein misfolding and neurodegenerative diseases. *Antioxid Redox Signal* 2008; **10**:87-101.

147. Nakamura T, Lipton SA. S-Nitrosylation of Critical Protein Thiols Mediates Protein Misfolding and Mitochondrial Dysfunction in Neurodegenerative Diseases. *Antioxid Redox Signal* 2010;
148. Tenneti L, D'Emilia DM, Lipton SA. Suppression of neuronal apoptosis by S-nitrosylation of caspases. *Neurosci Lett* 1997; **236**:139-142.
149. Pallast S, Arai K, Wang X, Lo EH, van Leyen K. 12/15-Lipoxygenase targets neuronal mitochondria under oxidative stress. *J Neurochem* 2009; **111**:882-889.
150. Grohm J, Plesnila N, Culmsee C. Bid mediates fission, membrane permeabilization and peri-nuclear accumulation of mitochondria as a prerequisite for oxidative neuronal cell death. *Brain Behav Immun* 2010; **24**:831-838.
151. Becattini B, Sareth S, Zhai D*, et al*. Targeting apoptosis via chemical design: inhibition of bid-induced cell death by small organic molecules. *Chem Biol* 2004; **11(8)**:1107-1117.
152. Almeida A, Bolanos JP. A transient inhibition of mitochondrial ATP synthesis by nitric oxide synthase activation triggered apoptosis in primary cortical neurons. *J Neurochem* 2001; **77(2)**:676-690.
153. Bedard K, Krause KH. The NOX family of ROS-generating NADPH oxidases: physiology and pathophysiology. *Physiol Rev* 2007; **87(1)**:245-313.
154. Brennan AM, Suh SW, Won SJ*, et al*. NADPH oxidase is the primary source of superoxide induced by NMDA receptor activation. *Nat Neurosci* 2009; **12(7)**:857-863.
155. Gandhi S, Wood-Kaczmar A, Yao *Z, et al*. PINK1-associated Parkinson's disease is caused by neuronal vulnerability to calcium-induced cell death. *Mol Cell* 2009; **33(5)**:627-638.
156. Kim YH, Koh JY. The role of NADPH oxidase and neuronal nitric oxide synthase in zinc-induced poly(ADP-ribose) polymerase activation and cell death in cortical culture. *Exp Neurol* 2002; **177**:407-418.
157. Susin SA, Lorenzo HK, Zamzami N*, et al*. Molecular characterization of mitochondrial apoptosis-inducing factor. *Nature* 1999; **397(6718)**:441-446.
158. Culmsee C, Zhu C, Landshamer S*, et al*. Apoptosis-inducing factor triggered by poly(ADP-ribose) polymerase and Bid mediates neuronal cell death after

oxygen-glucose deprivation and focal cerebral ischemia. *J Neurosci* 2005; **25**:10262-10272.

159. Zhu C, Wang X, Huang Z*, et al*. Apoptosis-inducing factor is a major contributor to neuronal loss induced by neonatal cerebral hypoxia-ischemia. *Cell Death Differ* 2007; **14**:775-784.
160. Seiler A, Schneider M, Forster H*, et al*. Glutathione peroxidase 4 senses and translates oxidative stress into 12/15-lipoxygenase dependent- and AIF-mediated cell death. *Cell Metab* 2008; **8**:237-248.
161. Plesnila N, Zinkel S, Amin-Hanjani S, Qiu J, Korsmeyer SJ, Moskowitz MA. Function of BID -- a molecule of the bcl-2 family -- in ischemic cell death in the brain. *Eur Surg Res* 2002; **34**:37-41.
162. Konig HG, Rehm M, Gudorf D*, et al*. Full length Bid is sufficient to induce apoptosis of cultured rat hippocampal neurons. *BMC Cell Biol* 2007; **8**:7.
163. Slemmer JE, Zhu C, Landshamer S*, et al*. Causal role of apoptosis-inducing factor for neuronal cell death following traumatic brain injury. *Am J Pathol* 2008; **173**:1795-1805.
164. Klein JA, Longo-Guess CM, Rossmann MP*, et al*. The harlequin mouse mutation downregulates apoptosis-inducing factor. *Nature* 2002; **419(6905)**:367-374.
165. Otera H, Ohsakaya S, Nagaura Z, Ishihara N, Mihara K. Export of mitochondrial AIF in response to proapoptotic stimuli depends on processing at the intermembrane space. *EMBO J* 2005; **24(7)**:1375-1386.
166. Yuste VJ, Moubarak RS, Delettre C*, et al*. Cysteine protease inhibition prevents mitochondrial apoptosis-inducing factor (AIF) release. *Cell Death Differ* 2005; **12(11)**:1445-1448.
167. Yu SW, Wang H, Poitras MF*, et al*. Mediation of poly(ADP-ribose) polymerase-1-dependent cell death by apoptosis-inducing factor. *Science* 2002; **297(5579)**:259-263.
168. Gao Y, Signore AP, Yin W*, et al*. Neuroprotection against focal ischemic brain injury by inhibition of c-Jun N-terminal kinase and attenuation of the mitochondrial apoptosis-signaling pathway. *J Cereb Blood Flow Metab* 2005; **25(6)**:694-712.

169. Xu X, Chua CC, Kong J*, et al*. Necrostatin-1 protects against glutamate-induced glutathione depletion and caspase-independent cell death in HT-22 cells. *J Neurochem* 2007; **103(5)**:2004-2014.
170. Yuan H, Gerencser AA, Liot G*, et al*. Mitochondrial fission is an upstream and required event for bax foci formation in response to nitric oxide in cortical neurons. *Cell Death Differ* 2007; **14(3)**:462-471.
171. Esposito E, Cuzzocrea S. New therapeutic strategy for Parkinson's and Alzheimer's disease. *Curr Med Chem* 2010; **17**:2764-2774.
172. Gu Z, Nakamura T, Lipton SA. Redox reactions induced by nitrosative stress mediate protein misfolding and mitochondrial dysfunction in neurodegenerative diseases. *Mol Neurobiol* 2010; **41**:55-72.
173. DeCostanzo AJ, Voloshyna I, Rosen ZB, Feinmark SJ, Siegelbaum SA. 12-Lipoxygenase regulates hippocampal long-term potentiation by modulating L-type Ca2+ channels. *J Neurosci* 2010; **30(5)**:1822-1831.
174. Lafon-Cazal M, Pietri S, Culcasi M, Bockaert J. NMDA-dependent superoxide production and neurotoxicity. *Nature* 1993; **364(6437)**:535-537.
175. MacDermott AB, Mayer ML, Westbrook GL, Smith SJ, Barker JL. NMDA-receptor activation increases cytoplasmic calcium concentration in cultured spinal cord neurones. *Nature* 1986; **321**:519-522.
176. Mandir AS, Poitras MF, Berliner AR*, et al*. NMDA but not non-NMDA excitotoxicity is mediated by Poly(ADP-ribose) polymerase. *J Neurosci* 2000; **20(21)**:8005-8011.
177. Klann E. Cell-permeable scavengers of superoxide prevent long-term potentiation in hippocampal area CA1. *J Neurophysiol* 1998; **80(1)**:452-457.
178. MacDonald JF, Jackson MF, Beazely MA. Hippocampal long-term synaptic plasticity and signal amplification of NMDA receptors. *Crit Rev Neurobiol* 2006; **18(1-2)**:71-84.
179. Aizenman E, Hartnett KA, Reynolds IJ. Oxygen free radicals regulate NMDA receptor function via a redox modulatory site. *Neuron* 1990; **5(6)**:841-846.
180. Patel M, Day BJ, Crapo JD, Fridovich I, McNamara JO. Requirement for superoxide in excitotoxic cell death. *Neuron* 1996; **16(2)**:345-355.
181. Tejada-Simon MV, Serrano F, Villasana LE*, et al*. Synaptic localization of a functional NADPH oxidase in the mouse hippocampus. *Mol Cell Neurosci* 2005; **29(1)**:97-106.

182. Mander P, Brown GC. Activation of microglial NADPH oxidase is synergistic with glial iNOS expression in inducing neuronal death: a dual-key mechanism of inflammatory neurodegeneration. *J Neuroinflammation* 2005; **2**:20.
183. Bae BI, Hara MR, Cascio MB*, et al*. Mutant huntingtin: nuclear translocation and cytotoxicity mediated by GAPDH. *Proc Natl Acad Sci U S A* 2006; **103(9)**:3405-3409.
184. Rosen DR, Siddique T, Patterson D*, et al*. Mutations in Cu/Zn superoxide dismutase gene are associated with familial amyotrophic lateral sclerosis. *Nature* 1993; **362(6415)**:59-62.
185. Fass U, Panickar K, Williams K, Nevels K, Personett D, McKinney M. The role of glutathione in nitric oxide donor toxicity to SN56 cholinergic neuron-like cells. *Brain Res* 2004; **1005(1-2)**:90-100.
186. Higgins GC, Beart PM, Nagley P. Oxidative stress triggers neuronal caspase-independent death: endonuclease G involvement in programmed cell death-type III. *Cell Mol Life Sci* 2009; **66(16)**:2773-2787.
187. Hattori Y, Hattori S, Kasai K. 4-hydroxynonenal prevents NO production in vascular smooth muscle cells by inhibiting nuclear factor-kappaB-dependent transcriptional activation of inducible NO synthase. *Arterioscler Thromb Vasc Biol* 2001; **21(7)**:1179-1183.
188. Liu W, Kato M, Itoigawa M*, et al*. Distinct involvement of NF-kappaB and p38 mitogen-activated protein kinase pathways in serum deprivation-mediated stimulation of inducible nitric oxide synthase and its inhibition by 4-hydroxynonenal. *J Cell Biochem* 2001; **83**:271-280.
189. Picklo MJ, Montine TJ, Amarnath V, Neely MD. Carbonyl toxicology and Alzheimer's disease. *Toxicol Appl Pharmacol* 2002; **184(3)**:187-197.

9. Acknowledgements

First of all I would like to thank my supervisor Prof. Dr. Carsten Culmsee for his support and his motivation. He always had time for discussions and guided me into the right direction. I am very happy that we obtained so many good results and managed to publish the CDD-paper despite of critical reviewers. Thank you also for the chance to attend several national and international meetings, which always were pleasant and unforgettable events.

Special thanks to all my colleagues and friends at the Institute of Pharmacology and Clinical Pharmacy, without their support my work would have been less successful and less fun. Thank you for all the discussions and the nice evenings with good food (Thanks to Anderson). It was always a big fun to spend time with you and I am very happy that we had this good and friendly atmosphere during the whole time of my PhD. I also want to thank Eva for the nice weekends at the Edersee and for the evenings that we spend together with a set square and a pair of compasses. Thanks also to Julia for the nice “sport-evenings” with sonny and all the other crazy coaches.

I also would like to mention Prof. Dr. Nikolaus Plesnila who supported all the projects and always had good ideas how to go on with the studies and papers.

Special thanks to Renate Hartmannsgruber, Sandra Engel and Emma Esser for their technical support, for teaching me important methods and for helping me with bureaucratic affairs. Special thanks to Renate for the nice time we were allowed to spend with her and Günter in their garden.

Thank you also to my “Wahlpflicht”-students who all did a very good job and helped me with several experiments.

Finally, I thank my parents, my grandma, my brother Jan and all my dear friends, without their support I would never have been able to complete this thesis. Thank you for reminding me that there is life outside of the lab. And special thank to Sebastian for his critical revision of my thesis and his help with all my computer problems.

10. Curriculum vitae

Personal data

Date of birth: 28.04.1983

Place of birth: Mölln, Germany

Marital status: unmarried

Education

01/2008 to present	PhD thesis at the Department of Pharmacology and Clinical Pharmacy, Philipps-University, Marburg, Germany; supervisor: Prof. Dr. Carsten Culmsee
12/2007	Licensure as pharmacist
05/2007-10/2007	Internship at Pfeil-Apotheke, Hamburg, Germany
11/2006-04/2007	Internship at Nordmark Arzneimittel GmbH & Co. KG, Uetersen, Germany
10/2002-10/2006	Studies of pharmacy, Philipps-University, Marburg, Germany
08/1993-06/2002	Secondary school, Lauenburgische Gelehrtenschule, Ratzeburg, Germany
07/1989-07/1993	Primary school, Grundschule Tanneck, Mölln, Germany